Exploring bicycle braking during a descent

C. van Trigt

TU Delft

Exploring bicycle braking during a descent

by

C. van Trigt

to obtain the degree of Master of Science
at the Delft University of Technology,
to be defended publicly on Friday April 12, 2019 at 10:00 AM.

Student number:	4141989	
Project duration:	February, 2017 – April, 2019	
Thesis committee:	Dr. ir. A. L. Schwab,	TU Delft, supervisor
	Dr. D. J. J. Bregman,	TU Delft, supervisor
	Dr. ir. R. Happee,	TU Delft
	MSc. T. Van Erp,	Team Sunweb

This thesis is confidential and cannot be made public until April 12, 2021.

TU Delft

Preface

My motivation for this project is that I want to help improve the performance of world class cyclists using science. It is interesting to see how important science has become in elite sport over the last decades. The differences between competitors have become smaller and smaller. The gains found using science can make a significant difference.

Within the project, I benefited from my knowledge and experiences as a competitive cyclist myself and all the weekends working at Sanders Tweewielers bicycle store in Haarlem. The practical knowledge gained there came in useful on several occasions.

Without the help of others, it would not be possible for me to complete this thesis. I would like to thank all who where involved and have helped me during the experiments and compilation of my thesis. Especially:

- Dr. Ir. Arend Schwab, my supervisor, for his support an flexibility throughout my graduation as well as reading and suggesting improvements for my report.
- Dr. Daan Bregman from the Sport Engineering Institute for providing a wide range of possible sport related projects to the TU Delft student's and his clear explanation on how to properly structure a scientific thesis.
- Teun van Erp, the movement scientist from Team Sunweb, for explaining many of the details behind professional cycling.
- Marco Reijne who was involved in the project from the TU Delft. He was of great help by assessing and filtering the GPS data and proofreading.
- Frank Schoenmaker from nSize for taking the photos during the experimental descents and involving me in the decision making and process of building the Sensor-Set mounts
- Wiebe Berkelaar from Berkelaar MRT who, during the production of the Sensor-Set, involved me in the production process and was interested in my opinion.
- Jos van Driel form the TU Meetshop has been very helpful by ordering the strain gauges and helped with the application of the strain gauges, a delicate process where an experienced helping hand is more than welcome.
- The personnel from the workshop of Industrial Design with their advice on how to manufacture the various parts for the Sensor-Set.
- The staff and members of Team Sunweb for the warm welcome I received during their training camp.

C. van Trigt
Delft, April 2019

Abstract

This exploration study focuses on the braking behaviour of World Tour cyclists during a descent. For this study, 8 riders descended over 6 trials using a 'sensor bike'.

As part of this particular study, a novel brake sensor is developed and validated in practice. The sensor package can be transferred between bicycles, allowing each rider to use his own bicycle.

Results of the exploration study indicate that for the chosen descent, braking and cornering skills are not decisive for overall time over the descent. However, significant time differences are found for the corner which is analysed. Time difference reported over this corner are approximately one second. With a shortest cornering time of 10.14 seconds this is a significant difference.

The brake behaviour of the World Tour cyclists could be split into two distinct braking strategies:

- 'stop brake late' (where braking is stopped late and well into the turn).
- 'stop brake early' (where braking is stopped before or early in the turn).

It was found in this study that the best brake strategy is 'stop brake late'.

The peak brake forces measured during the descent are much lower than the maximum brake forces reported in literature. This implies, that performance can still be improved by increasing brake forces at the first part of the braking action, so the braking can start later.

The results found in this study can contribute to optimise braking and cornering skills of riders by explaining and showing where improvements can be found.

An additional result is that the brake sensor revealed unexpected brake rub at certain parts of the descent, especially when riders are accelerating. Eliminating this brake rub, can improve rider performance.
The riders also shows clear signs of learning behaviour as can be observed in the obtained data.

For future research it is recommended to add a speed sensor to the sensor package. Recommended small improvements for the brake sensor are identified. Using this improved sensor package, trials could be rehearsed on a steeper descent, such that pedalling actions have less influence, exploring braking and cornering strategies further.

Contents

1 Introduction

In cycling, speed is the most important parameter. The cyclist with the highest average speed during a race will cross the line first and wins that race. The speed a cyclist reaches is determined by the forces that act on a cyclist. When cycling, a cyclist experiences the following forces:

- Pedalling force form the cyclist;
- Aerodynamic drag;
- Drive train loss;
- Rolling resistance;
- Gravity from road gradient;
- Brake force.

All these forces acting on a cyclist are shown in figure 1.1.

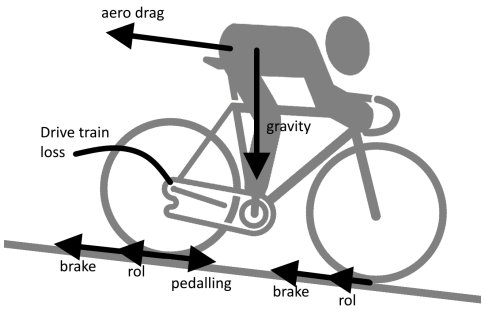

Figure 1.1: Schematic drawing of a cyclist and the forces acting on a cyclist.

In cycling research a large amount of literature focuses on the power production of a cyclist. Focus on power production in literature may be split in three fields: being modelling, improving and optimising power production. In general modelling has the goal to create a model of the power production over time. Most models are focused on the duration of maximum power production by a cyclist [14] [21]. Improving power production looks into methods to improve the power production of a cyclist. Research mainly focuses on finding the best bike geometry [15] or effects of nutrition on power production are investigated [7]. Optimising power production is about finding the best pacing strategy to minimise time to the finish [23] [4].

As said, most research is done on the power production of a cyclist. However, effects reducing cycling speed are much less investigated. Scientific literature on power losses during road cycling is mostly limited to aerodynamic losses. Changes in equipment and rider position could reduce aerodynamic losses. This results in lower power requirements and implies that a cyclist may keep the pace longer or has a higher speed.

The effect of aerodynamic losses is mostly researched for time trials. During and after time trials results may be more easily compared and evaluated [12].
Aerodynamic interactions of riding in groups is an important part of cycling aerodynamics. In racing the aerodynamic interaction between cyclist from drafting has large effects on power needs and race strategies used [10].
The scientific focus is mainly on aerodynamic losses because they can account for up to 96 % of the power losses in road cycling [14]. The smaller gains of lowering mechanical losses in bicycle components is mainly investigated and optimised by bicycle and component manufacturers. They work on the reduction of tire rolling resistance [25] and improvement off drive train efficiency [2].

Little to no scientific literature can be found on how cyclists brake or what the optimal brake strategy should look like during a corner. However, literature does report the braking forces and accelerations that can be expected. The data is stated in accelerations to make it independent of mass differences between cyclist. Pein, Wayne [19] states accelerations of -0.6 g as max braking for a heavily skilled cyclist and -0.35 g for a normal cyclist. Jim Papadopoulos [3] gives an acceleration of around -0.5 g for hard braking. R.F. Back [1] tested braking on multiple types of bicycles. Accelerations found for a road bicycle on asphalt are: -0.4 g with both brakes, -0.38 g front brake only and -0.27 g for rear only.
The only article found about braking power, is about the validation of a device designed to measure braking power for an disc brake MTB [17]. The device is extremely overbuild at 4.79 kg and thus not suited for experiments in races or race simulations, where weight is of importance.

Until this study, the differences between a good and bad braking techniques are unknown. Therefore, the aim of this study is to determine who has a good braking technique, who does not and how to optimise braking. To find out where a technically good and bad cyclist differ, their behaviour needs to be analysed: where are the braking points, how much energy do they lose by braking, do they brake during or before a corner and more. Answering such questions for different cyclists, the parameters that determine good performance may be found. When this is known, performance may eventually be improved by structured skills training.

Braking occurs on several occasions during a road cycling race. It is required to brake before most corners, and even on a completely straight road the brakes are sometimes used to avoid crashing into competitors or teammates. The frequency of braking actions is magnified during a technical descent. Descending is thus an interesting starting point for exploration on braking behaviour.

The above information summarises to the following research question: which are the best braking strategies resulting in a fast and safe cycling technique and optimum use of human power, leading to optimum results.

As demonstrated in literature [12], best comparisons are made during time trials. A descent is chosen as these are known to be able to make a difference during a race. Also frequent braking is required during a descent. It is therefore investigated if the braking behaviour of various cyclists impacts the time over the set course and may generate a significant impact.
This will be investigated by developing a custom sensor that measures braking forces. This brake sensor will be an addition to a currently existing interchangeable Sensor-Set used to record cycling techniques. After developing and producing the brake sensors, testing and calibration is done. The testing is done to describe sensor behaviour and the calibration is needed to determine the relation between brake force and sensor output. This research is conducted as an integral part of an overall research plan for optimising cycling using a 'sensor' bike explained in appendix P. The calibrated brake sensor will then be used to measure the braking technique during the overall experiment with 8 different riders on a descent.

2

Brake Sensor

The advantages of a brake sensor over other sensors that can be used to estimate brake points and forces are presented in Section 2.1. The requirements of a brake sensor are defined in section 2.2.1. Using these requirements, design choices are made in Section 2.2.2. These design choices result in a sensor design which is subsequently fabricated, as described in Section 2.3.

2.1. Advantages of a Brake Sensor

A true brake sensor measuring brake force independently from other parameters, i.e. instead of using derived data from other sensors such as a power meter or accelerometer, has various advantages. These are listed below.

- When using a brake sensor the output is zero when not braking. Using acceleration to estimate brake force, accelerations from pedalling will also give sensor output as well as other forces acting on the cyclist/bicycles.
- A brake sensor measures brake forces directly. Using an accelerometer, various parameters influence acceleration (e.g. road gradient due to gravity, aerodynamic drag, rolling resistance, etc.). Only when these all level out to zero acceleration, a negative acceleration can be directly linked to braking.
- In case the sum of forces does not level out to zero, the power balance of a cyclist needs to be used to more accurately estimate brake forces from an accelerometer. The cycling power balance contains one difficult to measure parameter, being the aerodynamic drag coefficient. Aerodynamic drag is related to rider, body position, equipment and moreover, these constantly change and differ per scenario.
- A brake sensor also works when aerodynamic drag is affected by many rapidly changing variables i.e. riding in a peloton. The acceleration data will then be not useful.
- The road gradient is required to remove gravity forces from the accelerometer data. As mentioned in Section 3, obtaining the road gradient accurately from GPS data is difficult.
- Brake sensor data may be used directly. Accelerometer data requires post processing of extra data. This lengthens the time needed to get the results ready for feedback to the riders. If a Sensor-Set is used for training purposes this is unwanted.
- Front and rear brake force distribution differences between riders and trials, cannot be measured using a accelerometer.
- The accelerations will be measured in the Sensor-Set that is mounted on the bicycle frame. It is not the acceleration of the centre of mass (rider +bicycle) that is measured. This implies that rider movement may give sensor output not related to accelerations of the complete system.

To summarise these points, the advantage of using a brake sensor is that true braking is directly measured whereas it is only possible to estimate brake forces from GPS, power and accelerometer data.

2.2. Brake Sensor Development

2.2.1. Sensor Requirements

The first step is to establish sensor requirements based on the final application and allowing for optimum measurements. The sensor has to work with the other equipment used in the experiment, experimental methods, research goal, participants and environmental conditions.

The experiments should be done using the bicycles of the participants. World Tour cyclist ride around 30.000 to 35.000 km annually [11]. This makes World Tour cyclists extremely sensitive to their riding position, bike settings and component changes. For the validity of the experimental data it is very important that the riders cycle on their own familiar bicycles, using the same settings and components. This implies that in order to record braking data, a sensor has to be developed that does not influence braking behaviour and may be used on normal brake callipers, changing as little as possible to the bike settings. In order to perform measurements with several cyclists, the sensor need to be able to be exchanged between bicycles relatively easy and quick.

The first step for the sensor development, is to categorise the bicycles of the Sunweb team. Team Sunweb uses 4 different bikes for their men World Tour, women World Tour and development team [24]. A rim brake Giant TCR is used by the World Tour men. The rim brake Liv Envie is used by the World Tour women. The Giant TCR Disc brake is used by the development team. The Giant Trinity with rim brakes is used as time trial bike for all three teams. The differences between disc and rim brake bicycles are to large to develop one solution for all bikes. The first experiment will be done with rim braked giant TCR from the World Tour men shown in figure 2.1. The first sensor that will be made will focus on the Giant TCR advanced. This TCR Advanced is equipped with Shimano Dura-ace 9000 brakes callipers as shown in figure 2.2. The brake pad on this caliper is mounted using a bolt. An added bonus would be if the brake sensor could work on the time trial bike and the woman's bike that have rim brakes from a different type.

Figure 2.1: The Giant TCR of Team Sunweb's world tour team

Figure 2.2: Dura-ace 9000 rim brake caliper

Braking is done to slow the bicycle down and starts by pulling the brake lever. The pulling force on the brake lever results in forces on multiple locations. From the brake lever the force is transferred through the brake cable. From the brake cable the force goes onto the brake caliper. This brake caliper pushes the brake pads onto the rim. The normal force on the brake pad in combination with the moving rim results in friction between the brake pad and rim. The friction force on the rim results in a force between the tyre and road that slows the bicycle down. When following the entire path from lever to road, there are many steps, each with their own force transmission and friction losses. These friction levels alter with equipment wear, lubrication, brand, type and weather conditions. This means that the force at the brake lever is not linearly related to the tyre road force. One of these two forces has to be selected as braking force. For this thesis, the tyre road force is chosen because this is what slows the bicycle down and makes calculations of braking energy possible. This means that the sensor is required to measure the force between road and tire after calibration.

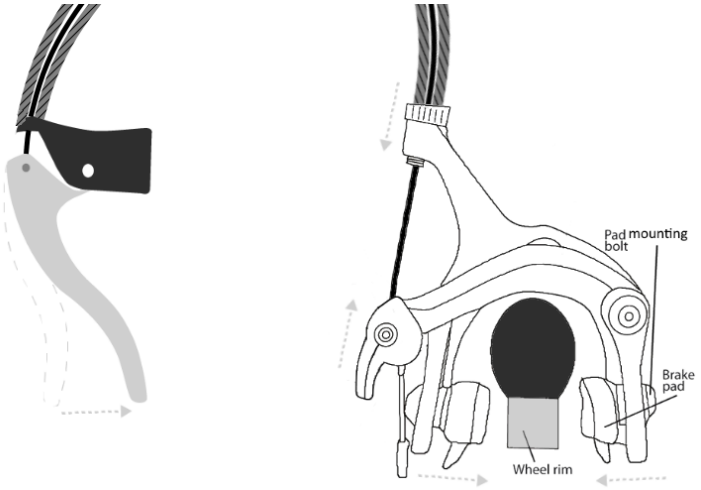

Figure 2.3: Schematic drawing of a rim brake system. With the brake lever on the left and the brake caliper on the right.

For the development of a sensor it is important to have an estimation of the force range that needs to be measured. In the scientific literature there are multiple values given for maximal braking forces, as can be seen in the literature study [24]. The maximal value for a road bicycle on asphalt [1] of -0.4 g for a 100 kg rider plus equipment or 400 N should be used as maximal force for the brake sensor. By using the highest road bike specific force from literature, it is assured that all the brake data recorded will be within the measurement range. The brake sensor should at least measure a maximal braking force of 400 N.

The development of the Sensor-Set is already started by Berkelaar MRT and the decisions on the electronic connection for the brake sensors are already made. The Sensor-Set will have 2 instrumentation amplifiers to connect a Wheatstone bridge load cell. The gain of the instrumentation amplifiers can be changed by switching an electronic resistor. The voltage output after the instrumentation amplifiers is made digital using a 12 bit Analogue to Digital Converter (ADC). This setup, using 2 connections for Wheatstone bridge load cells, gives the requirement to use strain gauges in a Wheatstone bridge configuration.

The environmental conditions during the experiment can be harsh on the equipment. To withstand these conditions, the sensor has to be water and vibration proof. Vibration proof is for the road imperfections and bumps that are transferred into the bicycle. Although the Sensor-Set is not completely water proof, the brake sensors have to be water proof. The brake sensor will likely be near the wheels and possible water/dew on the road surface can be splattered around by the wheels.

The brake sensor should do the following:

1. measure tire road brake force after calibration;
2. be easily swapped between Giant TCR bicycles;
3. not influence the bicycle behaviour;
4. measure a maximum of 400 N;
5. water proof;
6. vibration proof;
7. work with the Sensor-Set already built by Berkelaar MRT and use strain gauges in a Wheatstone bridge configuration.

2.2.2. Design Choices

With all sensor requirements defined in Section 2.2.1, a concept that fulfils these requirements is developed in this section. This concept involves a custom made brake pad holder and a Wheatstone bridge strain gauge pattern to isolate shear force.

Presented in Section 2.2.1 are the reasons to measure the brake force between the tyre and road surface. It is not feasible to directly measure forces between the road and tire. Road-Tire force shown in figure 2.4 should thus be measured at a location where there is a linearly related force. On the bicycle wheels there is the Rim-Brake force and the Hub force. These forces are linearly related to the Road-Tire force and need to add up to zero with the Road-Tire force.
The Rim-Brake force goes through the brake pad shown in figure 2.5 into the brake caliper shown in figure 2.6. At the brake pad, the shear forces are equal to the Rim-Brake force at the wheel. The normal force at the mounting point is related to the shear force through the friction coefficient between brake pad and rim. The moment at the mounting point is depending on pad thickness and wear pattern. Looking at the brake caliper the Rim-Brake force is transmitted to the mounting point of the brake pad on the caliper. For force equilibrium at the brake caliper a force equal to the Rim-Brake force and a moment needs to be present at the caliper mounting point on the frame/fork.
This information shows that there are multiple locations for brake force measurements before friction coefficients between brake pad/rim and moving caliper parts affect the forces. Looking at these force measurement locations, some are easily eliminated as feasible location. Measurements at the wheel hub will be affected by road vibrations and other non-brake related forces such as rider mass for example. The bicycle rim is not feasible due to the large surface area where the force could be applied. The brake callipers are not easily switched between bicycles. It has only has curved surfaces that make strain gauge application difficult. The brake pad and washer between the brake caliper and frame/fork shown in figure 2.6 are the two locations which are most feasible. Looking at the brake pad, advantages over the washer can be found. The brake pad only experiences forces during braking and is universal for several road bicycles, increasing the compatibility with the women's and time trial bikes. For these reasons, it is chosen to locate the sensor at the brake pad.

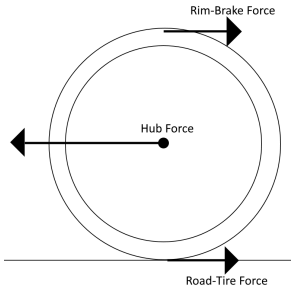

Figure 2.4: Forces at a bicycle wheel free body diagram

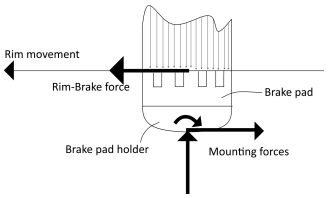

Figure 2.5: Top view of a brake pad with braking forces

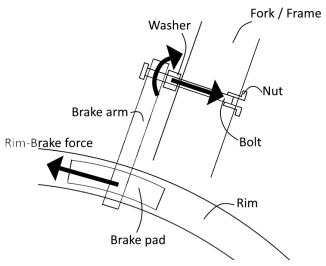

Figure 2.6: Forces at a rim brake caliper

Shown in figure 2.5 is the Rim-Brake force, the force that has to be measured. The Rim-Brake force puts a shear load on the brake pad. This shear in the brake pad has to be isolated from the compression and bending that are also present on the brake pad. Shown in figure 2.7 is the Shimano Dura-ace brake pad mounted on the Giant TCR with the forces that shear the pad. The brake pad consist of a rubber pad insert and an aluminium pad holder. Measuring in/on the rubber pad is not possible. The deformations are too large for strain gauges. Looking at the stock aluminium pad holder there is not much room for structured application of strain gauges. To make room for the strain gauge application a custom pad holder will be designed.

Figure 2.7: The stock Shimano Dura-ace brake pad

To measure isolated shear force on the brake pad holder, a dedicated strain gauge application and connection pattern is used. When strain gauges lengthen, their electronic resistance increases and shortening lowers the electric resistance. These changes in electric resistance are linear to the length changes. To isolate shear force, 4 strain gauges are applied as shown in figure 2.8.a. The deformation modes are shown in figure 2.8.b,c,d. These strain gauges have to be connected to the Sensor-Set in a Wheatstone bridge pattern shown in figure 2.9. The plus and minus signs shown in figure 2.9 represent the changes in electric resistance with the deformations shown in figure 2.8. With shear resistance 4 and 2 increase, 1 and 3 decrease. The voltage over 4 and 3 will no longer be equally spread. Resistance 4 will take more voltage and 3 less. On the other side 2 will take more voltage and 1 less. This will create a voltage over V-uit. With bending the voltage is equally spread on the left side and also on the right side so there will be no change in V-uit. During compression all the strain gauge resistances decrease by the same amount and V-uit will thus remain equal. Theoretically shear would thus be the only deformation effecting the output voltage of the Wheatstone bridge.

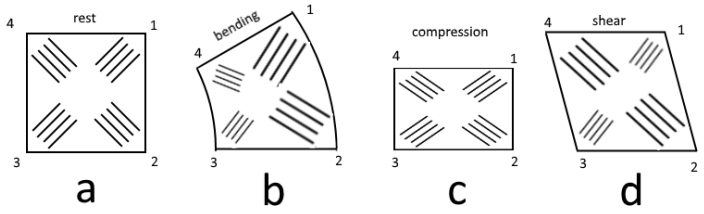

Figure 2.8: Deformations and corresponding strain gauge lengthening or shortening

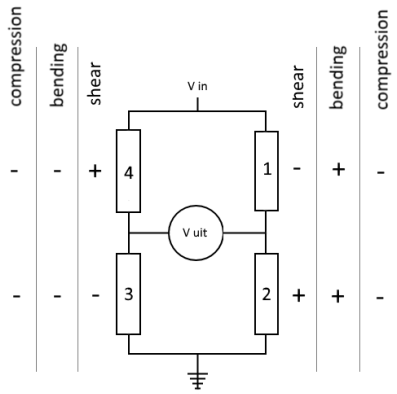

Figure 2.9: Strain gauge application pattern and how these strain gauges change length with different deformation modes

Before starting the design and manufacturing of a brake sensor a check of the strain gauge application and connection pattern is done at the TU Delft MeetShop together with Jos van Driel. For this a 10 mm X 10 mm square aluminium bar of length 300 mm and the following strain gauge assembly's brand: TML, model number: FCA-1-23-1L, gauge resistance: 120+-0.5 ohm are used. The strain gauges have 2 gauges orientated at 90 deg on a single backing plate as shown in figure 2.10. Fixating the left side in a vice and loading the bar on 3 distances from the fixation point as shown in figure 2.11. First the linearity is checked at the closest point around 1cm from the strain gauges. The data from the linearity check is shown in figure 2.12. The load output relation is linear, as expected. The dependency of the output on bending moments is tested by moving the largest test mass on the bar and noting the output voltage. The result is 0.909V at 1 cm, 0.909 V at 5 cm and 0.929 V at 10 cm. This implies that the strain gauge pattern is almost insensitive to bending.

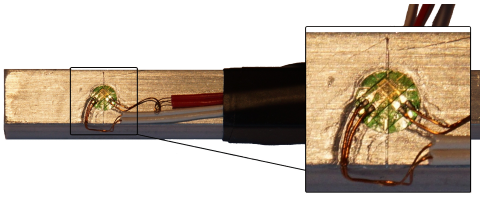

Figure 2.10: 10 mm X 10 mm square aluminium bar of length 300 mm with strain gauge's applied in shear isolation pattern

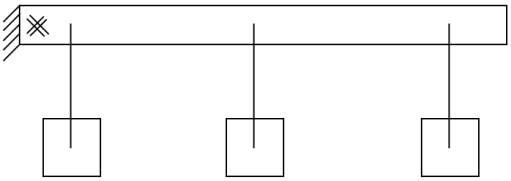

Figure 2.11: schematic drawing of the test setup to validate the strain gauge pattern for shear isolation

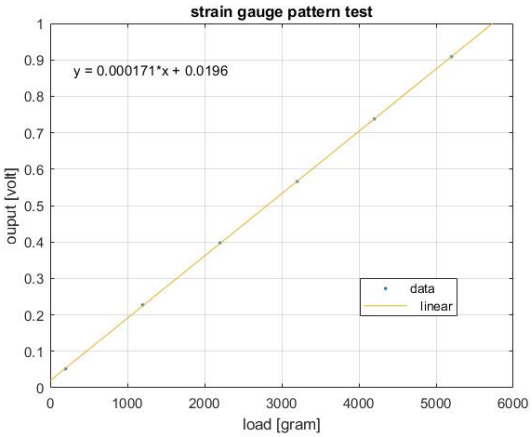

Figure 2.12: plot of test data

With a solution found to isolate shear, an custom brake pad holder with room for strain gauge application is designed. An 10x10 mm mounting post is used as strain gauge application surface. To make sure to not alter the braking behaviour the stock Shimano Dura-ace rubber pad needs to fit in the new pad holder. To achieve a good fit the old pad holder is measured and copied into the new holder.

2.3. Sensor Fabrication

Based on the design choices for the brake sensor, a construction drawing is made, as shown in figure 2.13. The mounting post is made square for easy mounting of the strain gauges. The brake pad mounting dimensions are taken from the Shimano Dura-Ace brake pad holder. The outside is a simple rectangle to simplify production.

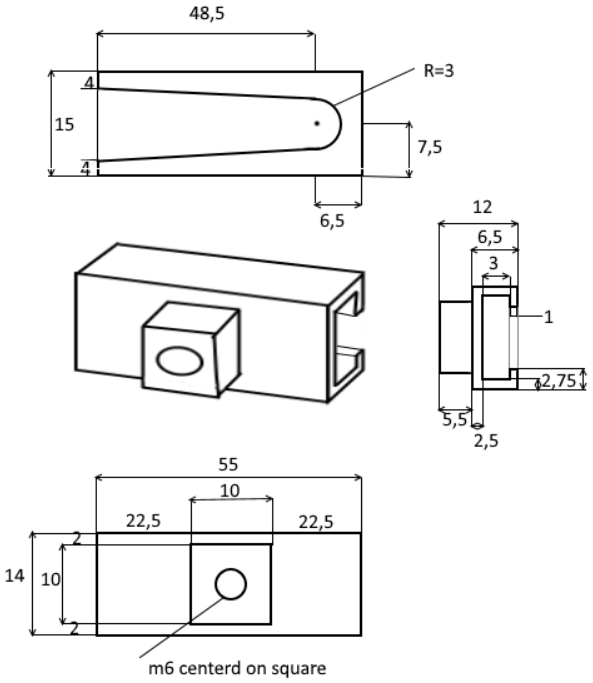

Figure 2.13: construction drawing of the custom pad holder

Two sensors are made at the Industrial Design Inloopwerkplaats by milling the part out of an 7075 t6 aluminium bar. When all milling was finished, a m6 tread for mounting the sensor was made using an thread tap. Shown in figure 2.14 is the resulting pad holder with a brake pad inserted.

Figure 2.14: Picture of the custom pad holder with a brake pad inserted

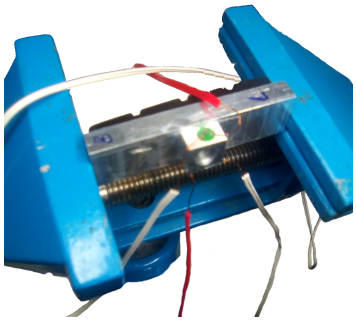

Figure 2.15: Strain gauge application at the TU Delft Meet-Shop

Strain gauge application is done at the MeetShop[1]. For application the following steps are made: sanding down the application surface, clean the application surface, apply glue, align and press down strain gauge to the surface. Due to the small application surface, strain gauge application was a difficult process. The first try was not always successful. The strain gauges either did not bound correctly and fell off or were not properly aligned. Shown in figure 2.15 is the custom pad holder with the just applied strain gauges. The used strain gauges are the same type as on the test bar, brand: TML, model number: FCA-1-23-1L, gauge resistance: 120+-0.5 ohm

The strain gauges are not waterproof yet, but they should be. Therefore, a solution needs to be found to make these strain gauges weather proof, as during field trials any type of weather may be present. Wa-

[1] Jos van Driel is acknowledged for preforming this dedicate process

terproofing the sensors is done by covering the strain gauges with glue. The same glue is used to secure the strain gauge connection wires to the custom aluminium pad holder. When pulling the connection wires, the force is transmitted from the wire through the glue onto the aluminium pad holder, instead of the forces going through the strain gauge and potentially damaging it. A picture of the final result is shown in figure 2.16

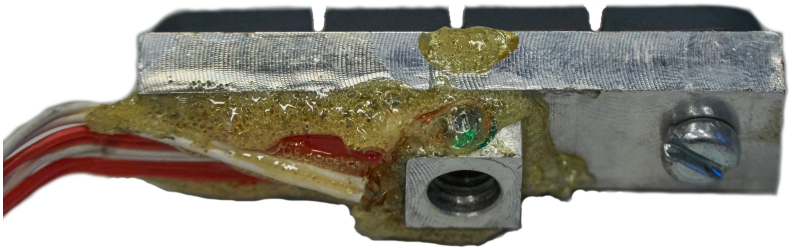

Figure 2.16: picture of the finished brake sensor

A detailed description of the prototype brake sensors validation and calibration is included in Appendix E.

3

Method

This graduation project is part of a larger exploration study about descending funded by Sportinnovator [22]. An exploration study implies that no interventions are made between different trials of riders. The exploration study about cyclist descending is done to obtain information about what differentiates a good and bad descent/descender. The recorded data will be used to identify the parameters that are important for descending performance. In other words what are the differences between a good or bad descent. This information can later be used to design an intervention study or structured training method for descending on a bicycle.

For the exploration study we have found 8 professional cyclist competing at UCI World Tour level willing to participate. Each of these riders will do 6 trials on a descent. The riders do the experiment in pairs of two. The two riders start at one minute interval on top of the descent, making it an individual exercise. When both riders have reached the bottom of the descent they are brought back to the start by the team car. Working in pairs of two saves time and makes it more enjoyable for the participants.

The first paragraph from the riders instruction paper explains the procedure for the riders in a short summary. *"For the experiment, you have to ride a descent of approximately 2 km as fast as possible (but safety first). The experiment is repeated 10 times. You must remain on the right lane at all times and be aware of other traffic. You are allowed to pedal and take on any position you like (be aware of the measurement system). The experiment will be performed with two riders at the same time (1 minute interval on the descent)."* For a more detailed explanation from a riders perspective extra information is included in appendix R. This appendix includes the complete instruction paper handed to the riders.

Before starting the experiment the riders have to read the informed consent included in appendix Q. In this informed consent the purpose, procedures, benefits, risks and possible discomforts of the study are explained. When they agree to participate after reading the informed consent they can sign the consent form.

To help explain and understand the recorded data each rider is interviewed after their descent. For this thesis, as part of the complete exploration study, the remarks made by the riders about each trial are used. The remarks given by the riders can be found in appendix J.

As explained before the experiment is done in pairs of two. For the first two riders the Sensor-Set's are mounted on their bicycle's at the team hotel. The two bikes and riders are driven to the descent with the team car. and also the two bicycles of the next two participants. After the first two riders have completed the experiment, they can wait a few minutes until the Sensor-Set is removed from their bicycle and cycle back to the hotel or, take a ride back with the team car and their bikes will follow later. The team car will pick up the two riders for the following round together with the bicycles for the round after that. During the travel the Sensor-Set's are mounted on the previously brought bicycles for the next participants. This process is repeated until every rider has completed the experiment. Using this method waiting time for the participants is minimised.

Data recording is started before the first trial of each rider and stopped after the last trial. Before starting with a new rider, the id number (wireless ant+ protocol) of power meter, speed and cadence sensor as well as rider information is entered into the Berkelaar MRT Sensor-Set interface. By making one file for each rider, time can be saved as no data processing is required in between trials.

After recording and storing one large data file per rider, the 6 trials have to be cut from this large data file. To simplify identification of the trials during post processing of the data, the video synchronisation button is used. When pushing the synchronisation button a LED lights up. The lighting of the LED can be used to synchronise the video images with the data file. In the recorded data file the synchronisation button is zero when not pushed and one when pushed. For trial identification the synchronisation button will also be used to mark the start and stop of each trial. Pushing 3 times marks the start of a trial, pushing 4 times marks the end of a good trial. For a trial that is not successful the synchronisation button is pushed 5 times. An unsuccessful trial could for example happen when a rider is caught behind slower traffic.

The descent chosen for the exploration study is an 1.85 km long section of the L218 near Vossenack, Germany with an average gradient of 5 %. Shown in figure 3.1 is a top view of the road section used. The road is split into 8 segments that each have their own characteristics.

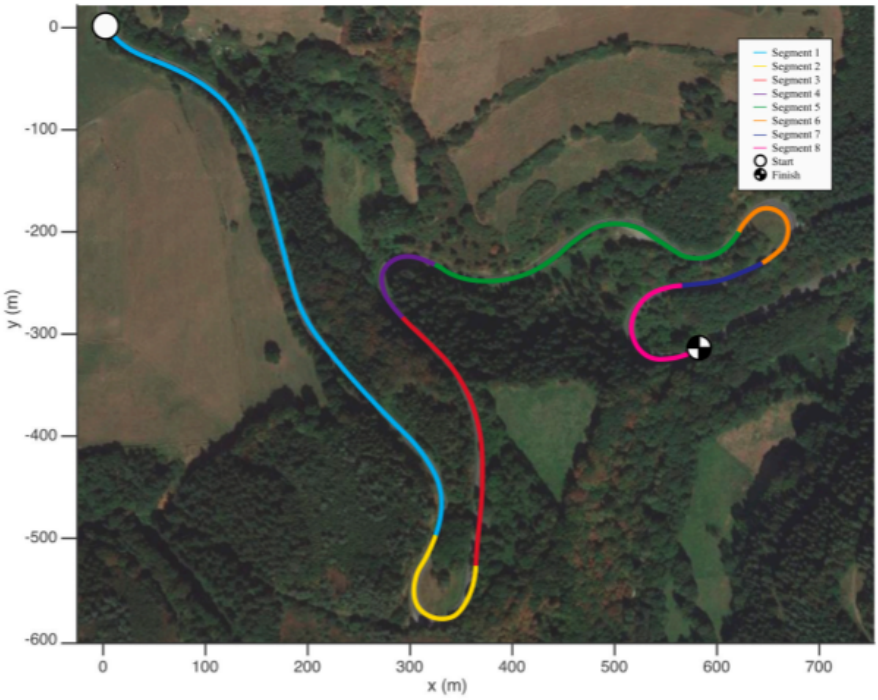

Figure 3.1: Location of the experiment is a 1.85 km part of road of the L218 near Vossenack, Germany. The average gradient of the descent is 5 degrees. Start location is at the top left. The descent is divided into eight segments to compare rider technique for different elements (e.g., straight parts, left hand corners, right hand corners).

For this study, the altitude data is important, as the road gradient is derived from this data. The road gradient is used to correct the acceleration data for gravity.
High quality GPS can measure position accurately, but height measurements remains a weak spot of GPS sensors. The sampling rate is not high enough to obtain reliable height data at the speeds reached during these experiments. Differential GPS is used to measure the track outlines of the descent before the experiment. With a low speed descent, sufficient GPS samples are recorded. After filtering, the large amount of samples will result in accurate road gradient data, as noise can be filtered without removing too much detail.

To guarantee that the best altitude and gradient data is used for each rider, the altitude data recorded during each individual trial, is replaced with that from the differential GPS measurements. This leads to all riders having uniform and high quality altitude and gradient data. Shown in figure 3.2 is a plot containing the road gradient data.

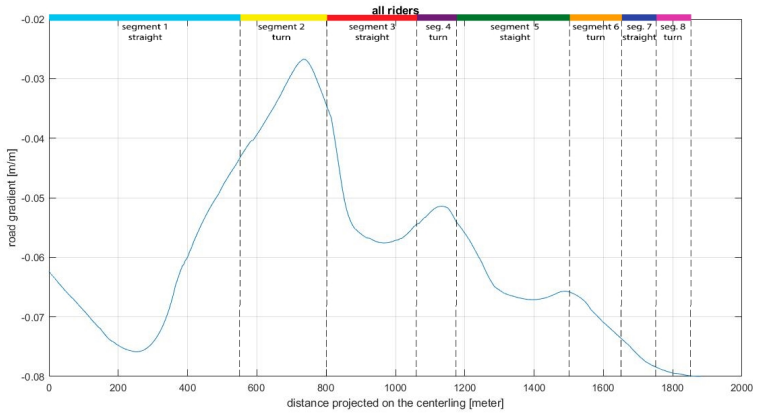

Figure 3.2: The road gradient used for all riders and trails.

During the descent the Sensor-Set shown in figure 3.3 is recording the follow information:

A Rider posture (video);

B Position;

C Steer angle;

D 3D orientation, rotational speed and linear acceleration of the rear frame;

E Brake force front and rear;

F Cadence, speed and pedal power.

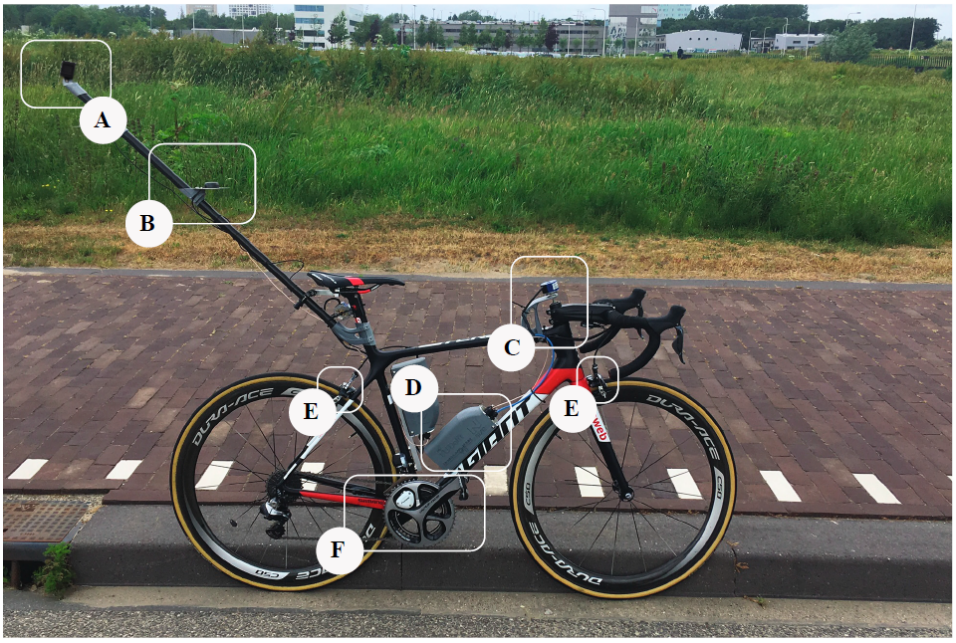

Figure 3.3: Picture source [20] with Measurement system installed on a bicycle. (A) GoPro camera and mount to record rider posture; (B) GNSS antenna to measure rider's position on the road; (C) optical encoder to measure steering angle; (D) IMU to measure roll angle and data acquisition system; (E) stain gauges on brake shoe to measure brake force; (F) speed and cadence sensor and power meter

The focus of this thesis will be on the braking part of descending skills. This does not mean that the recorded brake sensor output will be used as the only data. Without other data to put the brake sensor data

into context, it would be almost impossible to say something about braking during a descent. Therefore speed, position and linear accelerations are used to give context to the output of the brake sensor. Position data in combination with the brake data can for example be used to determine the braking points before a corner.

It is possible that riders take a different line during the descent. When the riders take different lines, the distance travelled from start to finish will be different. A standardised measure for distance travelled is therefore required. This is achieved by projecting the position of a rider on to the centreline. As shown in figure 3.4, the centreline is defined as the line in the middle between the track centreline (left track boundary) and the line on the right side of the road (right track boundary), i.e. the middle of the lane.
The point on the centreline with the shortest distance to the riders actual location is used, i.e. a line from the actual point, perpendicular to the centreline, see figure 3.4. The riders progression of the descent will be evaluated using this projected distance on the centreline. Rider A, B and C are shown in figure 3.4. Rider C has the the same progress on the descent as rider B, while rider A is much closer to rider B but has more progress.

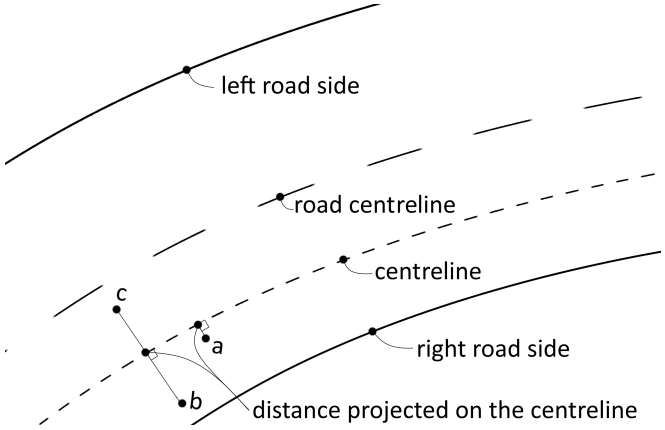

Figure 3.4: Distance projected on the centreline explained and three example riders

During tests of the Sensor-Set, it appeared that the data had a high frequency noise. This was expected beforehand and can be easily filtered out. This noise is contributed to imperfections in road surface, rider movement and other external disturbances. Acceleration, gyro, magnetometer, brake force and steering angle data is therefore filtered using a butter-worth filter set at 5 Hz cut of frequency.

The raw measurement data is filtered and synchronised with a Matlab script[1]. The GPS is synchronised with the other sensors. Acceleration, gyro, magnetometer, brake force and steering angle data is therefore filtered using a Butterworth filter set at 5 Hz cut of frequency. Movements faster than 5 Hz are not likely to be human input [20] and therefore neglected.

As experienced during the calibration, the brake sensor zero offset voltage is drifting during the experiments. This drift will have to be removed from the brake data. Removing the zero offset drift is done by translating the brake sensor data to match zero at the start and stop of every trial. The riders are not braking at the start and stop of the trial so the zero offset should be 0 there.

Now that the sensor drift is removed from the brake force data, a method to compare brake data between riders is needed. Each rider has a different mass and will thus require different braking forces to slow down an equal amount. That is why brake force is converted into acceleration using Newtons second law of motion $F = m * a$.
To normalise acceleration data between riders, the combined mass of rider and equipment is needed. Total mass is recorded minutes before the start of the experiment using a high quality person scale on a level surface. Quality of this data cannot be validated but is likely to be correct. In case a calibration off-set is present, this offset is present for each rider.

[1] credit is due to Marco Reijne for making the Matlab script

After dividing brake force by rider + equipment mass, the rider's mass differences are removed from the brake force. The resulting 'normalised' brake force data (acceleration) allows for multiple different comparisons:

- The accelerometer data can be compared to the brake sensor for brake sensor validation;
- The measured brake forces can be compared to values found in literature;
- What different riders do during the chosen descent.

4

Results

The results of the exploration study are presented in this Chapter. During the experiments and data processing some issues appeared, making data not suitable for drawing conclusions. These exceptions and exclusions are presented in Section 4.1.
The brake sensor developed was evaluated in a static setting. An additional validation of the brake sensor under actual conditions was done during the experiment and reported in Section 4.2. Results over the entire descent are presented in Section 4.3.
In sections 4.4 and 4.5, the cornering and braking techniques are analysed in depth.
All correlation factors calculated in this chapter are summarised for convenience in Appendix A.

4.1. Data Collection During Experiment

The trials are performed during a normal day with other traffic present. In some occasions the riders caught up traffic going at lower speed than themselves. This is denoted with a striked out result in the tables. These trials are excluded from further assessment and calculations. Rider remarks (Appendix J) and brake data (Appendix G.1) are used to determine when to strike out a result.

No brake data could be collected for rider 7 because the brake sensor did not fit on his bicycle. The Giant Propel from rider 7 is one of the very few road bicycles not using the standard sized brake pads. The Giant Propel has brake pads with the mounting bolt not in the center of the brake pad. The brake pad is positioned differently for aerodynamic reasons. With the brake sensor having the mounting bolt centred it was not clearing the bicycle frame and could thus not be fitted.

Figure 4.1: Picture of a Giant Propel rear brake. [13]

For rider 8 the recorded GPS data is of low quality. With the GPS data being used to determine position

it is difficult to calculate travelled distance projected on the road centreline. For trial 4 and 6 calculating the distance projected on the centreline was not feasible. Trial 4 and 6 are thus excluded from the results.

The GPS receiver did not perform as expected. For all trials, the GPS signal was lost for several seconds for varying locations due to occlusions of trees close to the side of the road. Therefore the position of the rider is unknown for several seconds. An example of the GPS position data collected for one trial is shown in figure 4.2.

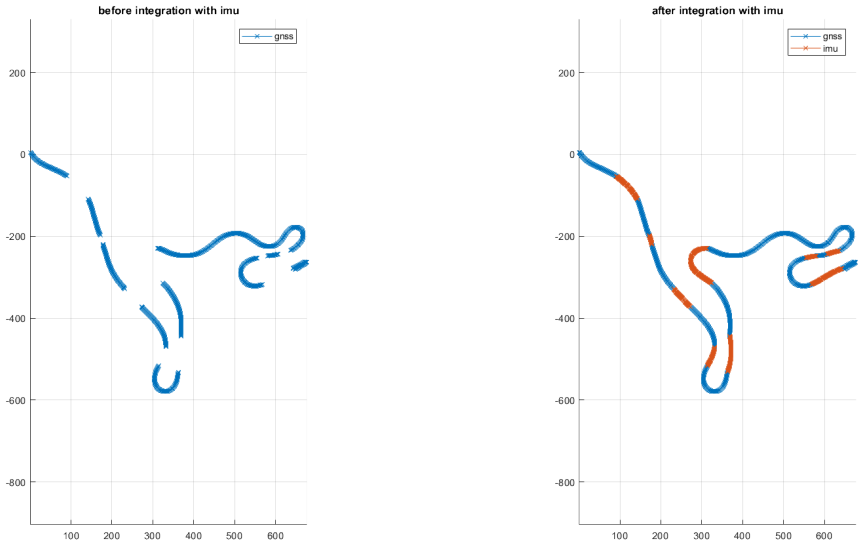

Figure 4.2: Example of a trajectory showing typical loss of position data (rider 1 trial 2). Shown left is the data recorded by GPS. Shown right is the GPS data and estimation (red).

The gaps in position data could be filled with an estimation of integrated IMU data, but results of this integration were assessed to be unreliable [20]. For the turns, there is only complete position data for every trial for segment 6. Therefore, only segment 6 can be evaluated on cornering and braking technique.

The speed and power data are recorded using the Ant+ speed sensor and power meter. These speed sensors and power meters are standard installed on the bicycles from Team Sunweb. The Sensor-Set is equipped with an Ant+ receiver to record the speed and power data. Speed data was planned to be used for verification of speed data derived from the GPS coordinates. The power data was planned be used to determine the moments riders generate power by pedalling and distinguish different descending techniques.
However, due to power meters entering sleep modes between the trials and the Sensor-Set not reconnecting automatically, the data is only partly recorded by the Sensor-Set.
For speed data, it was found that the wheel magnets triggering the speed sensor were missing and/or batteries were empty, again resulting in partly measured data.
The fact that Ant+ data is partially missing is not a large setback. With this data being send at a 1 *sec* interval, this is a too low interval for analysis, e.g. segment 6 only takes 10 *sec* to complete, resulting in 10 samples. In addition, speed data can also be derived from GPS and/or accelerometer.

After the experiments, speed and power data has been retrieved from the bicycles Head-Units (bicycle computers) used by Team Sunweb. The power data is analysed in Appendix M in order to determine the moments riders are pedalling to provide power. Due to limited data available and its accuracy, it is difficult to determine the moment where pedalling is started.
Another method to get information about pedalling behaviour is to analyse the high amplitude accelerations in each direction of the bike coordinate system. This shows the bicycle moving from pedalling loads and may be used to determine pedalling onset.
The accelerometer data included in Appendix H is assessed for such an analysis. Zooming in on segment 6, a feasibility check showed it would be hard to determine the exact location where riders start applying power in a quantitative way. However an estimation of the pedalling onset distance can made qualitative. This is

done by visually determining start of the high frequency and high peaks in Appendix H . Lines are drawn in the data sets to determine distance on the track. Shown in figure 4.3 is an example of such an analysis. The results of this analysis can be found in Section 4.5.4.

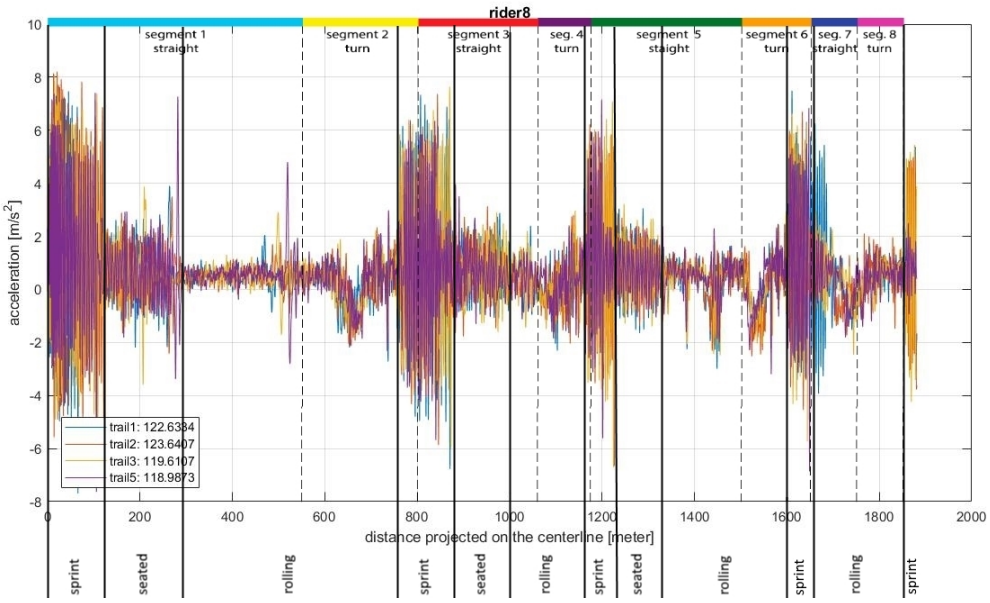

Figure 4.3: Acceleration data of rider 8 in forward direction. Including the sections where rider 8 sprint, pedals seated and is rolling.

The performance of the brake sensor during the experiment, as well as the data collected by the brake sensor during the experiment is discussed in Section 4.2.

4.2. Brake Sensor Validation

The brake sensor is validated under static laboratory conditions, see Appendix E. The accelerometer and GPS data is used to validate the brake sensor under actual experimental conditions.

The brake force is already normalised to m/s^2, allowing direct comparison to the accelerometer data. GPS data comparison requires the GPS speed (m/s) to be differentiated to m/s^2.

The GPS speed derivative is calculated using the $diff()$ function of the Matlab programming environment. The result is acceleration data with a low amount of detail (the GPS samples at 10 hz), but sufficient for the intended comparison.

The acceleration data is already transformed in the bike frame coordinates [1] and shows indications suggesting calibration and rotation errors (see Appendix L).
As accelerometers are known to be very reliable and accurate, it is likely that the transformation of the data requires improvement.
The raw acceleration data is transformed into bike frame coordinates using the following steps:

1. Calibrated according to the sensor data-sheet;
2. Filtered using a Butterworth 5 Hz cut off frequency;
3. Rotated into the bicycle frame coordinate system by assuming a level bicycle moving at steady state for a selected part of the descent.

[1] x being forward, y to the left and z upward relative to the bicycle frame

To improve data quality, an improvement is made to step 1 and 3.
For step 1 (accelerometer calibration), the accelerometer is calibrated inside the Sensor-Set housing coordinates system.
This calibration is done using 6 known orientations relative to the earth gravitational field and results in higher accuracy calibration parameters. After calibrating, the data has to be rotated (step 3).
Rotation is done around the y-axis that is pointing sideways as shown in figure 4.4. The amount of rotation required to translate from the Sensor-Set to bicycle coordinates, proofed to be depending on the bicycle frame size used by the rider. As the Sensor-Set is mounted on the bicycle down-tube this seems to be a logic consequence of the sensor position. The amount of rotation required is optimised for forward acceleration. Optimising is done by minimising the difference between the acceleration measured and gravity forces exerted for a straight segment of the descent, assuming speed is most constant on such a section (i.e. acceleration is zero). Included in appendix K is the calibration and rotation process with the resulting data.

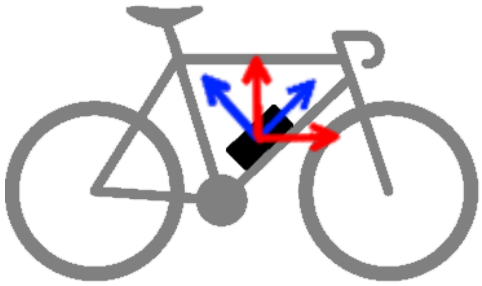

Figure 4.4: Schematic drawing of the chosen Sensor-Set and bike frame axis orientations.

The acceleration data is now calibrated and rotated with a higher accuracy, but gravity is still affecting the data. Included in Appendix E is the removal of gravity from the accelerometer data as well as the resulting plots containing the three different sensor data sets plotted into one graph.

Figure 4.5 and 4.6 show two example comparisons of the accelerations measured by the accelerometer, GPS and brake sensor.Figure 4.5 shows a good match of the decelerations during braking and figure 4.6 shows discrepancies between accelerometer and brake sensor data. In the data from rider 5 (figure 4.5), the for gravity corrected forward acceleration matches with the normalised brake force as well as the derivative of the speed data. In the data from rider 2 (figure 4.6), this match is only found for the pattern but not in the amplitude. Examining the data from every rider (included in appendix E) the same result is found. There is a visual match between normalised brake force and the other accelerations for riders 5, 6, 8 in magnitude and pattern observed. For riders 1, 2, 3 and 4 there is only a match in pattern and not in signal amplitude. This indicates that the brake sensor calibration is not correct for each rider.

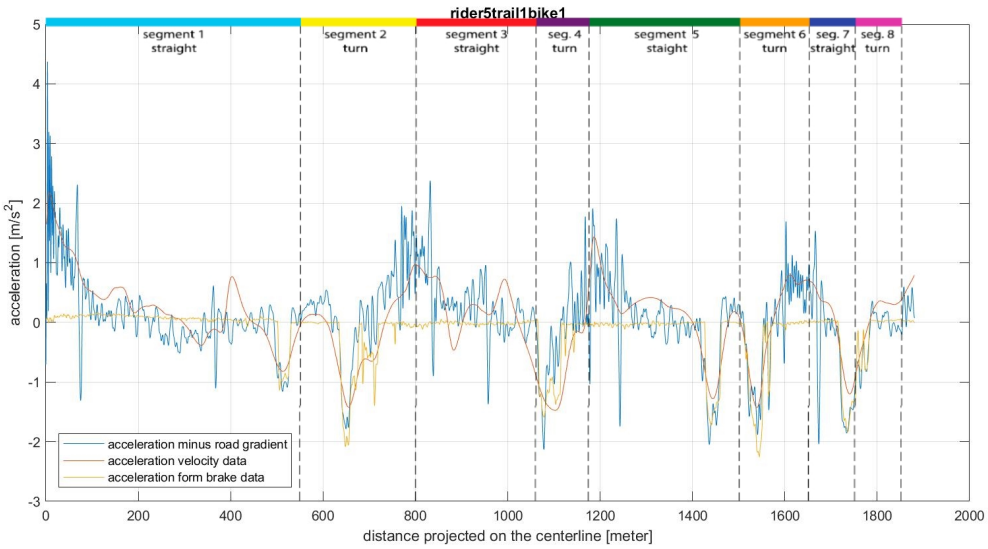

Figure 4.5: Normalised brake sensor data, derivative of the GPS speed data, forward bike frame acceleration filtered using a butter-worth filter with a 1.5 Hz cut of frequency that has gravity force from road incline removed. A good match between the three different methods to derive acceleration data is observed.

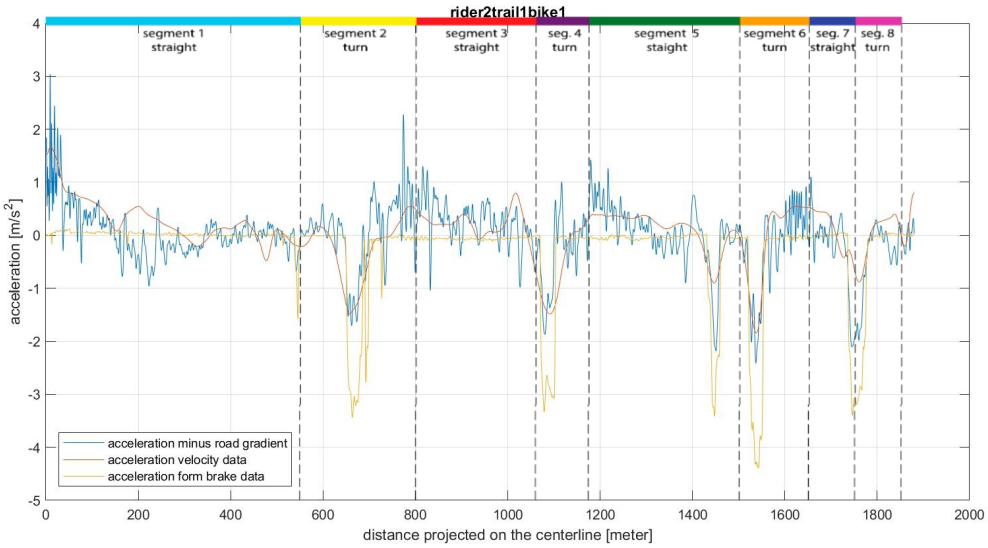

Figure 4.6: Normalised brake sensor data, derivative of the GPS speed data, forward bike frame acceleration filtered using a butter-worth filter with a 1.5 Hz cut of frequency that has gravity force from road incline removed. It can be observed that the brake sensor is more sensitive. A good match between GPS and accelerometer derived acceleration is observed. The normalised brake data, shows a higher amplitude. Despite the higher amplitudes, the patterns are matching.

The correct calibration of the brake force sensors cannot be linked to the use of Sensor-Set One or Two. For both Sensor-Set One and Two, there are riders where normalised brake force matches with the other accelerations and where it does not, see table 4.1.
During the experiment, it appeared two different types of Shimano brakes where used. The standard brake calliper used during the calibration in Section F.2 and a new unreleased prototype version from Shimano. Brake calliper configuration has been mapped using photos and videos taken during the experiment and is presented in table 4.1 as well. As can be seen from this table, all riders having brake force calibration errors are using the new prototype sensor.

In Appendix D, the effect of the prototype brake calliper on the brake sensor is explained in detail, as well as a solution to the observed mounting sensitivity.

	brake	calibration	sensor-set
rider 1	prototype	-	2
rider 2	prototype	-	1
rider 3	prototype	-	1
rider 4	prototype	-	1
rider 5	standard	+	1
rider 6	standard	+	2
rider 8	standard	+	2

Table 4.1: Type of brake used and quality of the brake sensor calibration during the descent

Re-calibration of the brake sensor for the prototype brake calliper would be the solution for obtaining correct data. However, the incorrect calibration was only revealed after assessment of the data. The bicycle with the prototype brake callipers was not available anymore, making re-calibration not possible.

In order to still obtain information on the braking behaviour from riders 1, 2, 3 and 4 the accelerometer data is used. The accelerometer data does not represent pure brake force, as discussed in Section 2.1. However, it is shown in figure 4.5 that when braking, the sum of these other forces is small in relation to the brake force, as both graphs show the same values. This allows the accelerometer data to be used as an estimate for the brake force.

4.3. Descending

In this section the most relevant results for the complete descent are reported. A complete set of plots, containing all the brake data is included in Appendix G.1.

Total time recorded for the 1.85 km descent for each rider is presented in table 4.2. The total time is used as the performance indicator: a shorter time is a better performance. The fastest trial for each rider is printed in **bold**. Average and standard deviation are calculated to examine the consistency of the concerned rider's performance. From table 4.2 it is observed that riders with a faster average time have a lower standard deviation. Calculating the correlation coefficient between average and standard deviation to verify the observation, an correlation coefficient of 0.7434 is found. This very strong correlation means that a shorter overall time is correlated to a lower standard deviation. This indicates that the faster riders show higher consistency in their performance.

	rider 1 *sec*	rider 2 *sec*	rider 3 *sec*	rider 4 *sec*	rider 5 *sec*	rider 6 *sec*	rider 8 *sec*
trial 1	117.01	122.90	117.46	122.33	117.88	~~128.15~~	122.63
trial 2	116.13	118.30	116.85	120.63	118.77	116.61	~~123.64~~
trial 3	116.38	118.17	**116.19**	119.14	~~118.39~~	116.16	**119.61**
trial 4	115.98	116.26	117.16	~~116.57~~	117.62	**114.91**	
trial 5	**115.73**	~~116.56~~	117.99	118.27	~~116.60~~	115.12	118.98
trial 6	116.89	**116.10**	119.37	**115.31**	**115.04**	~~116.20~~	
average	116.35	118.35	117.50	119.13	117.33	115.70	120.41
SD	0.50	2.74	1.09	2.63	1.60	0.81	1.95

Table 4.2: Table containing times from start to finish, the fastest time of each rider is in printed in **bold**. trials with a ~~strike out~~ are excluded from average and standard deviation calculations. For most of the striked out trials riders are caught behind slower traffic. Trial 4 of rider 4 is excluded because of an outlier in the exit speed of segment 6 see table 4.9. To illustrate differences between riders, the standard deviation over all valid trials is calculated (SD = 2,12 *sec*)

Taking the best performance of each rider by selecting their fastest trials from table 4.2 gives no informa-

tion on how time is gained or lost by the various riders. It is clear that rider 6 was the fastest and rider 8 the slowest. In order to find the locations where time is gained or lost relative to rider 6, figure 4.7 is made.
A downwards sloping line means time is lost to rider 6. An upwards sloping line means time is gained on rider 6. The highest located line is the fastest rider until that point. The strong peak over segment 1 by all riders compared to rider 6, is contributed to a dip in the GPS data for rider 6 during his fastest descent, see Appendix I.1, figure I.7 and is therefore not considered relevant.

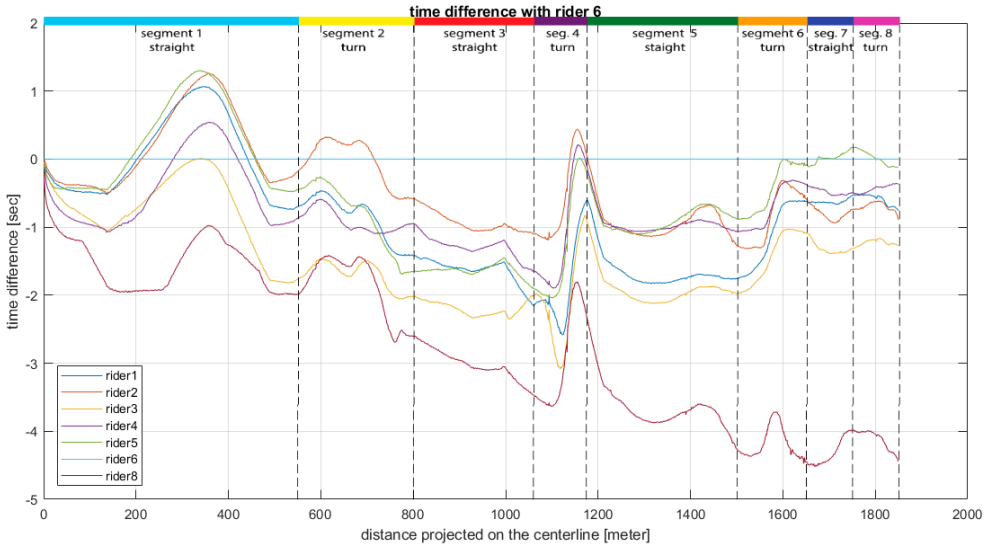

Figure 4.7: Time differences between each riders fastest trials relative to rider 6 who has the fastest time of all.

As shown in figure 4.7, the difference made by the fastest rider is made during segments 1, 2 and 3. All these segments are relatively straight with relative long pedalling actions.
Segments 4 and 6 are relative sharp corners, where all riders, except rider 8, gain time on rider 6. Over segment 5, the differences remains approximately the same. In this segment approximately 50% of the segment is pedalled and 50% cornered.

Because the power data is not completely recorded, it is not possible to compare the differences in power production between riders. This means, descending cannot be assessed on power generation and energy consumption.

Figure 4.7 shows that time differences between riders are constantly changing. This implies that the best overall performance does not originate from being the best performer on all segments. The time differences change most rapidly during the turns, showing the importance of cornering and braking techniques
The results also suggest learning behaviour see Appendix C

Due to the use of a brake force sensor, brake rub is observed in the data see Appendix B.

4.4. Cornering

For the in depth analysis segment 6 is selected as the segment has complete data sets for most riders. Segment 6 is the sharpest right handed turn on the entire descent, the corner is close to the previous corner, has unobstructed view through the corner, an average gradient of -6.95 %, good tarmac, smooth curvature and a clearly visible centreline. It is therefore the best segment for in-depth analysis. Shown in figure 4.8 is a still from the on-board camera footage at the start of segment 6. Segment 6 is not covered by trees, so almost every trial had proper GPS satellite connection to give quality data.

Figure 4.8: A still image from the on-board camera, at the start of segment 6 showing the turn and its characteristics

The time required for segment 6 for each rider is presented in table 4.3. The trial with fastest time over segment 6 is printed in **bold** for each rider. To highlight the best performance of each rider throughout this section, the best trial for each rider is printed in **bold** in every table.
Rider 6 has the fastest overall time of 114.91 *sec* as presented in table 4.2. This time is recorded during trial 4. However comparing the data presented in table 4.3, the fastest time over segment 6, 10.14 *sec*, is recorded by rider 1, trial 4 (10.14 *sec*). Further, it is noticed, that rider 6 during his fastest descent, recorded his slowest time (11.34 *sec*) over segment 6.

	rider 1 *sec*	rider 2 *sec*	rider 3 *sec*	rider 4 *sec*	rider 5 *sec*	rider 6 *sec*	rider 8 *sec*
trial 1	10.52	11.21	10.54	11.14	11.32	~~16.93~~	**11.22**
trial 2	10.46	10.71	10.52	11.44	10.93	11.31	~~12.53~~
trial 3	10.39	10.78	10.45	10.90	10.69	11.25	11.53
trial 4	**10.14**	**10.33**	10.38	~~10.65~~	10.77	11.34	
trial 5	10.21	10.82	**10.30**	10.68	10.98	11.12	11.55
trial 6	10.34	10.65	10.54	**10.66**	**10.56**	**11.02**	
average	10.34	10.75	10.46	10.91	10.87	11.21	11.43
SD	0.14	0.28	0.09	0.32	0.26	0.13	0.18

Table 4.3: Time trough segment 6 for each rider. Highlighted in **bold** is the fastest trial of each rider. To illustrate differences between riders, the standard deviation over all valid trials is calculated (SD = 0.39 *sec*)

A weak correlation of 0.4561 between total descent time and time through segment 6 is found. This implies that for this descent, time through the corner in segment 6 (cornering skills) is not decisive for final time. The speed/power output on the straight sections may be more important. Giving that the recording of the power meter data is not accurate during the experiment (Appendix M), it is difficult to judge if power production has a stronger correlation to overall performance than the cornering skills.
However, as reported in Section 4.3 and shown in figure 4.7, it is observed that rider 6 gains immediate advantage to the other riders during the first straight segment. This advantage is maintained throughout the rest of the descent. Indicating, that for this descent, the power developed during acceleration is a more determining factor than cornering skills.

The time difference between the best and worst performing rider for segment 6 is presented in table 4.3 and is more than a second (1.09 *sec*). In World Tour level cycling improving the worst performing rider by a whole second through corner training is still a significant gain to make.
The fastest rider overall (rider 6, table 4.2) has a relative weak performance in segment 6 (second to last). In case rider 6 would adapt the same strategy as rider 1 over segment 6, another full second may be won over the total descent.

To understand how consistency affects performance for segment 6, the average and standard deviation are calculated. Checking the correlation between the average and standard deviation, a correlation coefficient 0.2013 is found. This correlation coefficient implies that a more consistent performance is weakly correlated to a better performance for segment 6.

Shown in figure 4.9 is the time differences between each riders fastest trial over segment 6 relative to rider 1, similar as shown for the overall descent in Section 4.3, figure 4.7.
This plot can be used to see where in segment 6 the time differences between riders are made. A downwards sloping line means time is lost relative to rider 1 and an upwards slope means time is gained on rider 1. Figure 4.9 shows that, rider 1 gains time on each rider from the onset of segment 6 until approximately 1560 meter. At the 1560 meter mark, rider 2 and 8 are gaining time on rider 1. Rider 8 gains back so much time from 1560 till 1590 meter, that he reaches the 1590 meter mark in the same time as rider 1. From about 1590 meter onward most riders have approximately a constant time difference with rider 1. Again rider 2 and 8 are different from the other riders, as they lose time after the 1590 meter mark.

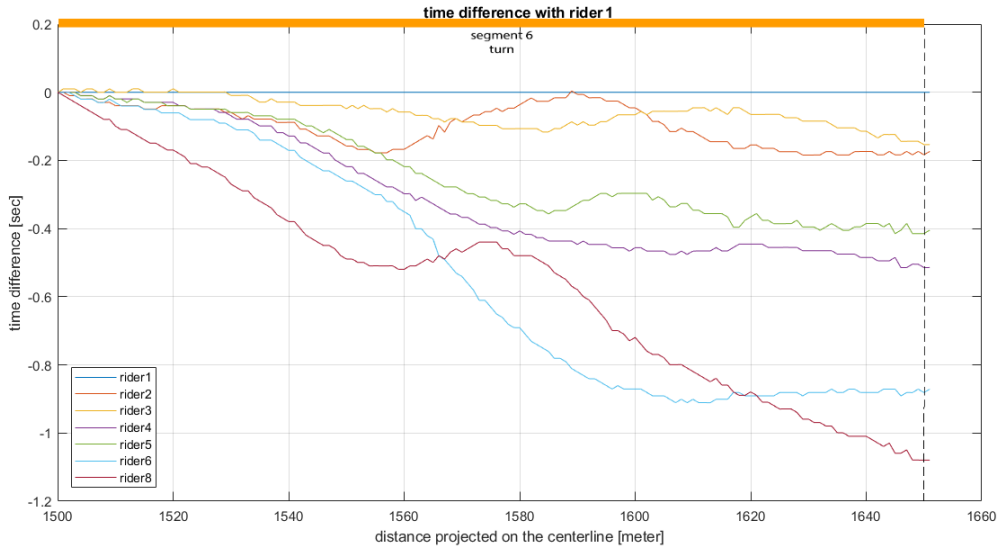

Figure 4.9: Time differences between riders fastest trial over segment 6 relative to rider 1 who has the fastest time of all

4.5. Braking

Knowing the performances of each rider, it is possible to examine which parts of the braking behaviour are indicators for a good overall performance. The focus will be on the braking behaviour of the riders and the speed at different locations since braking is done to control speed. The braking points (start and stop), the maximum braking force and the speed at the start and stop of braking are presented in the first three sections. The last two sections present the brake forces and their timing and the impact of braking on acceleration after the corner

4.5.1. Braking Points

Presented in table 4.4 is the point when braking is started in segment 6 for each trial. The given values are in meters of distance projected on the centreline from the onset of segment 6. For the correlation coefficient between time and the point where braking is started, a very strong negative correlation of -0.7303 is found. This implies that a faster time through segment 6 is very strongly correlated with a larger distance from the start of segment 6 until the braking point. Rider 3 has the latest braking point, during trial 2 he braked 34.3 meters after entering segment 6. The earliest braking is done in trial 1 of rider 4 and trial 5 of rider 8, they brake more than 30 meter earlier at 4.1 meters from the start of segment 6.

	rider 1 *m*	rider 2 *m*	rider 3 *m*	rider 4 *m*	rider 5 *m*	rider 6 *m*	rider 8 *m*
trial 1	33.7	19.7	27.3	4.1	12.5	~~2.6~~	**11.3**
trial 2	27.2	21.1	34.3	13.3	15.3	13.6	~~13.2~~
trial 3	25.4	20.9	31.7	10.0	21.4	15.3	13.8
trial 4	**24.8**	**17.4**	33.5	~~15.3~~	16.9	12.8	
trial 5	27.2	15.6	**29.3**	11.4	15.5	11.0	4.1
trial 6	27.6	21.4	34.0	**11.9**	**13.5**	**10.8**	
average	27.7	19.4	31.7	11.0	15.8	12.7	09.7
SD	3.2	2.3	2.8	3.8	3.1	1.9	5.0

Table 4.4: Points where braking is started measured from the start of segment 6 in meters. Highlighted in **bold** is the fastest trial of each rider. To illustrate differences between riders, the standard deviation over all valid trials is calculated (SD = 8.5 *m*)

The distance from start of segment 6 to the end of the braking action for each trial is presented in table 4.5. When calculating the correlation coefficient between the end of the braking actions and time through segment 6, a weak negative correlation of -0.3506 between time and stop braking point is found. Meaning that ending a braking action later is weakly correlated to shorter time for segment 6.

	rider 1 *m*	rider 2 *m*	rider 3 *m*	rider 4 *m*	rider 5 *m*	rider 6 *m*	rider 8 *m*
trial 1	80.9	55.2	74.2	53.2	71.7	~~66.1~~	**63.3**
trial 2	98.1	55.3	81.9	58.4	79.8	90.5	~~97.5~~
trial 3	96.6	58.9	77.3	53.9	77.4	59.8	62.3
trial 4	**92.2**	**52.8**	73.5	~~59.4~~	70.0	80.1	
trial 5	84.0	53.8	**77.0**	61.4	70.1	76.2	66.7
trial 6	82.3	54.6	76.5	**51.4**	**60.8**	**65.3**	
average	89,0	55,1	76,7	56,3	71,6	74,4	64,1
SD	7,6	2,1	3,0	4,0	6,7	12,1	2,3

Table 4.5: Points where braking is stopped measured from the start of segment 6 in meters. Highlighted in **bold** is the fastest trial of each rider. To illustrate differences between riders, the standard deviation over all valid trials is calculated (SD = 13.1 *m*)

Two brake point locations are identified: start braking and stop braking. The correlations between the different braking actions with the time through segment 6 are calculated. Very strong and weak correlations are found. The start of braking (-0.7303) has a very strong correlation and stop of braking (-0.3506) has a weak correlation.
These correlations indicate that braking later (start, stop) is beneficial for performance. This is as expected, but it seems counter intuitive that the location where braking is started has the highest correlation with performance.

For all of the in this report defined parameters, the point where braking is started has the highest correlation with segment 6 performance. With the distance from the start of segment 6 till the start of braking being such a good performance indicator, it should be one of the first focus points when developing a method to improve rider performance. Training riders to brake later may result in improved performance during cornering.

An interesting question to answer is, do the different riders have a different method for braking. The consistency in brake points for each rider over the trials is assessed using the standard deviation. In case a rider always brakes at the same moment, the standard deviation for a particular rider is low compared to the standard deviation over all trials. If riders break at different locations in the trials, the individual standard deviation should be similar to the overall standard deviation.
Table 4.4 shows that the standard deviation over the average brake point for all riders is relatively high (8.5 m) with respect to the maximum standard deviation for a specific rider (5.0 m). This implies, the brake point differs per rider, indicating that different strategies are used.

4.5.2. Braking in order to Control Speed

Braking is done to control speed. Therefore, the speed at the locations of start (table 4.4) and stop (table 4.5) of braking, are presented in table 4.6 and 4.7. The speed is given in m/s and is taken from the GPS data.

The correlation between the speed where braking is started and time over segment 6 is calculated. A correlation coefficient of -0.1771 is found between speed at the start of the braking action and time, meaning that no correlation is found.

	rider 1 m/s	rider 2 m/s	rider 3 m/s	rider 4 m/s	rider 5 m/s	rider 6 m/s	rider 8 m/s
trial 1	15.57	15.22	16.03	15.68	15.46	~~10.76~~	**14.94**
trial 2	15.54	16.08	15.74	15.78	15.62	16.34	~~15.83~~
trial 3	15.75	15.80	15.87	15.41	15.98	16.18	15.54
trial 4	**16.42**	**16.43**	15.64	~~15.88~~	15.55	16.12	
trial 5	16.22	16.54	**15.86**	15.99	16.32	16.21	16.34
trial 6	16.06	15.52	15.81	**16.33**	**16.51**	**16.05**	
average	15.93	15.93	15.82	15.84	15.91	16.18	15.6111
SD	0.36	0.51	0.13	0.30	0.43	0.10	0.6992

Table 4.6: Speed at start braking in m/s. Highlighted in **bold** is the fastest trial of each rider. To illustrate differences between riders, the standard deviation over all valid trials is calculated (SD = 0.38 m/s)

When calculating the correlation between the speed at the end of braking and time through segment 6, a correlation coefficient of -0.0946 is found. There is no correlation between time through segment 6 and speed at the end of braking.

	rider 1 m/s	rider 2 m/s	rider 3 m/s	rider 4 m/s	rider 5 m/s	rider 6 m/s	rider 8 m/s
trial 1	12.42	11.43	12.39	11.56	11.77	~~7.73~~	**12.39**
trial 2	12.77	12.15	12.76	13.27	12.32	12.13	~~11.06~~
trial 3	12.73	12.17	12.61	12.84	12.37	13.56	12.82
trial 4	**13.32**	**12.37**	12.86	~~13.56~~	11.88	12.37	
trial 5	12.81	12.03	**12.82**	13.04	11.73	12.70	13.71
trial 6	12.81	11.79	12.68	**12.97**	**12.40**	**12.66**	
average	12.81	11.99	12.69	12.87	12.08	12.68	12.97
SD	0.28	0.33	0.17	0.69	0.31	0.54	0.67

Table 4.7: Speed at stop braking in m/s. Highlighted in **bold** is the fastest trial of each rider. To illustrate differences between riders, the standard deviation over all valid trials is calculated (SD = 0.52 m/s)

In order to understand how the speed changes over segment 6, the speeds at the beginning and the end of segment 6 are compared. These speeds may show if riders slow down before braking due to wind resistance or gain speeds due to road decline.
Presented in table 4.8 is the speed when riders enter segment 6. When calculating the correlation between time over segment 6 and entry speed, a strong negative correlation of -0.6491 is found. The negative correlation means that a higher entry speed is strongly correlated to a shorter time over segment 6.

	rider 1 m/s	rider 2 m/s	rider 3 m/s	rider 4 m/s	rider 5 m/s	rider 6 m/s	rider 8 m/s
trial 1	16.73	15.65	17.24	15.74	15.51	~~10.83~~	**15.09**
trial 2	16.21	16.58	17.20	15.91	15.73	16.61	~~15.98~~
trial 3	16.39	16.37	17.37	15.31	16.21	16.50	15.71
trial 4	**17.20**	**17.04**	17.32	~~16.09~~	15.85	16.41	
trial 5	17.05	17.08	**17.10**	16.32	16.66	16.38	16.45
trial 6	16.94	16.27	17.32	**16.57**	**16.76**	**16.15**	
average	16.75	16.50	17.26	15.99	16.12	16.41	15.75
SD	0.38	0.53	0.09	0.44	0.51	0.17	0.68

Table 4.8: Speed at start segment 6 in m/s. Highlighted in **bold** is the fastest trial of each rider. To illustrate differences between riders, the standard deviation over all valid trials is calculated (SD = 0.60 m/s)

Comparing segment 6 entry speed with table 4.6, speed at braking onset, it can be observed that for almost every trial segment 6 entry speed is higher than speed at brake onset. Trial 3 from rider 4 is the only trial showing a gain in speed during segment 6 before braking is started.

Presented in table 4.9 is the speeds at the end (exit speed) of segment 6 for each rider. The correlation coefficient between segment 6 exit speed and time over segment 6 is -0.2525, meaning shorter time over segment 6 is weakly correlated to higher exit speed.

	rider 1 m/s	rider 2 m/s	rider 3 m/s	rider 4 m/s	rider 5 m/s	rider 6 m/s	rider 8 m/s
trial 1	15.26	14.34	14.13	14.44	15.07	~~11.62~~	**14.72**
trial 2	13.51	14.89	15.44	16.35	14.85	14.80	~~12.00~~
trial 3	15.02	14.72	14.37	13.74	15.36	15.77	16.30
trial 4	**15.51**	**15.66**	14.83	~~10.62~~	15.92	15.23	
trial 5	15.34	14.43	**14.36**	13.96	15.31	14.80	16.44
trial 6	15.30	14.88	14.40	**14.66**	**16.66**	**15.38**	
average	14.99	14.82	14.59	13.96	15.53	15.20	15.82
SD	0.74	0.47	0.47	1.87	0.66	0.40	0.95

Table 4.9: Speed at stop segment 6 in m/s. Highlighted in **bold** is the fastest trial of each rider. To illustrate differences between riders, the standard deviation over all valid trials is calculated (SD = 0.73 m/s)

Comparing speed at end of segment 6 to table 4.7, speed after braking it can be observed that speed is gained after braking during every trial.

When examining the accelerometer data in Appendix H it can be observed the riders did not produce power between the previous corner and the start of segment 6. The speed before segment 6 can thus not be increased by a larger power output and may be determined solely by the exit speed from the previous corner. Assuming that the higher exit speed from the previous corner is a result of better cornering skills, it can be expected that speed through segment 6 (also a corner) is also higher. This is supported by the strong correlation between entry speed of segment 6 and the time through segment 6.

A weak correlation of -0.2525 for time and speed at the end of segment 6 is found. This is lower than expected, as faster through segment 6 was expected to be linked strongly to speed at the end of segment 6. Form the accelerometer data, it can observed that riders already apply power before the end of segment 6. This explains the low correlation found. As speed is not only depending on cornering skills but now also on the amount of power each rider does produce. This is a key difference with the entry speed correlation, as no power is produced between segment 5 and 6. This implies that cornering skills determining entry speed of segment 6 and performance over segment 6.
That the riders apply power during segment 6 can be seen in Section 4.1. With each rider starting to pedal at a different location and with a different applied power, this pedalling may be the reason for the low correlation between speed at end of segment 6 and time through segment 6.

For the speed at the start and stop of the braking actions, no correlation is found with time through segment 6 (start -0.1771 and stop -0.0946).
This is somewhat surprising as a higher speed at the stop of braking was expected to result in better performance through segment 6. A possible explanation is found in the way riders differ in speed.
The way riders differ in the speed when starting or stopping their braking action is presented in table 4.6 and 4.7. The similarity of the average speed's calculated for each rider is what stands out. This is confirmed by calculating the standard deviations 0.17 m/s for the start and 0.37 m/s for the stop.

4.5.3. Brake Forces

It is interesting to look at how different riders slow down to the speed at which they enter the corner of segment 6. Throughout this and further sections, the normalised brake force is referred to as brake force. Similar, the for gravity corrected forward acceleration is referred to as acceleration.
The brake force measured during the fastest trial of each rider is shown in figure 4.10. For the dotted lines, brake force is estimated using the acceleration data, using a Butterworth filter with 0.75 hz cut of frequency.
The complete set of brake data from each rider is included in appendix G.2. Figure 4.10 shows that some riders brake once (one brake pulse) while other riders brake twice (two braking pulses).
However, identifying what is important for a best performance form this single plot is difficult. Therefore, parameters identifying the characteristics of the brake force curve are used. Location of peak brake force, peak brake force and average brake force are presented in table 4.10, 4.11 and 4.12.

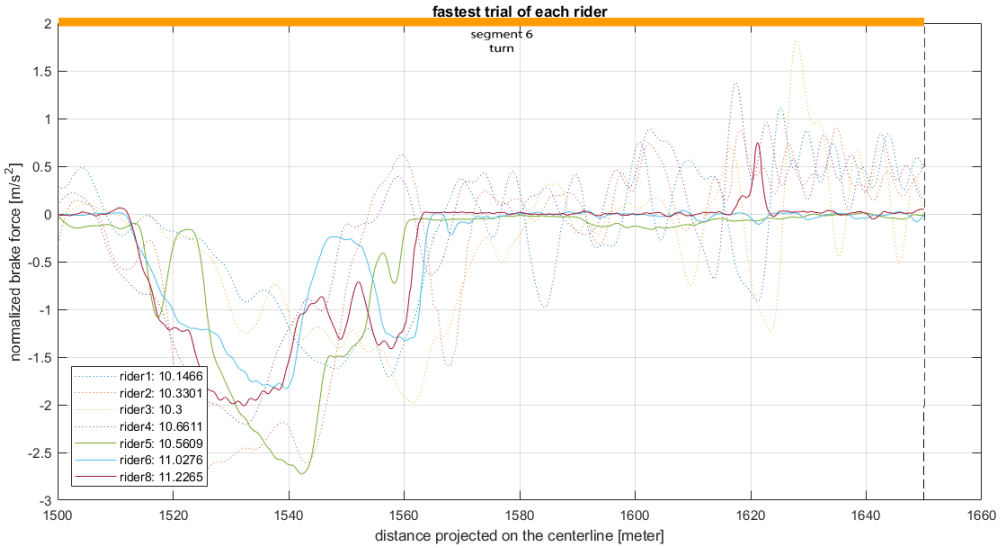

Figure 4.10: Normalised Brake Data of the fastest trial of each rider over segment 6

The peak brake force for each trial is presented in table 4.10. The highest brake force is recorded of -3.74 m/s^2 by rider 2 during trial 6.
The correlation coefficient between the peak brake force and the time through segment 6 is -0.0388. A higher peak brake force is thus not correlated to a shorter time over segment 6. Rider 1 who has the fastest average time through segment 6 has the lowest peak brake acceleration.

	rider 1 m/s^2	rider 2 m/s^2	rider 3 m/s^2	rider 4 m/s^2	rider 5 m/s^2	rider 6 m/s^2	rider 8 m/s^2
trial 1	-2.26	-2.41	-2.27	-1.84	-2.25	~~-2.01~~	**-2.01**
trial 2	-1.82	-2.62	-1.88	-2.24	-2.34	-1.81	~~-2.71~~
trial 3	-1.61	-2.51	-2.10	-2.06	-2.82	-1.42	-2.47
trial 4	**-1.70**	**-2.78**	-2.00	~~-1.95~~	-2.73	-1.89	
trial 5	-1.74	-3.09	**-1.97**	-2.24	-2.82	-1.97	-2.46
trial 6	-2.02	-3.74	-1.82	**-2.20**	**-2.72**	**-1.83**	
average	-1.86	-2.68	-2.01	-2.09	-2.61	-1.78	-2.31
SD	0.2385	0.4917	0.1611	0.1685	0.2513	0.2106	0.2655

Table 4.10: Peak brake acceleration in segment 6. For rider 1, 2, 3, 4 forward acceleration data from the accelerometer 1.5 hz cut-off is used. For rider 5, 6 and 8 brake sensor data is used. Highlighted in **bold** is the fastest trial of each rider. To illustrate differences between riders, the standard deviation over all valid trials is calculated (SD = 0.46 m/s^2)

The location at the peak brake force from table 4.10 is presented in table 4.11 in meters from the onset of segment 6. Rider 1 that has the fastest average time through segment 6 and the largest average distance to peak brake force from onset off segment 6. The correlation coefficient between peak brake force location and time through segment 6 is -0.5321. This implies, that having peak brake force later in segment 6, is strongly correlated to a shorter time over segment 6.

	rider 1 m	rider 2 m	rider 3 m	rider 4 m	rider 5 m	rider 6 m	rider 8 m
trial 1	56.9	37.4	58.6	38.0	45.2	~~18.6~~	**32.4**
trial 2	57.2	30.8	58.7	30.6	40.5	47.9	~~25.6~~
trial 3	48.3	29.2	45.7	19.6	41.6	49.6	31.5
trial 4	**57.6**	**24.5**	42.4	~~33.4~~	36.3	26.3	
trial 5	56.9	34.5	**61.6**	32.9	38.1	29.2	20.0
trial 6	48.6	29.0	43.9	**32.8**	**42.4**	**39.6**	
average	54.2	30.9	51.8	31.2	40.7	38.5	28.0
SD	4.5	4.5	8.7	6.2	3.2	10.6	6.9

Table 4.11: Point of peak brake force. For rider 1, 2, 3, 4 acceleration data from the accelerometer 1.5 hz cut-off is used. For rider 5, 6 and 8 brake sensor data is used. Highlighted in **bold** is the fastest trial of each rider. To illustrate differences between riders, the standard deviation over all valid trials is calculated (SD = 11.5 m)

The average brake force during braking is presented in table 4.12. The differences between average brake forces are large. Rider 1 and 6 have an average of -0.88 m/s^2 and rider 2 has an average of -1.76 m/s^2 that is twice the value of rider 1 and 6. Due to the large differences between riders, the correlation coefficient of average brake force and time through segment 6 is -0.0012. This non-meaningful correlation means there is no correlation found between average brake force and time through segment 6.

	rider 1 m/s^2	rider 2 m/s^2	rider 3 m/s^2	rider 4 m/s^2	rider 5 m/s^2	rider 6 m/s^2	rider 8 m/s^2
trial 1	-1.18	-1.45	-1.33	-1.20	-1.10	~~-0.74~~	**-1.25**
trial 2	-0.71	-1.74	-1.14	-1.07	-0.95	-0.73	~~-1.02~~
trial 3	-0.80	-1.55	-1.28	-1.32	-1.19	-1.14	-1.58
trial 4	**-0.69**	**-2.03**	-1.33	~~-0.91~~	-1.27	-0.82	
trial 5	-0.95	-2.07	**-1.17**	-1.08	-1.41	-0.76	-1.34
trial 6	-0.95	-1.73	-1.30	**-1.30**	**-1.38**	**-0.97**	
average	-0.88	-1.76	-1.26	-1.14	-1.22	-0.88	-1.39
SD	0.18	0.24	0.08	0.15	0.17	0.17	0.17

Table 4.12: Average normalised brake force in segment 6. For rider 1, 2, 3, 4 forward acceleration data from the accelerometer 1.5 hz cut-off is used. For rider 5, 6 and 8 brake sensor data is used. Highlighted in **bold** is the fastest trial of each rider. To illustrate differences between riders, the standard deviation over all valid trials is calculated (SD = 0.33 m/s)

When examining the distribution over time of the brake force, two values are of importance: average and maximum brake acceleration. These parameters have no correlation with time over segment 6, as maximum brake force correlated to time with -0.0388 and average brake force -0.0012.
This is an unexpected low correlation. It was expected before the experiment, that braking harder for a shorter duration would be the better and applied strategy. This strategy should result in a higher average brake force. Braking hard and late makes it possible to delay braking and to maintain entry speed for a longer period.
Some riders have a second brake action. It is obvious that the average break force is then lower, due to the used definition of braking points: the start and stop of a braking action is chosen as the first and last point where the brake fore is not zero in segment 6. This may be the explanation for the low correlation.

The distribution of braking force between front and rear brake is shown in Appendix O. Primarily, the front brake is used by all riders, except for rider 8. It is this rider that shows worst performance over the descent.
No further significant correlations for this study could be found.

4.5.4. Influence of Braking on Regaining Speed

In this section the influence of the braking on the location where the riders start to apply power and thus regain speed is investigated. For example investigation the possibility that if a rider has his last braking moment earlier in segment 6, his first pedalling moment is also earlier.

Examining the speed data included in Appendix I.2 it can be observed that riders gain speed (accelerate) immediately after braking is stopped. This acceleration is not from the rider applying power, as power application starts later (Appendix H). The acceleration is due to the road gradient and gravity, making riders accelerate. This acceleration could be the reason for the second brake pulse by some rider (see Section 4.5.3).

Rider 5, 6 and 8 start pedalling early (just before the 1600 meter mark), rider 2 and 4 start pedalling in the middle (around 1610 meters) and rider 1 and 3 start pedalling late (around 1620 meter). The location of braking and pedalling actions are shown in table 4.13.

	start brake			stop brake			start pedalling			average brake force		
	early	mid	late	early	mid	late	early	mid	late	low	mid	high
rider, time	m<15		m>25	m<65		m>75	~100	~110	~120	acc<1		acc>1.5
1, 10.34			X			X			X	X		
3, 10.46			X			X			X		X	
2, 10.75		X		X				X				X
5, 10.87		X			X		X				X	
4, 10.91	X			X				X			X	
6, 11.21	X				X		X			X		
8, 11.43	X			X			X				X	

Table 4.13: A table containing the location of braking and pedalling actions, sorted in three groups as early, mid and late.

A clear trend appears, this trend seems to indicate that starting pedalling later in segment 6 may be correlated with a better performance.
This is a surprising result, as pedalling increases the riders speed and pedalling for a longer period in segment 6 is expected to increase performance. Here the contrary is recorded. Thus there needs to be an explanation that pedalling later still allows for a better performance over segment 6.

For this analysis, the locations of start and stop braking are sorted in the same three groups (early, middle and late) and presented in table 4.13. For the location of braking onset, early is before 15 m, middle is before 25 m and late is after 25 m. For the location of end of braking, early is before 65 m, middle is before 75 m and late is after 75 m.
Apparently, the approximately 50 m that is pedalled in segment 6 is not sufficient in length to eliminate the advantage from late braking.

5

Discussion

The results of this exploitation study, as presented in chapter 4, are discussed in this chapter.
The importance of cornering performance is discussed in Section 5.1. For many sports this is considered crucial for fast times. The braking behaviour, being the actual main topic of this thesis, is discussed in Section 5.2. After discussing all individual aspects of braking behaviour, the last two sections discuss the breaking strategies applied (Section 5.3) and what the optimum brake strategy should be (Section 5.4).

5.1. Influence of Cornering on Descending

The elation of segment 6 with the overall performance is reported in 4.3. Analysis shows that the overall performance is not related to the performance over segment 6.

Do these results mean that cornering performance is of non-importance for road cycling? Maybe not as shown by the following discussion points:

- Despite not being decisive for overall performance, a potential performance gain of 1 sec over segment 6 is identified (see table 4.3). With a time of approximately 10 sec over segment 6, the potential gain of 10% is considered significant in the modern world of professional cycling;
- It is also reported that riders that have a higher entry speed at segment 6 (table 4.8) have a better performance over segment 6 (table 4.3), with correlation factor of 0.6491 (Section 4.4); Taking into account that segment 5 ends with a corner, it is likely that a better performance over segment 6 is linked to a better cornering performance in segment 5.
- In Section 4.3 it is shown that overall best performing rider 6 gains time over all other riders over the segments where is pedalled (segments 1, 2 and 3). For segments with large rolling parts (segment 7 and 8) and segment 5 (sprinting, rolling and cornering), the difference remains more or less constant.
  Over the cornering segments (segments 4 and 6), rider 6 loses time.

Summarising the results discussed above, cornering performance is important.

The results are only verified for the descent used during this study. Repeating the same experiment on multiple different types of descents is recommended. It is expected that a steeper, longer and more technical descent increases the correlation between corner and overall performance. Taking a steeper descent for example, the increased steepness will result in higher speeds and thus lowers the amount of time that pedalling is beneficial/possible, making the advantage gained by rider 6 less important.

5.2. Braking

The parameters affecting braking behaviour are ordered in three different groups: when, why and how riders brake.

- When is the location where the riders start, stop and have their maximum braking actions in segment 6. This is discussed in Section 5.2.1;
- Why braking is done by a cyclist in order to regulate speed before a technical section. Therefore, speed at key points in segment 6 will be discussed under braking behaviour as the second group in Section 5.2.2;
- How riders slow down during braking. This is done by examining the normalised brake force's (brake acceleration) recorded in segment 6 and discussing these in Section 5.2.3.

After this the location where riders start pedalling in order to regain speed is discussed. Mainly, if the timing of pedalling is dependant on the braking behaviour in Section 5.2.4.

5.2.1. Braking Points

Braking later (start, stop and peak) is beneficial for performance. This was expected, but it seems counter intuitive that the location where braking is started has the highest correlation with performance.
Before calculating the three correlation coefficients, it was expected that braking is done to slow down before a given point in segment 6 in order to obtain a "maximum" possible cornering speed. As a result of this assumption, it would be logical that the location where braking is stopped has the highest correlation. However, this is not the case for segment 6. The point of start braking is of more importance for performance.

The importance of the point when braking starts, may be explained by that braking later allows a rider to keep its entry speed for a longer period of time. Keeping this entry speed longer, results in a shorter time for the first part of segment 6. The total length of segment 6 is 150 meters and the average distance from segment start until braking for the fastest rider (rider 1) is 22.7 meters. Rider 1 can keep his entry speed for 18.4 % of the segment. In comparison, rider 8 brakes after 9.7 meter on average, which is only 6.4 % of the segment length. Speed data is included in Appendix I.2. There it can be seen that the highest speeds recorded in segment 6 are at the start of segment 6. These high speeds at the start of segment 6 may explain the importance of a late braking onset. The simplified example speed data shown in figure 5.1 shows the speed being higher at the start of segment 6 then at the exit and how this leads to improved performance when braking later.

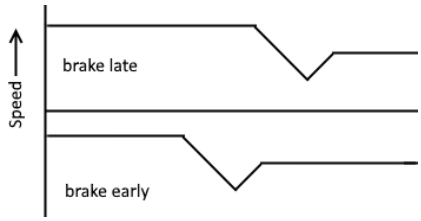

Figure 5.1: Drawing of speed through segment 6 in order to explain the strong correlation location of braking onset with performance in segment 6. On top are late braking point and at the bottom early braking points.

5.2.2. Braking in order to Control Speed

The various aspects of speed are discussed in this section.

A strong correlation of -0.6491 between speed at the start of segment 6 and the time through segment 6 is found. This could be originating from two different scenarios or a combination of them.
The first and most obvious possible origin for the strong correlation is that a higher entry speed lowers the time needed to reach the braking point. The further this brake point is, the faster the time over segment 6, especially as exit speed of segment 6 is considerably lower than the entry speed (see table 4.8 and table 4.9). Keeping speed as long as possible is then the optimum strategy.
The strong correlation may also be originating from the close proximity of a corner before the start of segment

6. Riders do not pedal in between these two corners (H.1 to H.7). It is to be expected that riders cornering better in segment 5 have a higher entry speed and are cornering better in segment 6 as well.

The best riders, continue to brake in the corner, see table 4.5. This seems counter intuitive, as generally, it is believed that braking is ideally stopped just before the corner. However, as riders gain speed when the brake action is stopped (see AppendixI.2), due to gravity, the best riders keep a constant high speed using their brakes. It is likely, this speed is close to what these riders feel to be the maximum cornering speed.

5.2.3. Brake Forces

Various aspects of braking are measured and reported in Section 4.4 and discussed below: peak brake force, average brake force and brake distribution. Peak and average brake forces are used to simplify the brake data included in Appendix G.2.

The measured peak brake forces are presented in table 4.10. These are the maximum braking forces applied by the riders in segment 6. The recorded brake forces are significant lower than those reported in literature. In literature the reported forces range from -0.38 *g* [1] to -0.6 *g* [19]. These values are very high compared to the maximum of -0.29 *g* recorded in this study (see table 4.10).
Two important remarks can be made on these observed differences. One, the literature studies mostly use normal bicycles. On racing bikes, the riders center of mass is positioned more towards the front of the bicycle, making hard braking more dangerous. It is demonstrated in the literature [1] that a more rearward position allows for much higher breaking forces. Secondly, in literature, peak brake force is only tested on a straight line in an isolated experiment. The current study is a real life descent which apparently does not require maximal breaking or does not allow for maximal breaking close to values reported in literature.

Below the hypothesis for the non-existing correlation between brake forces and performance are postulated and discussed:

1. Less strong braking (low brake acceleration) may allow for more precise braking, steering and speed regulation;
2. The use of different braking strategies, may very well have a different optimum for the brake forces, influencing the correlation as groups of data influence the calculation;
3. Braking harder results in a increased risk of losing traction and/or crashing.

Ad 1: No correlation between speed at end of breaking and time over segment 6 is found. This makes this hypothesis unlikely.

Ad 2: A rider can brake short and hard slowing down to a speed below fastest possible cornering speed and gaining speed again. In this scenario it is demonstrated (table 5.1) that late and harder braking is better in order to keep entry speed as long as possible.
Alternatively, a rider brakes with less force, but for a longer period, maintaining a speed more closely to the maximum cornering speed as shown in figure 5.3. Using this strategy, the average brake force becomes lower as the time interval increases;

Ad 3: The increase in risk does not outweigh the performance gain for the riders and the 'decision' is made to not brake near the maximal possible. To test this theory an experiment with riders doing a descent and an isolated max braking test needs to be done.

5.2.4. Influence of Breaking on Regaining Speed

In this section the influence of the braking on the location where the riders start to apply power and so regain speed, is discussed.

As presented in table 4.13, braking late, stopping brake late and starting pedalling late result in best performance. As shown in figure 5.1, keeping the entry speed for a longer period results in better performance, especially as the exit speed of segment 6 is lower than the entry speed (see tables 4.8 and 4.9).
Apparently, the approximately 50 m that can be pedalled in segment 6 after braking, is not sufficient in length to compensate the late braking advantage. While better performance is clearly the main benefit of this action, valuable energy resources from the riders are also saved by starting pedalling later.

5.3. Best Performing Brake Strategy

In the previous sections, is discussed several times that distinct braking strategies may be used by the riders. This is a surprising result as world's best cyclist participated in this study. It was expected that a near perfect strategy would be known and applied by all.

The data and correlation factors direct to two distinguishing strategies being utilised. This is depicted in figure 5.2 where the start and stop brake points for each rider are plotted on segment 6. The two best performing riders (1 and 3) brake late and stop braking late, see figure 5.2

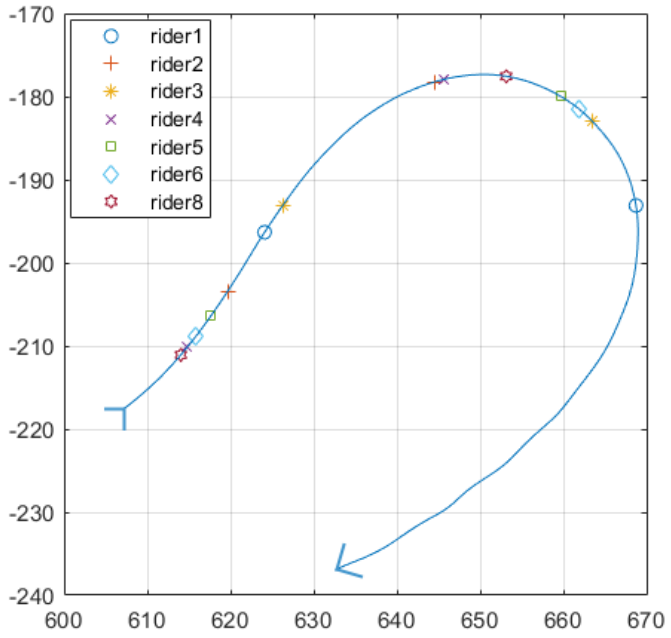

Figure 5.2: Top view of segment 6, containing the average locations where braking is started and stopped, taken from tables 4.4 and 4.5.

It seems that rider 1 is using a different method/approach to segment 6 than the other riders, resulting in the best performance.
The method utilised by rider 1 will be called the 'stop brake late' method and the other method utilised the 'stop brake early' method.
Rider 1:

- starts late (table 4.4)
- stops late (table 4.5)
- lowest brakes force (table 4.12)
- highest speed at end of breaking 4.7)

With the 'stop brake late' method the rider slows down to a given speed (likely the maximal cornering speed) and keeps braking to hold this speed while gravity pulls on the rider. After keeping constant speed, the brakes are released late (when maximal cornering speed becomes higher for the actual location).
With the 'stop brake early' method, a rider slows down firmly and then release his brakes early. After releasing the brake, the rider starts to increase speed by the gravity pulling down along the road gradient.
Both methods are depicted in figure 5.3. Utilising the 'stop brake late' method, allows a rider to control his speed closely to the maximal cornering speed. While the 'stop brake early' method creates the need for a rider to slow down far below the maximal cornering speed as his speed will increase after stopping to brake.
Rider 2 is a good example of this strategy:

- starts early (table 4.4)

- stops early (table 4.5)
- brakes the hardest (tables 4.10, 4.12)
- lowest speed at end of breaking (table 4.7)

However, by perfecting 'stop brake early', rider 2 is third best in segment 6.

These two strategies are already know in the cycling world as braking before (compare to 'stop brake early') or braking in the corner (compare to 'stop brake late'). Braking before or in the corner is a topic often discussed by cyclist. The correct answer may potentially be depending on the combination of road gradient and maximal cornering speed.
It should be noted that when cornering on a level segment, the speed increase, after braking is ended, is not present. As a result, these two strategies may not result in such a distinct difference when road gradient is zero.

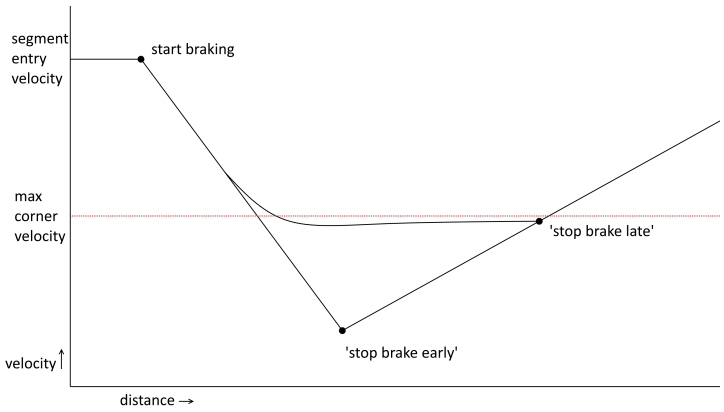

Figure 5.3: drawing of speed through segment 6 for two braking strategies. For illustrative purpose the effect is amplified considerably.

The idea that there are potentially two braking strategies being utilised, has an effect on the correlation coefficients calculated. Using strategy 'stop brake late' doing something i.e. later, faster or stronger can give a better result, while the same actions could be worse for the strategy 'stop brake early'. This may be making a correlation coefficient calculated on the complete group less informative/strong.

The 'stop brake late' strategy is supported by the strong correlation (0.7392) between average brake force and position at the end of breaking (Appendix A). If riders brake softer/lighter they also stop later. This correlation is not present for the start brake point, as no correlation (0.0540) is found. This implies, that slow braking does not mean early braking, braking is simply stopped later in the corner in such case. The general assumption is that riders finish breaking before the corner and are fully prepared for the corner. This is apparently not valid for this group and segment. Breaking late in the corner is the advantageous strategy.

5.4. Optimum Brake Strategy

In order to understand brake forces better, the time gained by utilising a higher average brake force is modelled and calculated. All calculated values resulting from the model described below are presented in table 5.1.
For the model, the speed at the starting and stopping of the brake action from rider 1 is taken. This rider has the fastest time over segment 6 and is using a distinct braking strategy over all of his trials. The speed of rider 1 at stop braking allowed this rider to continue the segment without additional breaking. This speed is therefore assumed to be close to the maximum cornering speed.
In order to demonstrate the advantageous effect of this strategy, three scenarios are calculated, each with a different average brake force. Brake forces are chosen based on results obtained during the trials:

- Low scenario, using the acceleration of rider 1 and rider 6, being the lowest measured;
- Medium scenario, using the acceleration of rider, 2 being the highest measured and twice as high as the low scenario;
- High scenario, being twice the medium scenario and still well below maximum literature values, so assumed a realistic value.

The required time to brake to the desired cornering speed is calculated for each scenario. After this step, the distance travelled during this brake time can be calculated. By doing so for all three scenarios, a difference in the start braking point (distance from the start of segment 6) is found. This difference may be travelled at the higher speed before starting to brake. The time gained travelling longer at higher speed is calculated. All results are presented in table 5.1.

	brake_acc	brake_time	brake_distance	extra_distance	total_time	time_gain
low	-0.88	3.54	39.8	0	3.54	0
high	-1.76	1.77	19.9	19.9	3.02	0.52
max	-3.52	0.88	9.9	29.9	2.76	0.78

Table 5.1: Example accelerations and the resulting time savings when slowing down to the same speed at the same location.

It is demonstrated that a time gain of 0.78 *sec* is possible over a total of 3 *sec* of braking which is a considerable 30 %.

The best used strategy, 'stop brake late' may not be performed at its full potential yet. As rider 1 has a low peak brake force (-1.86 m/s^2 or -0.18 g). This low peak brake force, means that harder braking can be done before velocity is kept constant during the difficult part of segment 6 by applying light braking.
Increasing peak brake force at the beginning of braking may potentially lead to an extra performance improvement.

6

Conclusions

Reaching a conclusion for the research question: 'Which are the best braking strategies resulting in a fast and safe cycling technique and optimum use of human power, leading to optimum results', the following conclusions can be drawn:

- This study shows clearly that two distinct brake strategies are used, resulting in a difference of approximately 1 *sec* over a sharp right-hand corner: 'stop brake late' (where braking is stopped late and well into the turn) and 'stop brake early' (where braking is stopped before or early in the turn). Popular believe is, braking being ready before the corner starts but, using 'stop brake late' results in a better performance in a sharp right-hand corner. As a result of the link between late braking and late pedalling onset, 'stop brake late' is also resulting in optimum use of human power.
- The best theoretical braking method is: starting to brake late and hard for the first part to reach max cornering speed at the onset of sharpest radius. The brake force should then be lowered instead of stopped to compensate for the acceleration caused by gravity. keeping the speed close to the maximal cornering speed throughout the corner.
- The best used strategy, 'stop brake late' may not be performed at its full potential yet. Increasing (peak) brake force at the first part of the braking action, will allow to brake later, resulting to an extra performance improvement.
- For all of the in this report defined braking parameters, the point where braking is started has the highest correlation with performance. With the distance until the start of braking being such a good performance indicator, training riders to brake later may result in improved performance during cornering.
- Braking harder can result in increased performance as, from all the riders using the 'stop brake early' method, the best performing rider has the highest recorded brake forces.

7

Recommendations

Brake Rub

During the data analysis, brake rub is found, see Appendix B, This brake rub was unexpected and unnoticed by the riders. It is recommended to gain a better understanding of brake rub and how to resolve it. Resolving brake rub will result in an immediate performance improvement. This performance improvement is extra valuable as no extra time, energy or power investment from the riders is required.

Learning Behaviour

During this exploration study, learning behaviour is observed, as discussed in appendix C. In general, riders become faster after each descent. Some riders braked the first trial for a corner, during later descents, the corner was taken without braking.
It is recommended to investigate the best method for course reconnaissance and the corresponding performance increase. Having this information will allow to make an educated choice on the benefit and method of performing course reconnaissance.

Experimental

Braking and cornering strategies are not the decisive elements in the current descent. By rehearsing the trials on a descent, containing more corners and having a steeper gradient, the effects found in this study are expected to become more pronounced.
GPS fix proved to be crucial, a course with open GSP fix should be selected for further experiments.

The peak brake forces found in this study are lower than the value's reported in literature. It can be investigated what the maximal brake accelerations are for professional road cyclist in tests similar to the tests found in literature. This way it can be verified if the riders cannot brake harder given the current equipment or do not require to brake maximal on this descent or are afraid losing traction/grip.

Improving Performance

For all of the in this report defined parameters, the point where braking is started has the highest correlation with segment 6 performance. It should be one of the first focus points when developing a method to improve rider performance. Training riders to brake late can improve performance during cornering.

Sensor Improvements

The brake sensor can be improved by changing the design of the aluminium brake pad holder, lowering the vulnerability to calibration. Instead of a threaded hole in the brake pad holder, where the mounting bolts thread into, a threaded stud could be mounted on the brake pad holder. Fixing the brake sensor to the brake calliper using a threaded nut.

It is recommended to invest in a dedicated speed sensor sampling at 100 Hz. By using a dedicated speed sensor, recorded data will improve in both quality and reliability, making the Sensor-Set less dependent on GPS fix.

The reliability of the power meter data recording of the Sensor-Set can improved. Although most commercial power meters send data at a relative low 1 Hz, the data is useful to determine the importance of power production for descending performance.
Power meter sampling at 10 or 100 Hz is preferred, aligning with the other used sensors sampling rate and allowing for detailed analysis.

A

Correlation Coefficients

For this thesis the correlations of multiple parameters describing braking behaviour with time through segment 6 are calculated.
In addition to the correlations with segment 6 time (performance), the correlations between all the other parameters are calculated and stated in this Appendix.

The correlation coefficients between all braking parameters that are used in this report. Table A.1 is for each trial with good data quality in segment 6.

	brake_acc_max	brake_acc_mean	loaction_max_brake	point_start_brake	point_stop_brake	speed_start_brake	speed_start_segment	speed_stop_brake	speed_stop_segment	time_descent	time_segment	trial_number
brake_acc_max	1.0000	0.7278	0.4497	0.1480	0.5017	-0.0416	0.0867	0.4771	-0.1596	-0.0189	-0.0388	-0.1907
brake_acc_mean	0.7278	1.0000	0.4435	0.0540	0.7392	-0.0444	-0.0738	0.3333	-0.0624	-0.1839	0.0012	-0.0970
loaction_max_brake	0.4497	0.4435	1.0000	0.6797	0.6714	0.0172	0.4716	0.1000	-0.1312	-0.2422	-0.5321	-0.1796
point_start_brake	0.1480	0.0540	0.6797	1.0000	0.5193	-0.1253	0.6490	0.0743	-0.2087	-0.2330	-0.7303	-0.0297
point_stop_brake	0.5017	0.7392	0.6714	0.5193	1.0000	0.0274	0.3180	0.2105	-0.0758	-0.3591	-0.3506	-0.0917
speed_start_brake	-0.0416	-0.0444	0.0172	-0.1253	0.0274	1.0000	0.6128	0.2715	0.3074	-0.6324	-0.1771	0.5425
speed_start_segment	0.0867	-0.0738	0.4716	0.6490	0.3180	0.6128	1.0000	0.2652	0.0154	-0.5737	-0.6491	0.3994
speed_stop_brake	0.4771	0.3333	0.1000	0.0743	0.2105	0.2715	0.2652	1.0000	0.2473	-0.2268	-0.0946	0.2768
speed_stop_segment	-0.1596	-0.0624	-0.1312	-0.2087	-0.0758	0.3074	0.0154	0.2473	1.0000	-0.1357	0.2525	0.1949
time_descent	-0.0189	-0.1839	-0.2422	-0.2330	-0.3591	-0.6324	-0.5737	-0.2268	-0.1357	1.0000	0.4234	-0.5143
time_segment	-0.0388	0.0012	-0.5321	-0.7303	-0.3506	-0.1771	-0.6491	-0.0946	0.2525	0.4234	1.0000	-0.2807
trial_number	-0.1907	-0.0970	-0.1796	-0.0297	-0.0917	0.5425	0.3994	0.2768	0.1949	-0.5143	-0.2807	1.0000

Table A.1: Correlation Coefficients between all the used braking parameters. The data used is of all trials with good data in segment6

The correlation coefficients between all braking parameters that are used in this report. Table A.2 is for each trial with good data quality during the whole descent.

	brake_acc_max	brake_acc_mean	loaction_max_brake	point_start_brake	point_stop_brake	speed_start_brake	speed_start_segment	speed_stop_brake	speed_stop_segment	time_descent	time_segment	trial_number
brake_acc_max	1.0000	0.7057	0.4754	0.1604	0.5379	0.1084	0.1730	0.4181	-0.2093	-0.0420	-0.0480	-0.1827
brake_acc_mean	0.7057	1.0000	0.4558	0.0394	0.7582	0.1059	0.0177	0.2764	-0.1412	-0.2477	0.0029	-0.0554
loaction_max_brake	0.4754	0.4558	1.0000	0.6851	0.6730	0.0531	0.5018	0.0823	-0.1438	-0.2610	-0.5335	-0.1671
point_start_brake	0.1604	0.0394	0.6851	1.0000	0.5143	-0.0861	0.6834	0.0544	-0.2110	-0.2789	-0.7273	0.0392
point_stop_brake	0.5379	0.7582	0.6730	0.5143	1.0000	0.0985	0.3732	0.1975	-0.1102	-0.4094	-0.3506	-0.0433
speed_start_brake	0.1084	0.1059	0.0531	-0.0861	0.0985	1.0000	0.6144	0.4125	0.3534	-0.6355	-0.2148	0.5146
speed_start_segment	0.1730	0.0177	0.5018	0.6834	0.3732	0.6144	1.0000	0.3305	0.0482	-0.5820	-0.6707	0.4149
speed_stop_brake	0.4181	0.2764	0.0823	0.0544	0.1975	0.4125	0.3305	1.0000	0.2601	-0.2737	-0.0846	0.3664
speed_stop_segment	-0.2093	-0.1412	-0.1438	-0.2110	-0.1102	0.3534	0.0482	0.2601	1.0000	-0.1418	0.2516	0.2033
time_descent	-0.0420	-0.2477	-0.2610	-0.2789	-0.4094	-0.6355	-0.5820	-0.2737	-0.1418	1.0000	0.4561	-0.4911
time_segment	-0.0480	0.0029	-0.5335	-0.7273	-0.3506	-0.2148	-0.6707	-0.0846	0.2516	0.4561	1.0000	-0.3404
trial_number	-0.1827	-0.0554	-0.1671	0.0392	-0.0433	0.5146	0.4149	0.3664	0.2033	-0.4911	-0.3404	1

Table A.2: Correlation Coefficients between all the used braking parameters. The data used is of all trials with good data for the whole descent

B

Brake Rub

B.1. Results

In figure B.1, a pulsating brake force is recorded by the brake sensor for rider 1 (rider 4 see figure G.4 and rider 6 see figure G.6). This brake force occurs when riders are not likely to brake (for example at start or after a corner) but rather are likely to be accelerating. Examining the brake data from rider 1 shown in figure B.1, a very consistent oscillation can be observed at the descent start and after each brake action. The pulsating brake forces occur on a constant distance rather than on time. The occurrence on distance rather than time indicates the effect is related to the drive train of the bicycle.

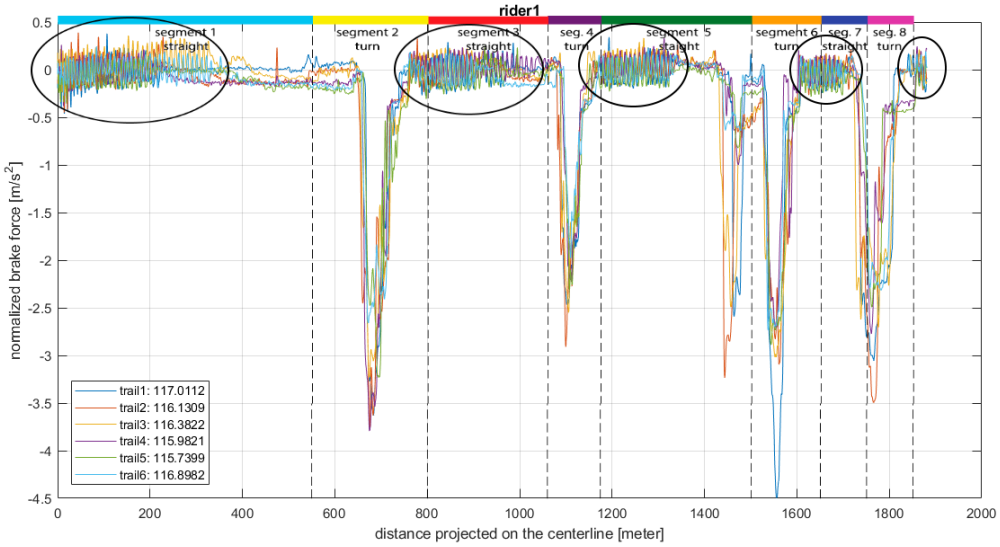

Figure B.1: Brake data from rider 1 with sensor drift removed. Inside the circles pulsating brake forces are observed.

B.2. Discussion

The pulsating brake forces reported in Section B.1 and shown in figure B.1 are contributed to brake rub.

As reported, the pulses are contributed to an effect linked to the drive train of the bicycle. The pulses occur at the start and after each braking action, points where riders apply the largest forces when pedalling. The pedals are linked to the drive train, explaining why the pulses occur on distance rather than time.

When pedalling a bicycle, the forces applied by the rider flex the bicycle. This flex can be large enough to make the brake pad contact, rubbing, the wheels [9] [5], as shown in figure B.2.
When a wheel is loaded in sideways direction at the bottom, the top of the wheel will move in the opposite direction of the load. On top of this, the bicycle frame will also flex [5] due to the pedalling forces, making the rim and brake pad move even closer together or touch (rub) in the worst case.
Widening the gap between brake pad and rim could be a solution but this may negatively affects braking feel of the bicycle. A better solution would be to strategically alter the stiffness in both bicycle frame and wheel.

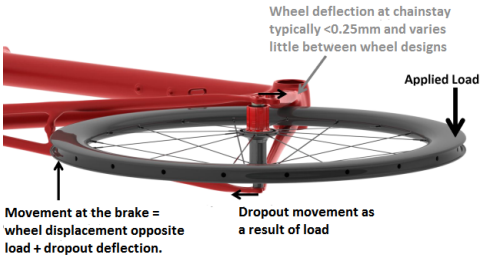

Figure B.2: Drawing of frame and wheel flex that cause brake rub [9]

Logically brake rub is unwanted because of the extra resistance it generates. Surprisingly none of the riders have mentioned brake rub when asked if anything special happened during the run.
It is likely that this unnoticed brake rub also occurs during actual races. This is both negative and positive news as, brake rub consumes valuable riders energy. However, avoiding brake rub results in immediately improved performances. This performance increase comes without extra time or effort investment from the rider. This is important because time and effort investment from the riders is already on the edge of whats possible without negatively affecting performance. This is why brake rub deserves a better understanding and possible solution. Avoiding brake rub requires changes to the bicycle frame, brake construction, bicycle wheels, installation and/or adjustment.

B.3. Conclusion

The advantage of a brake sensor, is clearly demonstrated by the finding of unexpected and unnoticed brake rub. One can conclude that this brake rub also happens during actual races. Elimination of this brake rub will immediately positively affect riders performance without any extra investment of the riders.

C

Learning Behaviour

C.1. Results

Shown in figure C.1 is the brake data of rider 5 with two distinct braking actions in segment one. The same result is observed with rider 2 (see figure G.2) but not with the other riders, see Appendix G.1 for all detailed graphs. For both riders this was during the first or second run. This indicates learning behaviour.

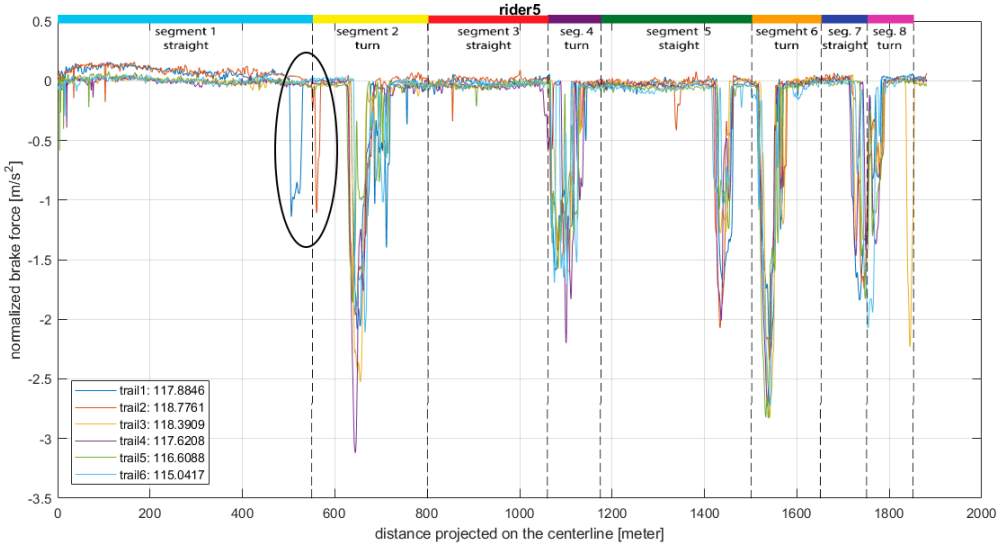

Figure C.1: Brake data from rider 5 with sensor drift removed. Inside the circled area the extra brake actions are shown

From the total descent and segment 6 times presented in table 4.2 and 4.3, it can be observed that the best performances are located towards the end of the trials. For the whole descent, none of the seven riders has his best performance in the first two trials and three have it during their last trial. For segment 6 time only rider 8 has his best trial within the first 3 trials. This is a strong indication that riders learn during the trials.

In Appendix A, the correlation coefficients between all calculated parameters as well as the trial numbers are presented in two tables. One table has the data for the whole descent and the other presents the data throughout segment 6. Data influenced by other traffic are skipped from this overview.

Using the data for the whole descent, a correlation of -0.4911 over the total number of trials is calculated. This negative correlation implies that riders learn throughout the trials, as later trials are correlated to lower (shorter) times over the whole descent.

Taking the data of segment 6, a correlation of -0.2807 is found for segment 6 time with trial number. This shows that learning is less pronounced for segment 6 time than for overall time.

Shown in figure C.1 and G.2 are riders 2 and 5 braking at the end of segment 1 during the first descents, during later descents no braking action is recorded at this location. Unnecessary braking before this fast and blind corner during the first trials is a clear example of learning behaviour, as during later trials both rider 2 and 5 learned there is no need to brake.

Looking at the overall times presented in table 4.2, it is observed that for the average overall times and standard deviations calculated, the smaller the standard deviation is for a rider, the faster the average overall time seems to be. With a correlation coefficient of 0.7434 this idea is confirmed. This suggests, that consistency over the trials is more important than a single strong effort. It also shows that the faster riders experience less improvements over the consecutive trials. This indicates that these riders have a natural feeling for the descent.

An interesting observation is made in table 4.7. For 6 out of the 7 riders their first trials have the lowest speed at the end of braking. Rider 5 is the exception with trial 5 at 11.73 m/s and trial one only marginally faster at 11.77 m/s.

C.2. Discussion

In this section, the learning effects over consecutive trials are combined and discussed.

In section 4.3, the overall times are presented in table 4.2. The smaller the standard deviation is for a rider, the faster the average overall time. Consistency over the trials is more important than a single strong effort. It also shows that the faster rider experiences less improvement over the consecutive trials. This shows these riders have a natural feeling for the descent

Section C, shows the best performances are located towards the end of the trials. For the whole descent, none of the seven riders has his best performance in the first two trials and 3 have it during their last trial.
This is confirmed by the correlations factors for the complete descent (-0.4911) and for segment 6 only (-0.2807), see Appendix A.
Rider 2 and 5 brake at the end of segment 1 during the first descents, during later descents no braking action is recorded at this location.

Taking these results, course reconnaissance can be very useful. In order to investigate how to best do a course reconnaissance, an intervention study may be done.

Many benefits for course reconnaissance can be listed. By doing so, also a disadvantage appeared that may result in lower performance: as riders may be given instruction to be careful in a certain corner, they may be constantly waiting for that one sharp corner that was somewhere in the descent, slowing down more than needed for other turns.

During this study riders were learning from repeatedly experiencing the descent themselves, as they did roughly 6 trials in 1 hour. Below are listed other methods for course reconnaissance.

1. Experience the descent multiple times in a short time frame;
2. A single reconnaissance descent long before the relevant event;
3. Descending multiple times long before the relevant event;
4. Reconnaissance by driving the route in a car;
5. Video reconnaissance either with or without explanation;
6. Looking at Google street view;
7. Less official but still a form of reconnaissance, listening to a team mate explaining the descent.

C.3. Conclusion

Combining the previously discussed information it can be concluded that performance increases from repeatedly experiencing a descent.

D

Brake Sensor Improvements

D.1. Problem analysis

From the equipment used, the brake sensor is discussed in detail in this Appendix as the development of this brake sensor is an important element of this thesis.

In Section 4.2, the brake calliper used is identified as the cause for the incorrect calibration. How the brake calliper design affects the brake sensors input/output relation is discussed in the following.

The electric side of the sensor does not change by using a different brake calliper and will thus not contain the cause for the calibration error.
For other explanations, the mechanical aspect of the brake sensors needs to be examined. The patterns present in the gravity corrected forward acceleration are matching with the normalised brake force (Appendix E). This implies, that the sensors worked properly with only the calibration being wrong.

The brake sensor is measuring deformation using strain gauges, so a difference in deformation of the sensor due to brake calliper design is looked into first as a possible cause.
When using different brake callipers, the length of the mounting bolt that is threaded into the brake sensor differs. This is shown in figure D.1, different calliper thickness (C1 and C2) alter the length of the bolt present in the aluminium brake pad holder (D1 and D2). When a shorter part of the bolt is present inside the brake pad holder, this lowers the stiffness. This implies that the sensor sensitivity is higher, as a less stiffer body deforms more. It is this deformation that is measured with the strain gauge mounted inside the brake sensor. The prototype brake calliper has a higher sensitivity, see figure 4.5 and figure 4.6, confirming the prototype design is identified as cause for the incorrect calibration.

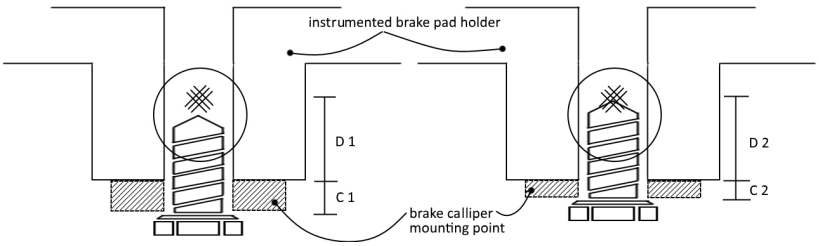

Figure D.1: Drawing of the different amounts of bolt present in the aluminium brake pad holder.

Although the current brake sensor design is found to be sensitive for its mounting method, brake points can still be reliably measured. The strong correlation between acceleration and brake forces, shown in Section 4.2, allows using the acceleration data where brake force data is less reliable and vice versa.

As part of this study, a brake sensor is developed and fabricated. The design principle of the brake sensor is proven to work during the experimental application.

Although some of the data measured by a brake sensor may be obtained from other sensors already present, the use of a dedicated brake sensor has distinct benefits. These benefits are already presented in Section 2.1 sensor advantage.
An important result, found due to the brake sensor is discussed in Section B.2.

D.2. Improved Brake Sensor Design

The brake sensor can be improved by using a threaded stud on the sensor. This will make the calibration of the brake sensor independent of the mounting method and brake calliper design. As a nut can be used on the threads to mount the brake sensor. This does not result in a different stiffness at the strain gauge location.
Production of this improved brake sensor can be done by machining new brake pad holders with a threaded stud extending out of the sensors. However, a cheaper solution would be to glue threaded rods into the current brake sensors.

E

Brake Sensor Validation

As summarised in Chapter 4, Section 4.2, the brake sensor is validated against the accelerometer and compared against GPS data.

In this Appendix, the data from the brake sensor, the accelerometer and the GPS are plotted in one graph for each rider for his first descent.

The forward acceleration data is effected by gravity with the road inclination. In order to compare the data directly, the gravity component is removed from the accelerometer data. The distortion form gravity on the acceleration data is given by (E.1).

$$xaccelerationroadincline = \frac{(-9.81 * roadgradient}{\sqrt{1 + roadgradient^2}}; \tag{E.1}$$

This equation is solved for every data sample. The result is subtracted form the forward acceleration data. The normalised acceleration data is compared with the normalised brake sensor data in Figures E.1, E.2, E.3, E.4, E.5, E.6 and E.7.

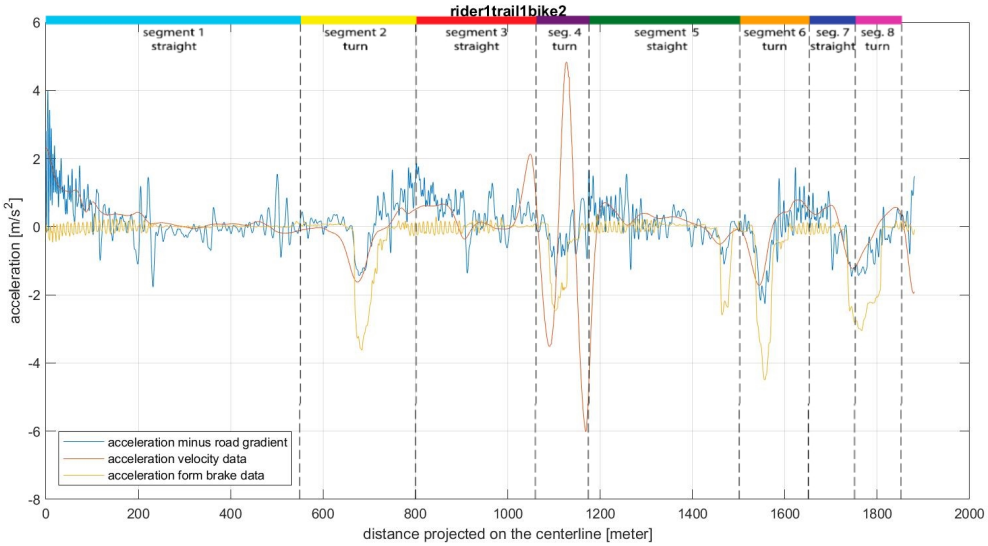

Figure E.1: Normalised brake sensor data, derivative of the GPS velocity data, forward bike frame acceleration filtered using a butterworth filter with a 1.5 hz cut of frequency that has gravity force from road incline removed.

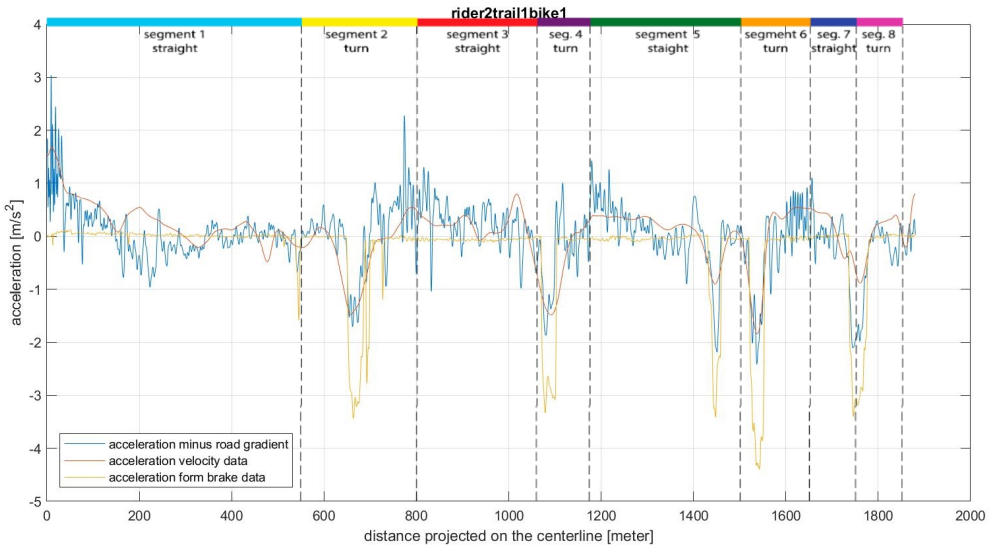

Figure E.2: Normalised brake sensor data, derivative of the GPS velocity data, forward bike frame acceleration filtered using a butterworth filter with a 1.5 hz cut of frequency that has gravity force from road incline removed.

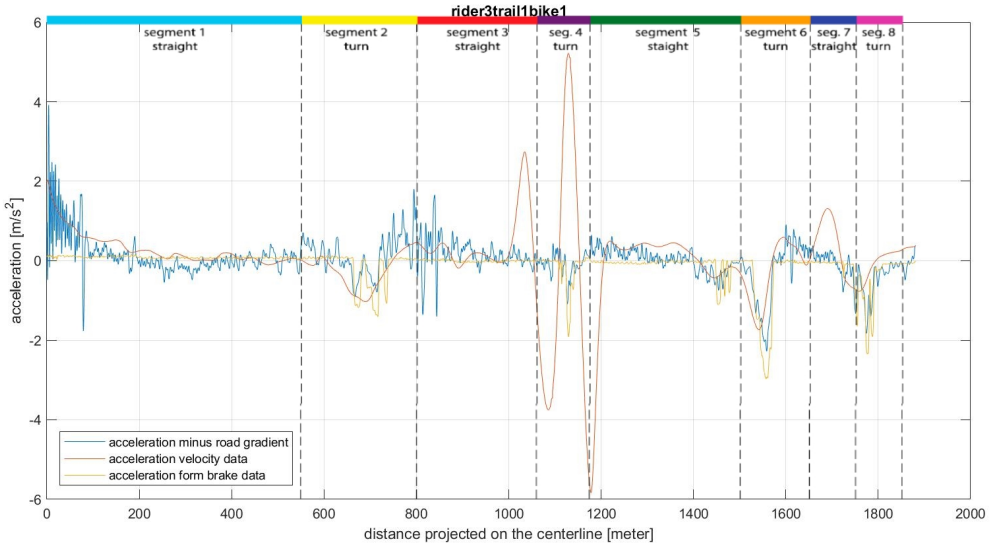

Figure E.3: Normalised brake sensor data, derivative of the GPS velocity data, forward bike frame acceleration filtered using a butterworth filter with a 1.5 hz cut of frequency that has gravity force from road incline removed.

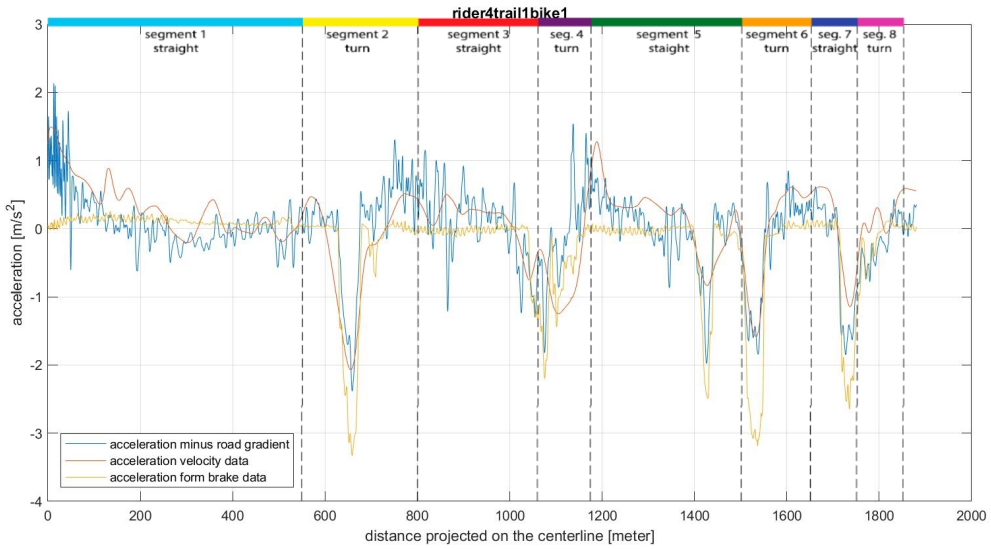

Figure E.4: Normalised brake sensor data, derivative of the GPS velocity data, forward bike frame acceleration filtered using a butterworth filter with a 1.5 hz cut of frequency that has gravity force from road incline removed.

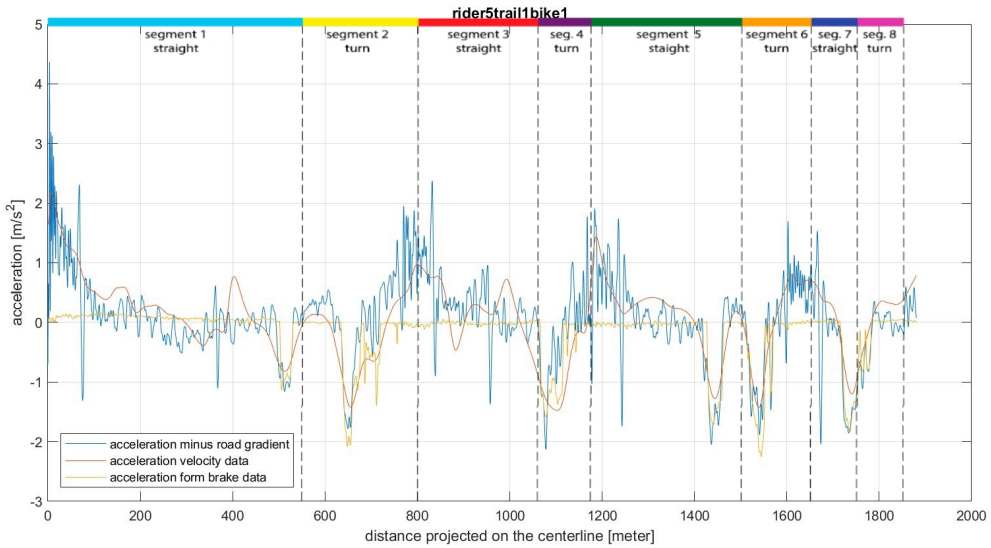

Figure E.5: Normalised brake sensor data, derivative of the GPS velocity data, forward bike frame acceleration filtered using a butterworth filter with a 1.5 hz cut of frequency that has gravity force from road incline removed.

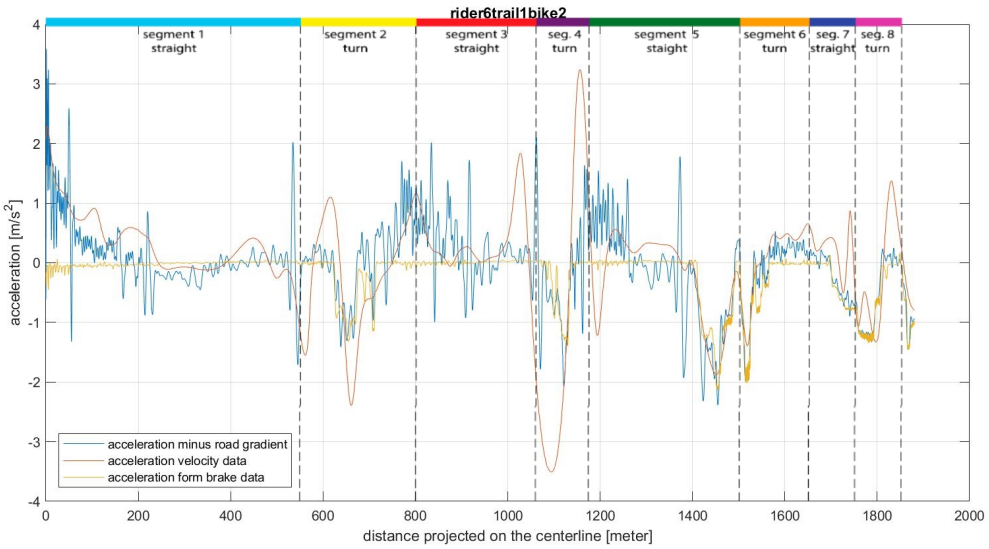

Figure E.6: Normalised brake sensor data, derivative of the GPS velocity data, forward bike frame acceleration filtered using a butterworth filter with a 1.5 hz cut of frequency that has gravity force from road incline removed.

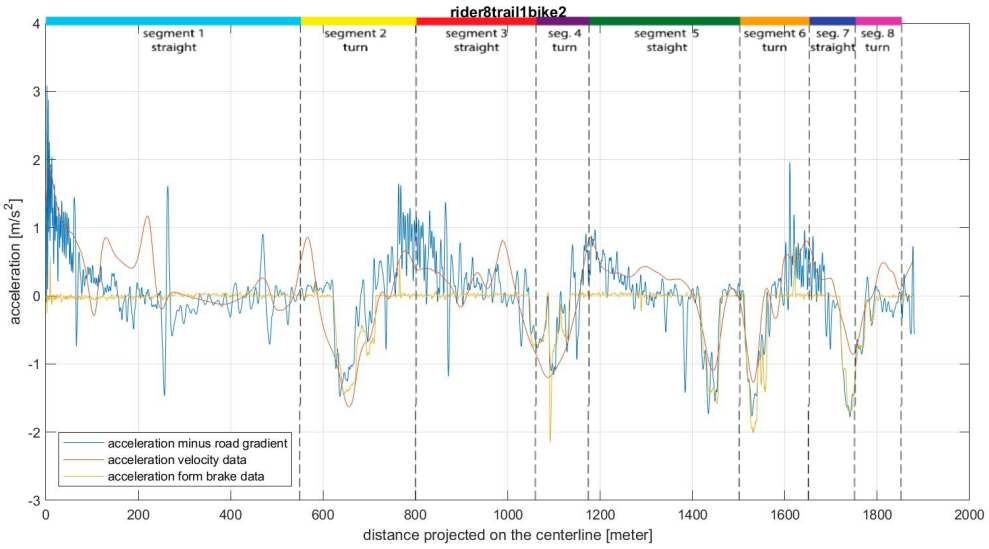

Figure E.7: Normalised brake sensor data, derivative of the GPS velocity data, forward bike frame acceleration filtered using a butterworth filter with a 1.5 hz cut of frequency that has gravity force from road incline removed.

F

Brake Sensor Validation and Calibration - Laboratory

After developing two prototype brake sensors in Chapter 2, the functioning of the prototype sensors has to be validated. The validation of the brake sensors is done by evaluating the reaction of the brake sensors during multiple different tests in Section F.1. These tests are chosen to evaluate the prototype brake sensors on:

- Zero offset drift;
- Shear force isolation;
- Zero offset repeatability when remounting and;
- Linearity of the relation between load and output voltage.

In case of satisfactory results, another series of brake sensors are manufactured. A total of 6 brake sensors is required for the experimental application in chapter 3.

From the 6 brake sensors that are now produced, four sensors are going to be calibrated in combination with the two Sensor-Sets in Section F.2, leaving two reserve sensors in case of damage. This calibration is needed because each sensor has a slightly different load-output relation. This relation is dependent on the sensor read out electronics that are used. Before the calibration can be started, the input output relation that is determined in Section F.1 is used to calculate the gain for the instrumentation amplifier in the Sensor-Set's. Changing the test setup and protocol to closely resemble the final application and executing the calibration protocol, makes the brake sensors ready for use during the experimental application.

F.1. Brake Sensor Design Validation

In this section the behaviour of the prototype brake sensors is evaluated to validate the sensor design and production process. After making a test setup to load the brake sensors inside the lab environment, the prototype brake sensors are evaluated on:

1. Sensor drift;
2. Shear force isolation;
3. Offset repeatability when remounting;
4. Linearity of the relation between load and output voltage.

The goal of this validation is not to find the calibration parameter that will be used during the experimental application but, the goal is to verify sensor design. When the brake sensors design is verified and the brake sensors do what they are intended for, the project can continue by producing the extra brake sensors needed for the experimental application.

F.1.1. Method

The two sensors that are made will both be tested and compared to each other and the expected results. If they are proven to be working the production of four extra sensors is started. To prove that the sensors are working a test setup is made. Different tests to verify sensor design and manufacturing are used to get an idea of the sensor behaviour.

For loading the brake sensor with a known load as close to the loading situation on the real bicycle, a test setup is made. The test setup consists of an old front fork mounted in a bicycle stand. On this front fork a brake, the brake sensors and a wheel are mounted. A rope is wrapped around the wheel, attaching known weights to the rope applies a known load that the brake sensors should measure. In this setup, it is easy to change the input to the brake sensor. To show the corresponding sensor output the sensor electronics are connected to a Scaime CJP rail instrumentation amplifier. The input voltage to the Wheatstone bridge is set to 5 V and the gain of the amplifier is 0.40-0.56 mV/V. To measure the output voltage of the amplifier a Fluke 117 true RMS multi meter is used. This complete setup is shown in figure F.1

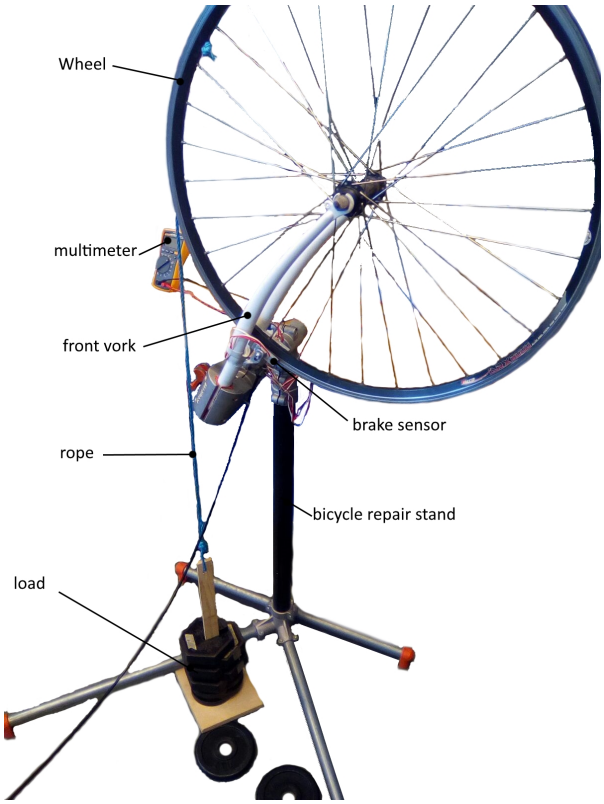

Figure F.1: Setup for sensor behaviour testing

With a test setup ready to read out and load the brake sensors, the first step in evaluating sensor drift will be to turn on the electronics and look for possible short circuit. After starting up the electronics the zero offset will be set to zero volt. Now the electronics reading the sensor output are activated, an electric current runs through the sensor and equipment. This current warms up the sensor and equipment effecting the sensor resistance and output voltage. This results in drift and is normal although excessive and non-stabilising drift can be an indication of production errors or other problems. The amount of drift of the brake sensors is written down so the sensor drifting can be evaluated.

During the final experimental application of the brake sensor it has to be switched between the bicycles of different riders. It is very important to have a repeatable zero offset after remounting the sensor. The Sensor-Set from Berkelaar MRT does not have zero offset adjustment. For the testing of this characteristic both brake sensor mounting bolts will be loosened and tightened multiple times. During this the researcher will be monitoring what happens to the zero offset.

During the design of the brake sensor in chapter 2 a strain gauge pattern to isolate shear force is shown. The question is does this pattern work on the brake pad holder with a mounting bolt adding extra deformations. Evaluating this is done by gripping the brake lever from very light to maximum grip force. When the rim/rope is not loaded this result in normal force on the brake sensors. Looking at the brake sensor output the effect of normal force on sensor output is visible. With known grip force this gives enough information to identify if normal force is isolated from the sensor output.

Now the output voltage when the wheel is loaded with known weights can be evaluated. I loaded the setup shown in figure (F.1) with 0.5, 4.5, 8.5, 12.5 and 16.5 kg to do a first calibration test. The goal of this first static calibration is to see if the sensors have a linear relation between load and output voltage. The results can also be used to determine the gain of the Sensor-Set instrumentation amplifier.
The calibration protocol consist of the following steps:

1. Zeroing the output voltage of the instrument amplifier;
2. Wait until sensor and amplifier are warmed up (the voltage slowly drifts when starting up);
3. Load the sensor with the rope and weight holder;
4. Note down voltage when the rim is just sliding through the brake pads;
5. Note down voltage when brake lever is gripped with max force;
6. Note down voltage when sensor is not weighted;
7. Add 4 kg to the weight holder and repeat step (4),(5)and(6);
8. Repeat step (7) until 16 kg of weights is reached;
9. Wait 10 minutes and note the voltage at the end;
10. Load the weight holder with 16 kg and then repeat step (4),(5)and(6);
11. Remove 4 kg from the weight holder and repeat step (4),(5)and(6) until there are no weights on the weight holder.

F.1.2. Results

Turning on the electronics did not result in a short circuit or other problems. This allows for the tests to be executed.

First, the zero offset of the sensors is set to 0 V, this is done by turning the zero offset adjustment screw on the Scaime CPJ rail instrumentation amplifier. Sensor number 1 could be zeroed without many difficulties. It became apparent that for sensor 2, the zero offset could not be easily adjusted to 0 V due to rapid drifting. In order to monitor the sensor drifting, it was decided to keep the sensors drifting for a prolonged period. After approximately half an hour, both sensors started to display stable values. Sensor 1 drifted a total of 0.180 V. Sensor 2 drifted -0,864 V. it can be seen that sensor 2 drifts significantly more than sensor 1, the absolute amount of drift is almost 5 times more. Now both sensors have stabilised, the zero offset voltage can be set to 0 V

The second test is to investigate the influence of dismounting and mounting the sensor again on the same brake calliper. This is to establish how sensor exchange between riders during the actual trials may affect the measurements. For this the brake sensor mounting bolts where loosened and tightened. After tightening the bolts both sensor 1 and 2 had a different zero offset. While tightening the bolts the output voltage of the sensors moved with increasing bolt torque. The tightening was done using an Allen key and will thus not have a repeatable mounting torque value. Repeating this multiple times a variant of around 1 V is found for both sensors.

The third test consists of establishing the effects of pulling the brake lever without loading the bicycle wheel. Or in other words does normal force effect sensor output. Pulling the brake lever without loading the wheel did result in a change in output voltage. This implies that the normal force is not completely filtered by the sensor. The method did not include a way to measure the normal force applied on the brake pad. In order to give an indication of the effect of normal force, the output voltage is drawn against how hard the grip

force felt. These drawings are shown in figure F.2 and F.3. Interesting to note is the difference in reaction to normal force from both sensors. Sensor 1 has a small drop in voltage and then rises. Sensor 2 has a more linear reaction with a downward slope.

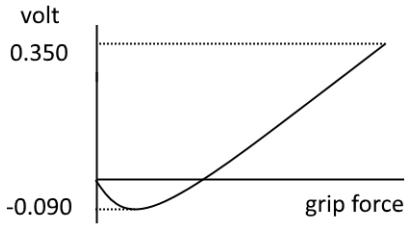

Figure F.2: Graph that shows how the brake grip force is related to the brake sensor 1 output voltage with a non-loaded rim

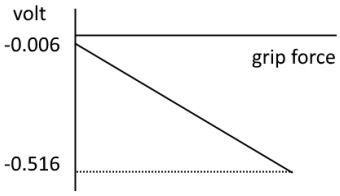

Figure F.3: Graph that shows how the brake grip force is related to the brake sensor 2 output voltage with a non-loaded rim

The calibration data from sensor 1 is shown in figure F.4 and F.5. As shown in figure F.4 a difference between the input output relation with increasing load or decreasing load can be observed. This difference is largest at the smallest load, during the smallest load the time difference between samples is maximal. The increase in difference with time points in the direction of sensor drift. To test the theory of sensor drift the zero offset voltage noted down during the experiment is removed from the data. Shown in figure F.5 is the data with zero offset voltages removed. A smaller difference between adding and removing weights from the setup is the result, supporting that the difference comes from zero offset drift.

Looking at the data for maximum grip force and the wheel slowly slipping through the brake pads. A difference between the output voltage of the slip and maximum force samples can be observed. For sensor 1 the maximal grip results in a higher output voltage.

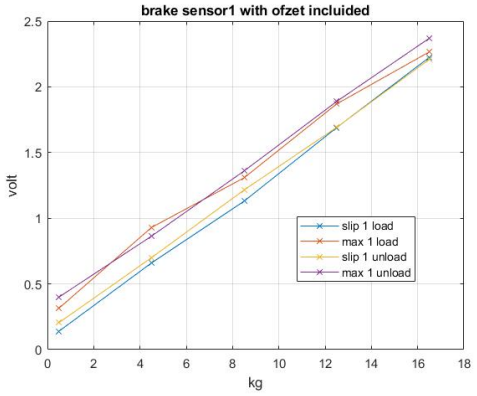

Figure F.4: Plot of the voltages during loading for the first rough calibration for sensor 1. The R^2 values are: $slip_{load}$ = 0.9993, max_{load} = 0.9942, $slip_{unload}$ = 0.9999, max_{unload} = 0.9996

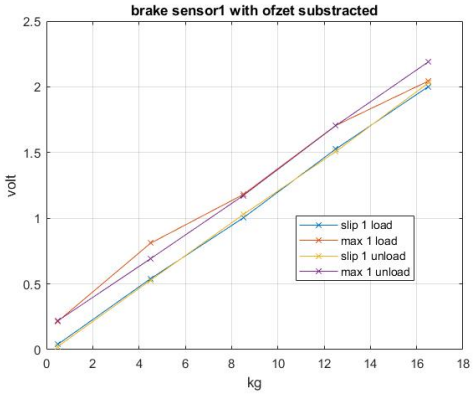

Figure F.5: Plot of the voltage during loading minus the zero offset voltage for sensor 1. The R^2 values are: $slip_{load}$ = 0.9997, max_{load} = 0.9920, $slip_{unload}$ = 0.9999, max_{unload} = 0.9996

The calibration data from sensor 2 is shown in figure F.6 and F.7. The sensor was still drifting when the calibration protocol was started. In figure F.6 it can be seen that the differences between loading and unloading are a lot larger for sensor 2 than sensor 1. Removing the zero offset drift from sensor 2 results in the data shown in figure F.7. The result is that the loading and unloading curves come together. The shape or linearity of the data does not change suggesting that, zero offset drift can be removed without affecting data quality.

Looking at the difference in output data between maximum grip force and the wheel slowly slipping through the brake pads. A difference between slip and maximum grip for Sensor 2 can be observed. With the maximum force output being lower than the slip output, the effect is the reverse to sensor 1.

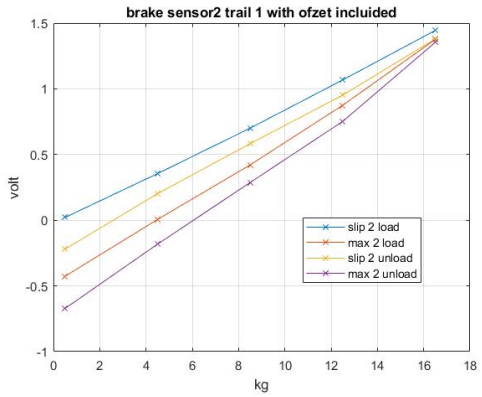

Figure F.6: Plot of the voltages during loading for the first rough calibration for sensor 2. The R^2 values are: $slip_{load}$ = 0.9994, max_{load} = 0.9987, $slip_{unload}$ = 0.9993, max_{unload} = 0.9975

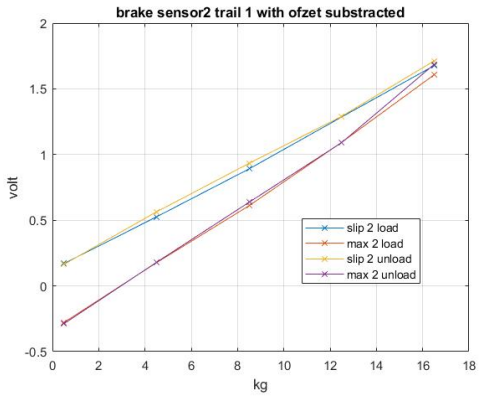

Figure F.7: Plot of the voltage during loading minus the zero offset voltage for sensor 2. The R^2 values are: $slip_{load}$ = 0.9995, max_{load} = 0.9989, $slip_{unload}$ = 0.9993, max_{unload} = 0.9970

After the zero offset drift of sensor 2 had stabilised, a second calibration for sensor 2 is done. The results of this calibration are shown in figure F.8 and F.9. With the zero offset no longer drifting, The data with the zero offset included is very close to the data with the zero offset removed. Comparing the results off this calibration with those shown in figure F.7 the results are very close. This indicates that zero offset drift can be removed without effecting data quality.

Figure F.8: Plot of the voltages during loading for the first rough calibration for sensor 2 after the zero offset drift has settled. The R^2 values are: $slip_{load}$ = 0.9981, max_{load} = 0.9999, $slip_{unload}$ = 0.9976, max_{unload} = 1.0000

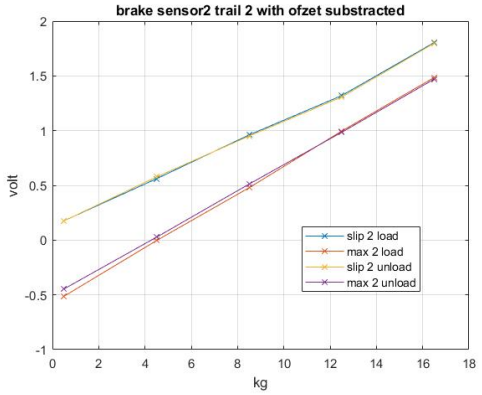

Figure F.9: Plot of the voltage during loading minus the zero offset voltage for sensor 2 after the zero offset drift has settled. The R^2 values are: $slip_{load}$ = 0.9977, max_{load} = 0.9999, $slip_{unload}$ = 0.9969, max_{unload} = 1.0000

F.1.3. Discussion

Discussing the possible options for the excessive drift of sensor 2, it was concluded that the most likely cause of the drifting strain gauges is the bonding to the metal pad. In case a strain gauge is not properly bonded to the aluminium pad holder, the strain gauge has a limited thermal connection with the aluminium brake pad. Normally this aluminium brake pad will act as heat sink and absorb the heat produced by the strain gauge and the strain gauge would reach stable equilibrium in the readings.

However, the excessive zero offset drift in sensor 2 could potentially be problematic during the experimental application. Therefore, the strain gauges of sensor 2 are removed and a new set of strain gauges are applied to verify if the drift problem may be eliminated. After applying a new set of strain gauges the zero offset drift was solved. This confirms that the excessive zero offset drift is a result from faulty brake sensor production.

The goal of the brake sensor design is to cancel out all forces other than the shear force that is transmitted

from rim to the brake pad. The normal forces applied perpendicular to the rim, should be cancelled out. When examining the test results it was clear that normal force is present in the measured values. For sensor 1 maximum lever grip force without load results in 0.35 V compared to the 2.0 V at a 16.5 kg load. For sensor 2 maximum grip force without load results in -0.51 V compared to 1.7 V at a 16.5 kg load. Normal forces lead to output voltage increase for sensor 1, as shown in figure F.4 and F.5, this lead to the slip line being below the max grip line. For sensor 2, normal forces lead to a lowering voltage output, the slip line is now lower than the maximum grip line as shown in figure F.6, F.7, F.8 and F.9. This normal force sensitivity is unexpected. Despite this normal force sensitivity the R^2 values of the calibration listed in below the figures, show that the output voltage is correlated to the sensor load. The lowest R^2 value of 0.9920 for sensor 1 during max grip when loading with the zero offset subtracted is still good. This good R^2 values could be explained by the fact that the brake pad normal force is related to the shear force by the friction coefficient between brake pad and rim. Add to this that normal force output from maximum grip results in smaller voltage changes than the shear force loads used, and the sensor could be usable.

While the brake sensor does not isolate shear force, both sensor 1 and 2 do not react in the same manner to normal force. As shown in figure F.2 and F.3 the change in output voltage from the two sensors is different in amplitude and direction. This suggest that small variations within the production of the sensors lead to the normal force sensitivity. Bad sensor design would result in both sensors showing similar unwanted behaviour. Remaking the sensors with more precision could lead to improvements on the results currently made.

To validate that the removal of zero offset is not affecting the data, two checks on the recorded data are done. First the plots containing calibration data with the offset included shown in figure F.4, F.6 and F.8 are compared to the ones with the zero offset subtracted shown in figure F.5, F.7 and F.9. For each of these trials, removing the zero offset from the sensors output brings the voltage during loading and unloading closer to together. Looking at the R^2 values not much changes in the linearity of the results. Second is comparing the result from sensor 2 trial 1 and trial 2, if removing the sensor drift results in similar input output relation for both trials removing drift can be done. Looking at trial 1 and trial 2 shown in figure F.7 and F.9, The data with maximum grip force is not equal but this can be explained by different grip force. The data from the rim slipping through the brake pads looks very similar for both trials, especially considering the rapid zero offset drifting of the brake sensor in trial one. Combining the results from the two checks it is very likely that the drift can be removed from sensor data without affecting the results.

An important question to answer is how does remounting the sensor on a different bike affect the brake sensor. In Section F.1.2, the zero offset changed during remounting of the brake sensor. A change in zero offset of around 1 volt occurred. However, this will not be a problem as the sensor drift may be removed in post processing of the result, without affecting sensor data quality. During the final experiment it is beneficial to use a torque wrench to further lower the variation between multiple remounts.

F.1.4. Conclusions

The points discussed in Section F.1.3 can be summarised to the following 6 conclusions.

1. The excessive zero offset drift observed in brake sensor 2 is the result of faulty manufacturing;
2. Shear force is not perfectly isolated as normal forces do affect the brake sensor output;
3. The effect of normal force on the brake sensor output is not large enough to make brake sensor non-functional;
4. Differences in reaction to normal force between brake sensor 1 and 2 are observed, this implies that the normal force sensitivity can be lowered by improving manufacturing precision;
5. Removal of zero offset drift from the brake sensor data does not harm the quality of the recorded data;
6. Remounting the brake sensor changes the zero offset of the brake sensor with a range of 1 V. These small changes can be digitally removed after the experiment data is recorded.

Having proven the first sensor design is working and being short on time to try multiple other sensor iterations, it is decided to produce 4 extra sensors with the design from chapter 2. The total amount of sensor will then be six. Four sensors will be connected and calibrated with the two Sensor-Set electronics and tow sensors will be reserve in case one of the others fail.

F.2. Sensor-set Calibration

In Section F.1 the brake sensor design from chapter 2 is validated and it is decided to use the sensor design from chapter 2 for the experimental application. Even though the input-output relationship has been determined in Section F.1 a new calibration is needed. This new calibration is needed due to changes in the electronics attached to the brake sensor. For the experimental application in chapter 3, the brake sensors will be attached to the Sensor-Set produced by Berkelaar MRT, this change could slightly alter the input-output relation of the brake sensor. The extra brake sensors that are produced will also all have a slightly different input-output relation. To do the final calibration as close to the intended use case as possible, four brake sensors are calibrated together with the two Sensor-Sets made by Berkelaar MRT. The calibration is done using the bike and brake type that will be used during the first experiment to further improve comparability with the experimental application. The 2 reserve brake sensor will not be calibrated. During the unlikely scenario that a brake sensor fails during the experiment, calibration of the replacement brake sensor can be done after the experiments.

F.2.1. Method

With a first calibration done in Section F.1, the instrumentation amplifier gain needed for the final measurements can be determined. This amplifier gain should be implemented in the Sensor-Set made by Berkelaar MRT. The gain of the integrated instrumentation amplifier can be changed by soldering a SMD resistor on the Sensor-Set circuit board. This is a time consuming task with the risk of overheating other components on the circuit board, so it is best to have the gain correct at the first try.

The selection of the amplifier gain is a trade off between two things, step size and measurement range. Step size of the brake force sensor data is the amount of Newton per bit in the stored sensor data. Measurement range is the range between minimum (zero) and maximum measurable brake sensor load. Increasing the amplifier gain will result in a smaller step size per data bit and a smaller measuring range. The advantage of the smaller step size is a higher resolution in the final data. But the resulting smaller range could lead to the output signal moving out of the measuring range. Shown in figure F.10 is a visual explanation of step size and amplifier gain.

With the brake sensor having a different zero offset every time it is remounted, it is important to make sure the sensor output is inside the measuring range of the Sensor-Set electronics. The zero offset of the brake sensors varied with around 1 V when remounting the brake sensor. To adjust the zero-offset inside the measurement range, an adjustable resistor can be used to balance the brake sensors Wheatstone bridge. The adjustable resistant will be placed across one of the strain gauges as shown in figure F.11. Adjusting the resistance until the zero offset is at 0 V is a possibility to solve the altering zero offset using hardware. Using a adjustable resistant will be slowing down the Sensor-Set mounting a lot, given the fact that it is not possible to read out the zero offset voltage live without, removing the Sensor-Set housing to connect a multi meter.

As mentioned in Section F.1.3, zero offset and sensor drift can be digitally removed from the recorded brake data during post-processing. When the zero offset is higher than zero and thus inside the Sensor-Set measurement range, digitally removing the zero offset in post processing is possible. But if mounting the brake sensor leads to a zero offset below 0 V, the data is outside of the Sensor-Set the measurement range and nothing will be recorded. When nothing is recorded digital removal of the zero offset is not possible. A trick to keep the zero offset from the brake sensor inside the Sensor-Set measurement is used, the zero offset of the brake sensors is set higher than the voltage changes recorded during remounting of the brake sensors. By doing this, the variation in zero offset reserves a part of the Sensor-Set measuring range. As a result the gain of the instrumentation amplifier has to be lower to keep the voltage change during the maximal load below the maximal measured voltage. Shown in figure F.10 is a visual representation of all possible combinations in

zero offset and amplifier gain. Minimal step size in Newton per data bit without going outside of the measurement range will normally be reached by using settings denoted as perfect gain and perfect zero offset. But as the light grey lines representing the possible zero offset variation after remounting show, this will lead to the brake sensor output possible being outside the measuring range. Using the bottom left combination of low gain an high zero offset the brake sensor output will stay inside the measurement range. With the brake sensor output staying inside the measurement range, zero offset removal can be done after the experiments, for example by using the Matlab programming environment.

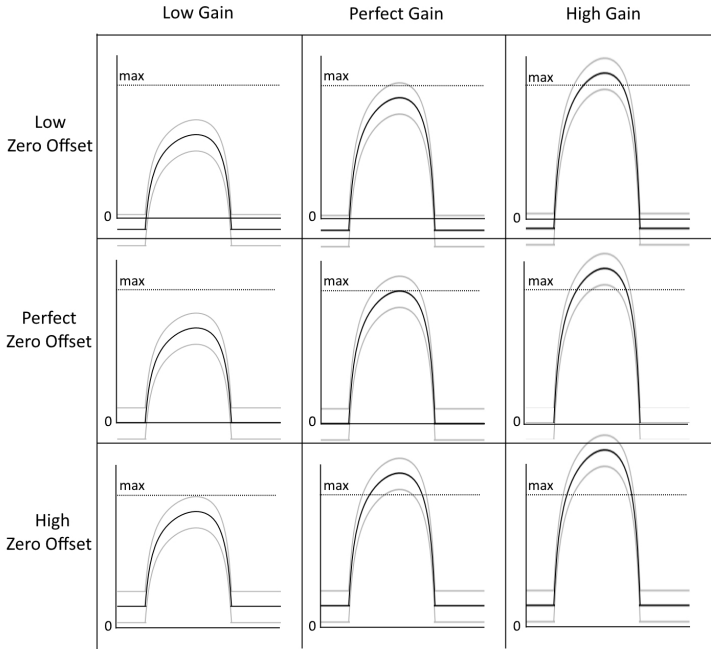

Figure F.10: The trade off between low and high gain

The instrumentation amplifier used in Section F.1 has a gain that is adjustable between 0.44 and 0.56 V/mV by turning a adjustment knob. As a result of the adjustability, the exact gain of the instrumentation amplifier is unknown. The 0.44-0.56 V/mV range combined with a Wheatstone bridge input voltage of 5 V, results in a output of 2.0 V for sensor 1 and 1.7 V for sensor 2 at a 161 N load. When estimating the amplifier gain at 0.5 V/mV right in the middle of the adjustment range for further calculations, the maximal expected load of 400 N would result in a output voltage of around 4.9 V for sensor 1 and around 4.2 V for sensor 2.

The estimated gain of the test setup is prefect for the final experiment. With the brake sensor output for a 400 N load that is found as expected maximal braking force [1], the output voltage stays just within the Sensor-Set measurement range. The room that is left in the voltage measurement range can be used for digital removal of the zero offset. Given this information it was requested to Berkelaar MRT, to set the amplifier gain to 0.5 V/mV.

With the brake sensors validated and the instrumentation amplifier gain adjusted to fit the expected loads, everything has to be calibrated. This new brake sensor calibration in combination with the Berkelaar MRT Sensor-Set is needed because, changing the electronics can have an effect on the input output relation of load cell. It is best practise to do the final calibration in circumstances as close to the final use case as possible. The setup from Section F.1 is replaced by, a Giant TCR bicycle equipped with a Shimano Dura-ace 9000 brake calliper as used by team Sunweb. The bicycle is supported using a cycling home-trainer. To let the front wheel rotate freely a custom made wooden support is used. For the application of a known load to the brake sensor, a rope is attached on the outer diameter of the bicycle wheel. placing this complete setup on-top of the workbench inside the bicycle lab, this creates enough height for the attachment of calibration weights onto

the rope. A picture of the setup is shown in figure F.12.

During the connecting of the brake sensors with the two Sensor-Set's, one of the brake sensors had a zero offset below 0 V and thus outside of the measurement range. To solve this problem the brake sensors needed balancing of the Wheatstone bridges. To balance the Wheatstone bridge of the brake sensor a balancing resistor is placed in parallel to one of the strain gauges as shown in figure F.11. This parallel balancing resistor lowers the resistance over the stain gauge and can make the Wheatstone bridge in balance again.

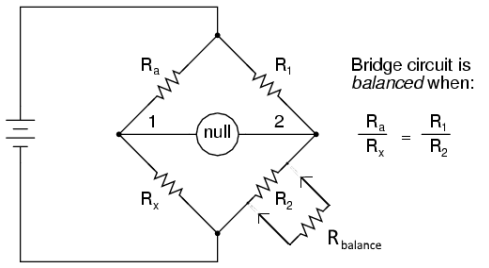

Figure F.11: Balancing a Wheatstone bridge

It is decided to mount both brake sensors on the front brake calliper. Mounting both brake sensors on one brake calliper, allows for possible force differences between the left and right brake pad to be quantified. The brake sensor meant for use on the rear during the final experiment sits on the right side of the bicycle, during the final experiment is will also be on the right side. The front brake will be on the exact same location during the calibration and final experiment.

For the Sensor-Set calibration, a few things are different from the calibration done in Section F.1.1. The differences between both calibrations are listed below.

1. A large advantage of using the Sensor-Set is that the Sensor-Set can record the brake sensor output during the whole calibration. Starting data recording at the beginning removes the need of writing down the brake sensor output values;

2. Due to mounting both brake sensors at the front brake loading, both sensors will be done simultaneously;

3. The calibration weights are increased to 10.5, 20, 30.5 and 40 kg. This increase is done to cover the full range of expected forces;

4. Each of these weights is used to load the brake sensor 5 times. By taking the averages of the measured output a more accurate result can be reached;

5. The maximal lever grip force test will not be done, this is not representative of the circumstances found during the final application;

6. Output data will be given in bit as recorded by the Sensor-Set instead of voltage that was previously used;

7. Zero offset and output during loading will not be separately taken from the recorded data. The delta created by sensor loading will be used in the results section.

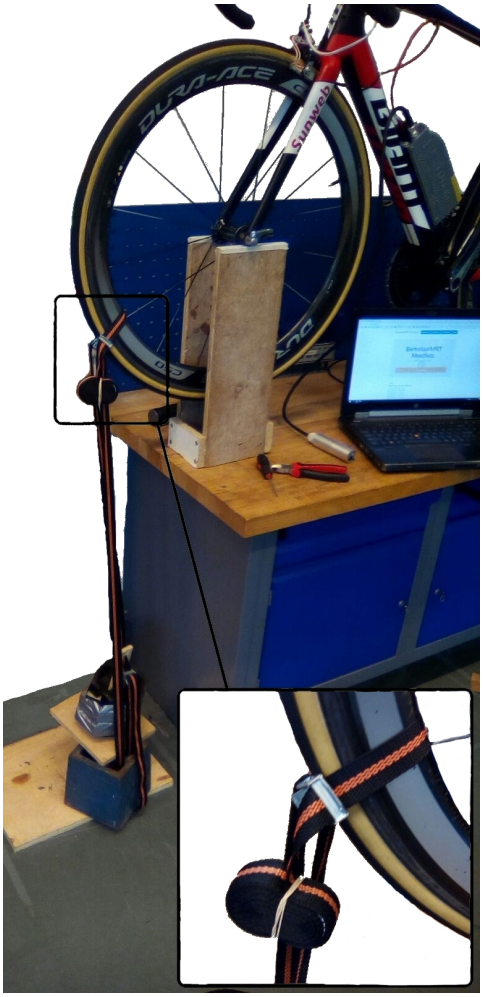

Figure F.12: Static calibration setup with the Giant TCR

F.2.2. Results

The results from the brake sensor calibration in combination with the Sensor-Set are shown in figures F.13, F.14, F.15 and F.16. Doing the calibration with the increased weights was more difficult than expected. To keep 30 and 40 kg loads in the air using the brake required very high grip force on the brake lever.

For Sensor-Set 1 the data is shown in figure F.13. Looking at the R^2 values to test the linearity between brake sensor input and output, An R^2 value of 0.9976 is found for brake sensor 1 and R^2 = 0.9898 for brake sensor 2. Shown in figure F.14 is the data from brake sensor 1 and 2 are added together. Calculating the R^2 value for the summed brake sensor data a value of 0.9963 is found.

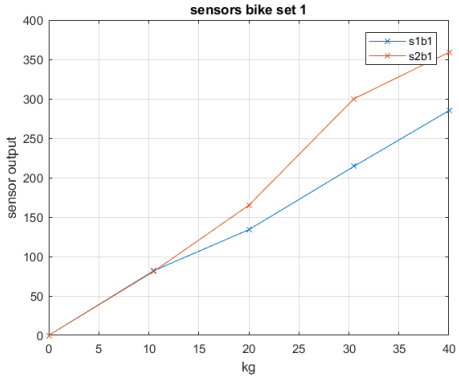

Figure F.13: Plot R^2: s1=0.9976 s2=0.9898

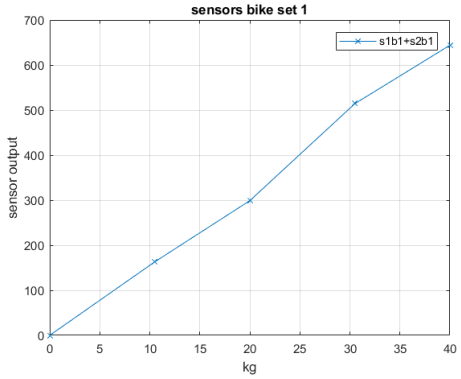

Figure F.14: Plot R^2: 0.9963

For Sensor-Set 2 the data is shown in figure F.15. Looking at the R^2 values to test the linearity between brake sensor input and output, An R^2 value of 0.9927 is found for brake sensor 1 and R^2 = 0.9932 for brake sensor 2. Shown in F.16 is the data from brake sensor 1 and 2 are added together. Calculating the R^2 value for the summed brake sensor data a value of 0.9961 is found.

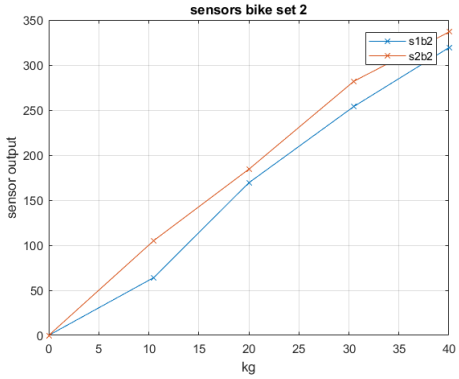

Figure F.15: Plot R^2: s1=0.9927 s2=0.9932

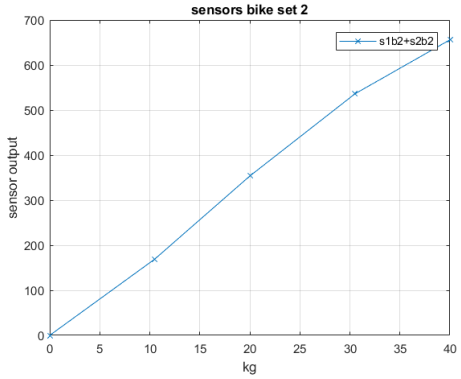

Figure F.16: Plot R^2: 0.9961

A least square fit on the brake sensor calibration data is done using the curve fit tool present in the Matlab programming environment. The curve fit tool is used to find the best fitting line through (0,0) and the 4 data points in bit and Newton. The directional coefficient of this line will be used for the conversion from bit to Newton. The resulting conversion factors/calibration parameters are:

- Sensor 1 bike 1 is 1.40 N/step;
- Sensor 2 bike 1 is 1.09 N/step;
- Sensor 1 bike 2 is 1.22 N/step;
- Sensor 2 bike 2 is 1.12 N/step.

F.2.3. Discussion

The difficulty experienced to grip the brake lever hard enough to keep the 40 kg load suspended in the air, feels not similar to the grip force experience during hard braking on my own road bicycle. From how hard the grip force felt I would not expect to find 400 N brake force during the final experiment. This difficulty is unlikely to affect the data quality. The Sensor-Set samples at 100 hz and an average over 5 trials is taken, making the change of missing the peak brake force very small.

The lowest R^2 value found is 0.9898 for brake sensor 2 on Sensor-Set 1, indicates a good linearity of the calibration points. This amount of linearity suggest that the sensor have a good quality and no large errors where made during brake sensor production.

Looking at the increase in R^2 that is found for both Sensor-Set when the left and right brake pad output are summed, it can be assumed that data quality will improve from using four instead of two brake sensors. However, the question is whether this is necessary. Without the improvement it is already possible to get high quality data showing the braking tactics of different riders. Moving to four brake sensors instead of two will also has some drawbacks as, time to mount a Sensor-Set and cost of production will increase.

The calibration parameters of the brake sensors are 1.40, 1.09, 1.22 and 1.12. Looking at these four numbers the large differences between them immediately stand out. This is surprising given that the brake sensors are made using the exact same design. The most likely cause of differences in the calibration parameters is the precision of strain gauges application. The strain gauges are applied by hand, the strain gauge location on the aluminium brake pad holder can be closer to the mounting point or brake pad. These different locations could have a slight differences in stiffness possibly resulting in the different input output relations.

F.2.4. Conclusion

From the calibration results it is concluded that the sensor are usable to answer the formulated research question, 'Which are the best braking strategies resulting in a fast and safe cycling technique and optimum use of human power, leading to optimum results'. An improvement in brake data quality can be made by using two instead of one brake sensor per brake calliper. Although this would not be necessary as the current data quality is expected to be sufficient to differentiate braking strategies of different riders.

The calibration parameters that will be used during the experiment are:

- Sensor 1 bike 1 is 1.40 N/step;
- Sensor 2 bike 1 is 1.09 N/step;
- Sensor 1 bike 2 is 1.22 N/step;
- Sensor 2 bike 2 is 1.12 N/step.

G

Brake Data

In this Appendix, the normalised brake data, after removal of zero-offset (see Appendix N) is presented. Section G.1 contains data of the full descent. For a more detailed view of segment 6, Section G.2 can be used, containing only data from segment 6.

G.1. Results of full descent trial

The figures below contain the shifted and normalised brake sensor data for the full descent.

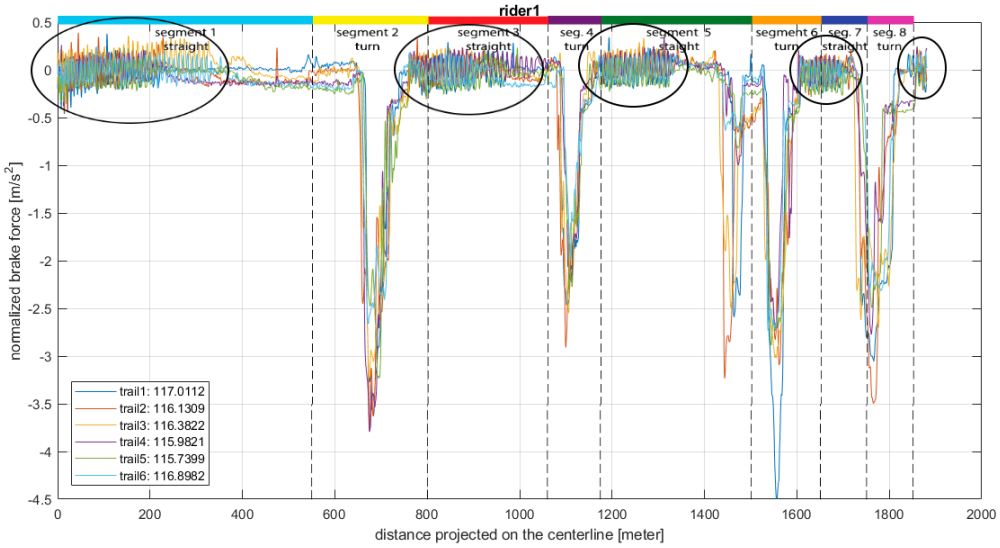

Figure G.1: Brake data from rider 1 with sensor drift removed

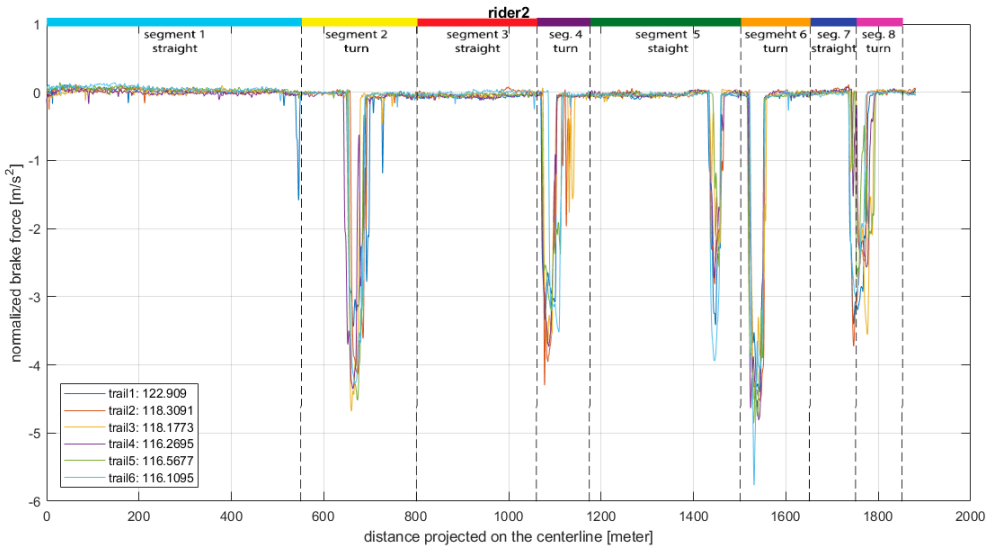

Figure G.2: Brake data from rider 2 with sensor drift removed

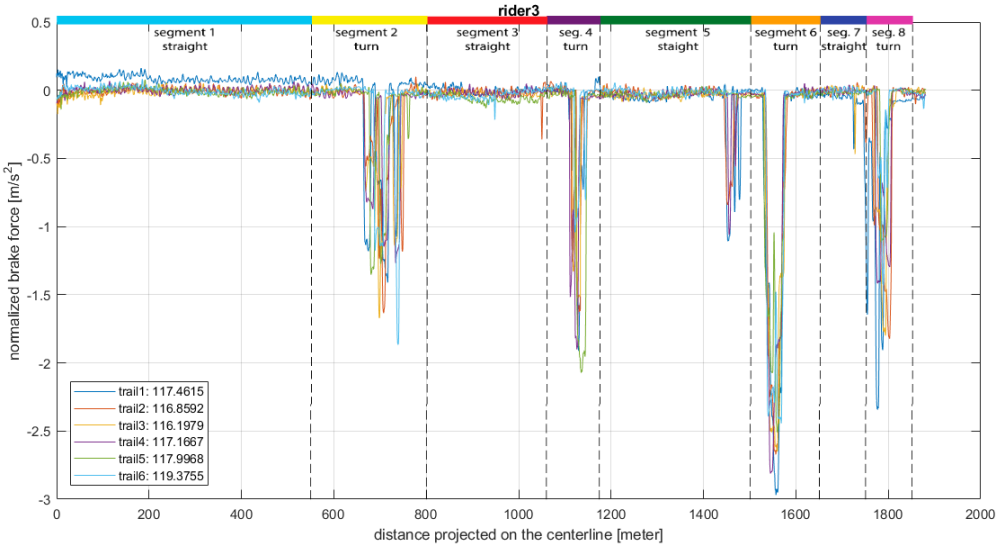

Figure G.3: Brake data from rider 3 with sensor drift removed

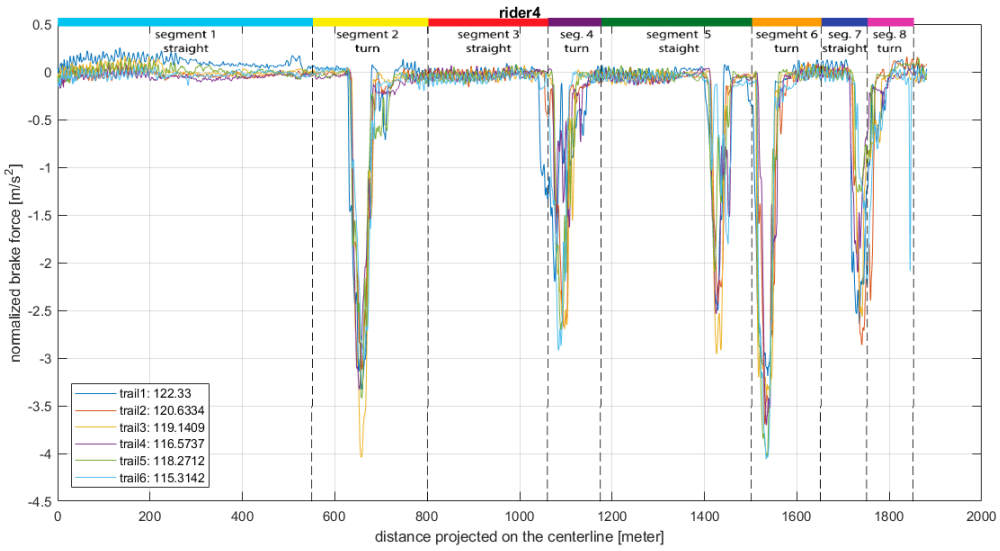

Figure G.4: Brake data from rider 4 with sensor drift removed

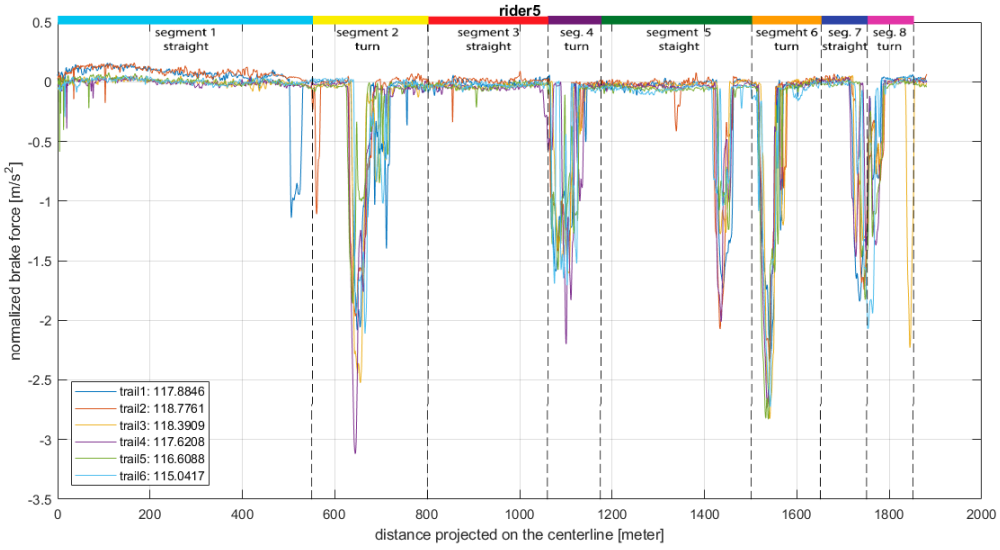

Figure G.5: Brake data from rider 5 with sensor drift removed

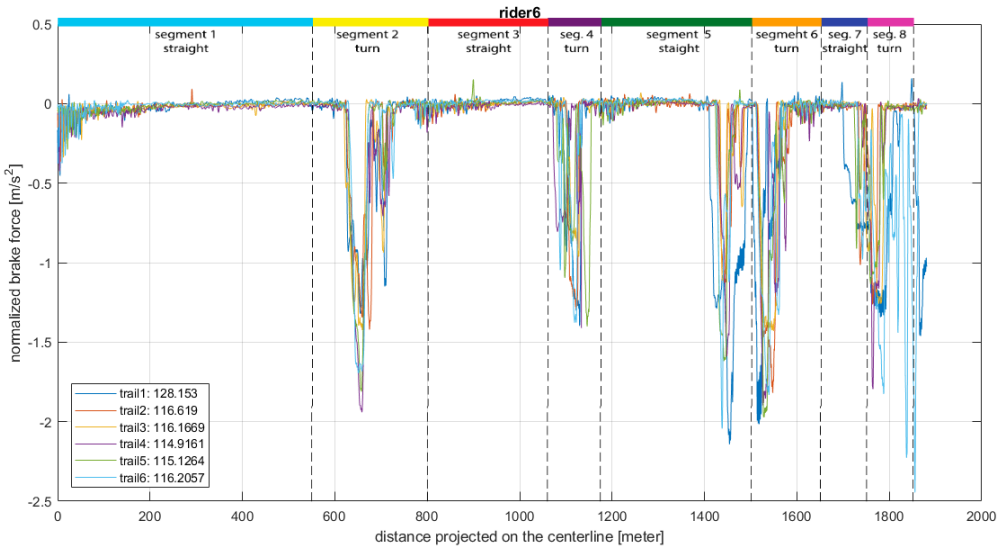

Figure G.6: Brake data from rider 6 with sensor drift removed

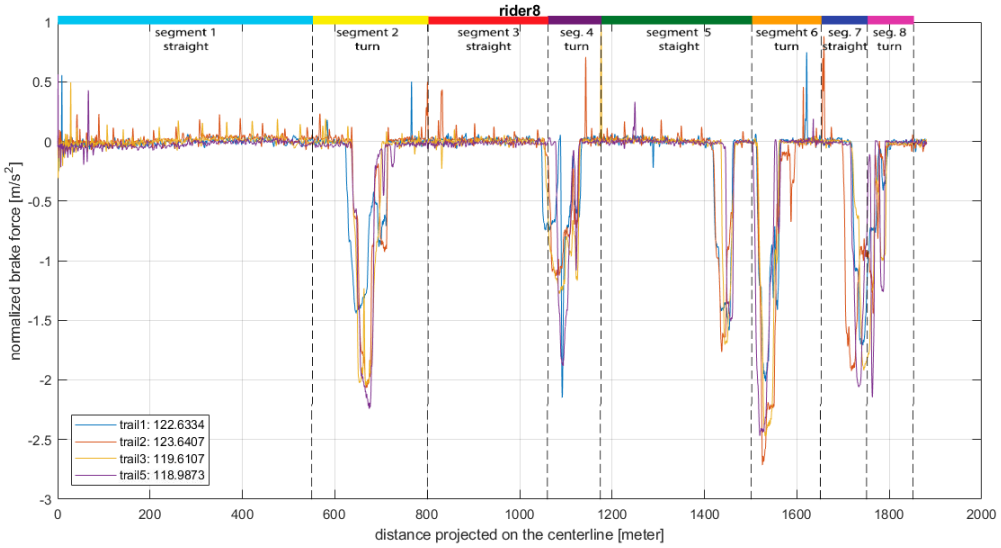

Figure G.7: Brake data from rider 8 with sensor drift removed

G.2. Cornering - Segment 6

The figures below contain plot brake data plot zoomed in on segment 6. Brake sensor data is used for all parameters, except for the break force of riders 1, 2, 3 and 4 as the brake sensor was not properly calibrated. For the brake forces, the dotted forward acceleration data is used as an estimate. The acceleration data needed filtering to make it readable. Filtering is done using a Butterworht filter with 0.75 hz cut of frequency.

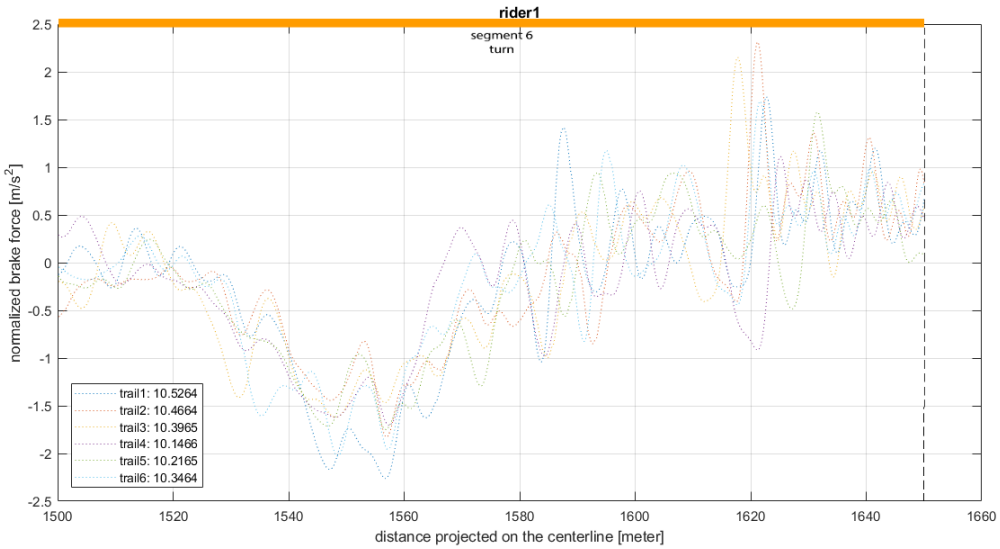

Figure G.8: Estimated brake data from rider 1 with sensor drift removed

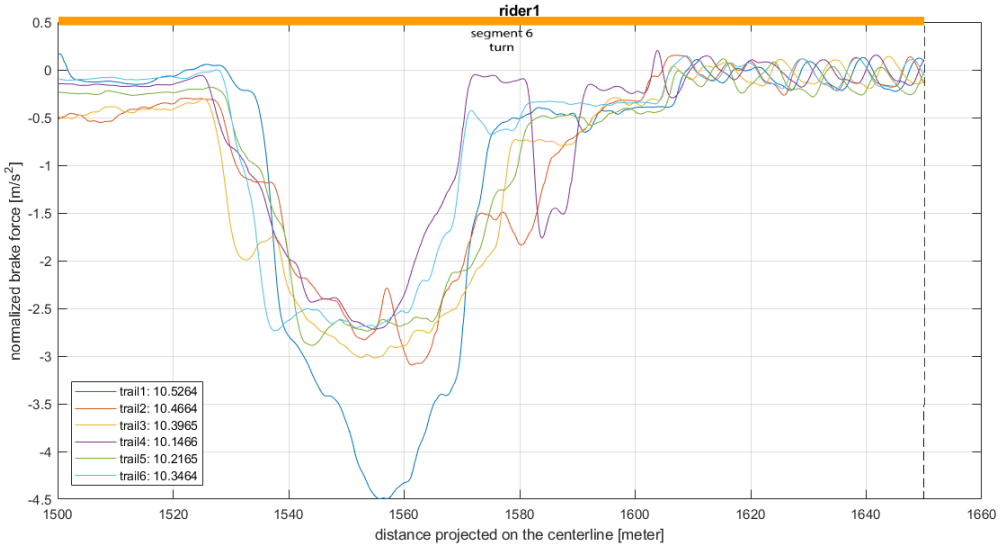

Figure G.9: Brake sensor data from rider 1 with sensor drift removed

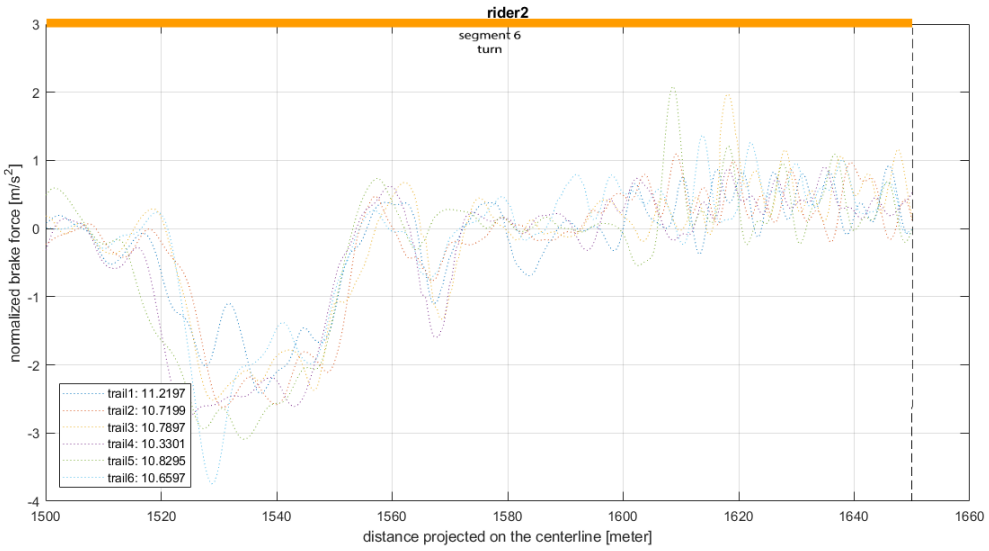

Figure G.10: Estimated brake data from rider 2 with sensor drift removed

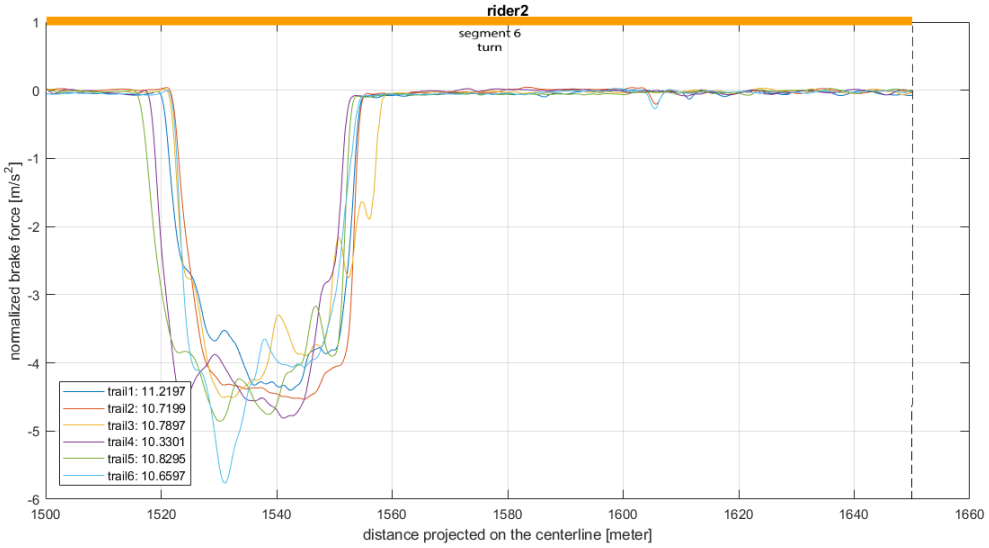

Figure G.11: Brake sensor data from rider 2 with sensor drift removed

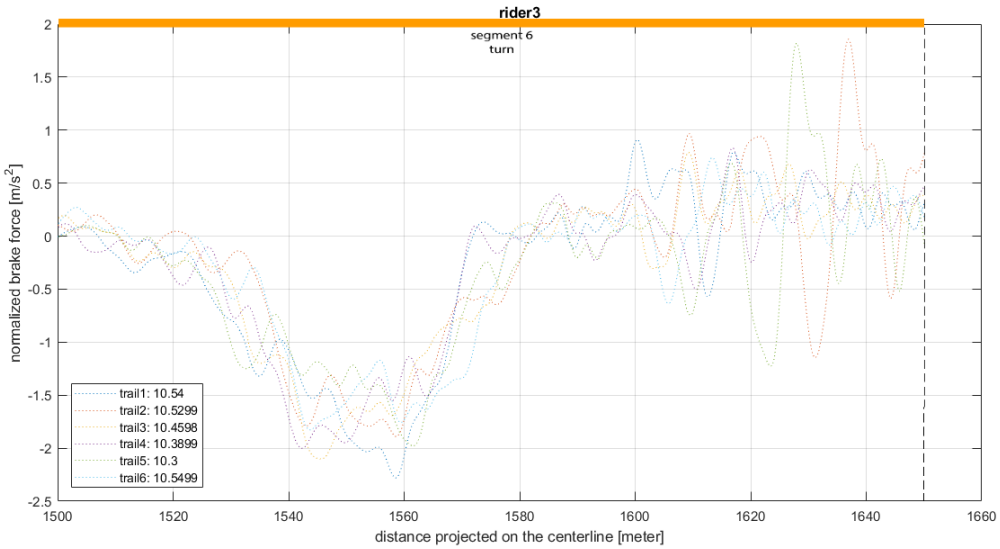

Figure G.12: Estimated brake data from rider 3 with sensor drift removed

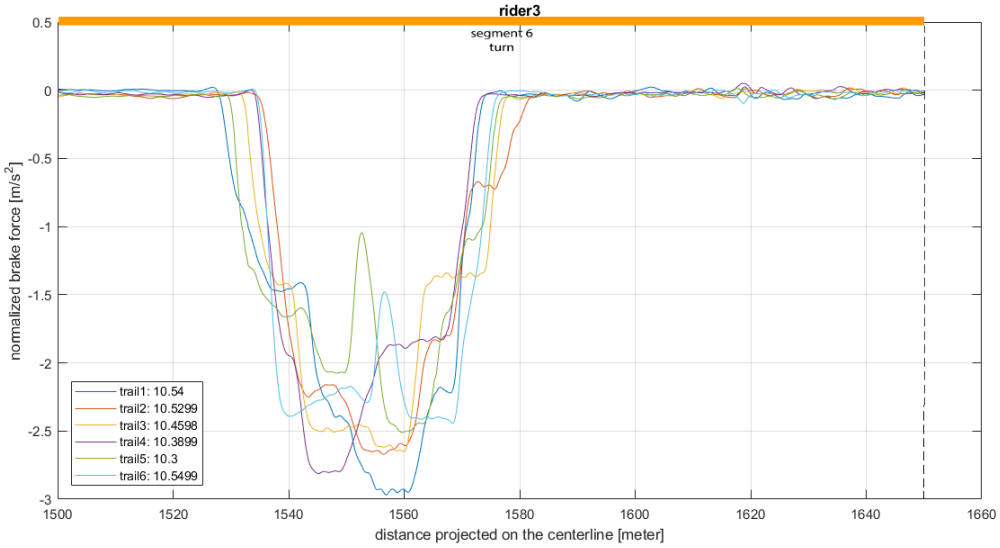

Figure G.13: Brake sensor data from rider 3 with sensor drift removed

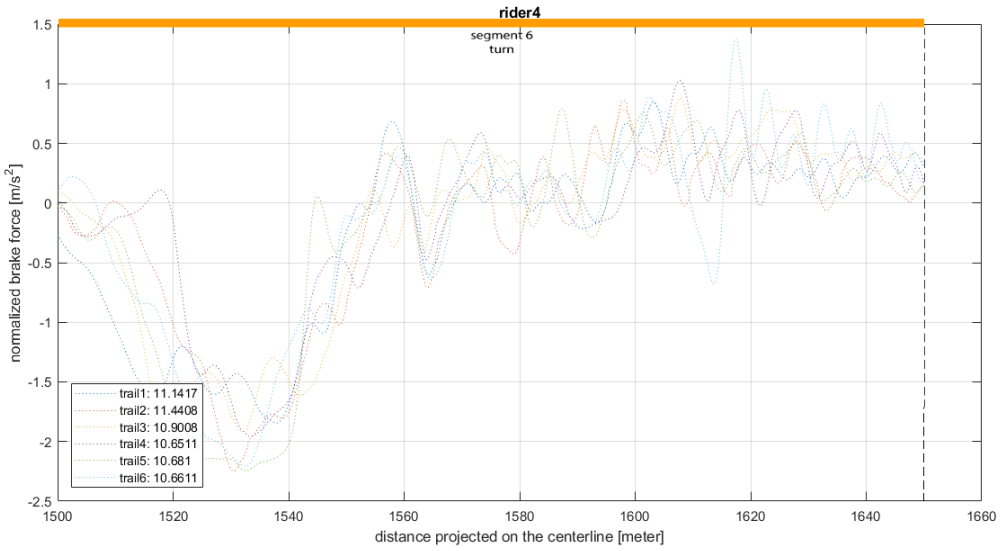

Figure G.14: Estimated brake data from rider 4 with sensor drift removed

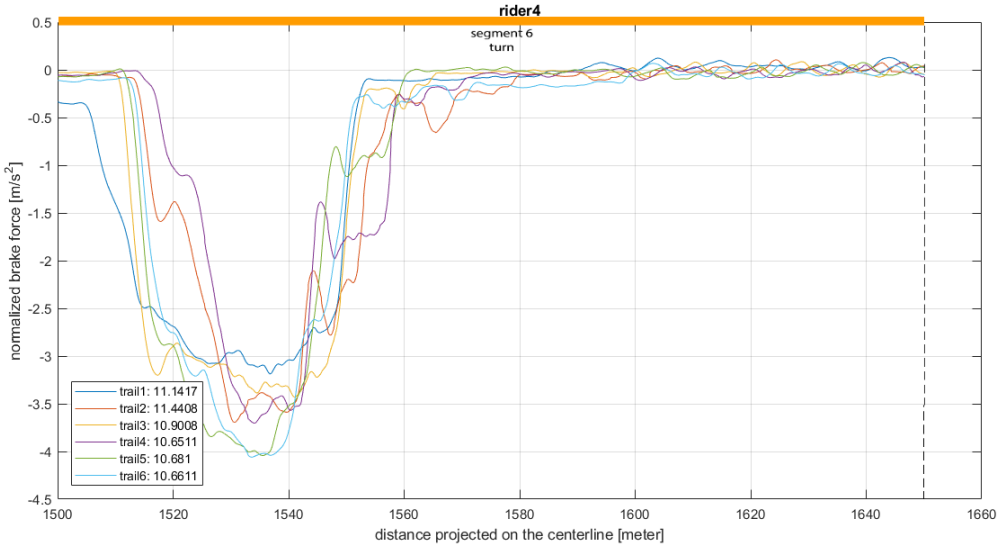

Figure G.15: Brake sensor data from rider 4 with sensor drift removed

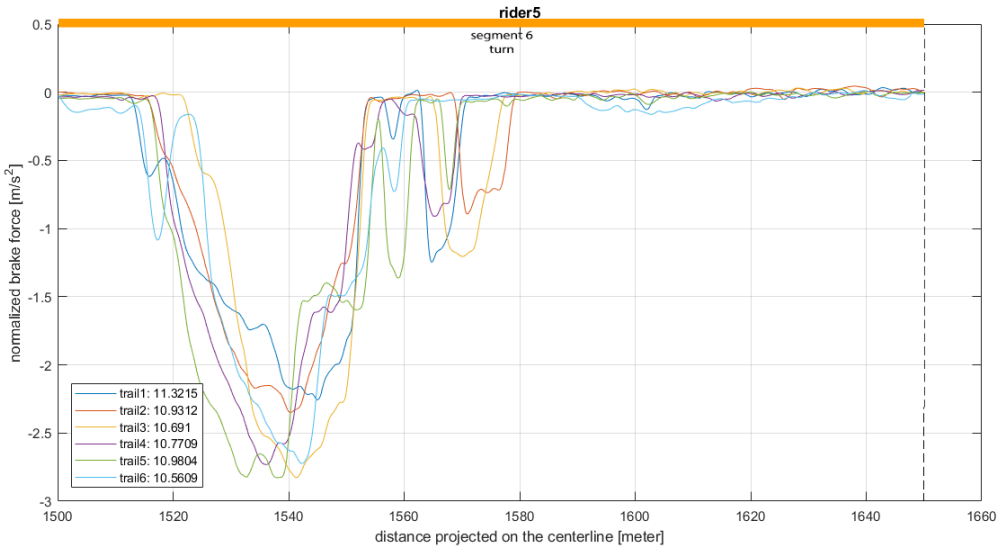

Figure G.16: Brake sensor data from rider 5 with sensor drift removed

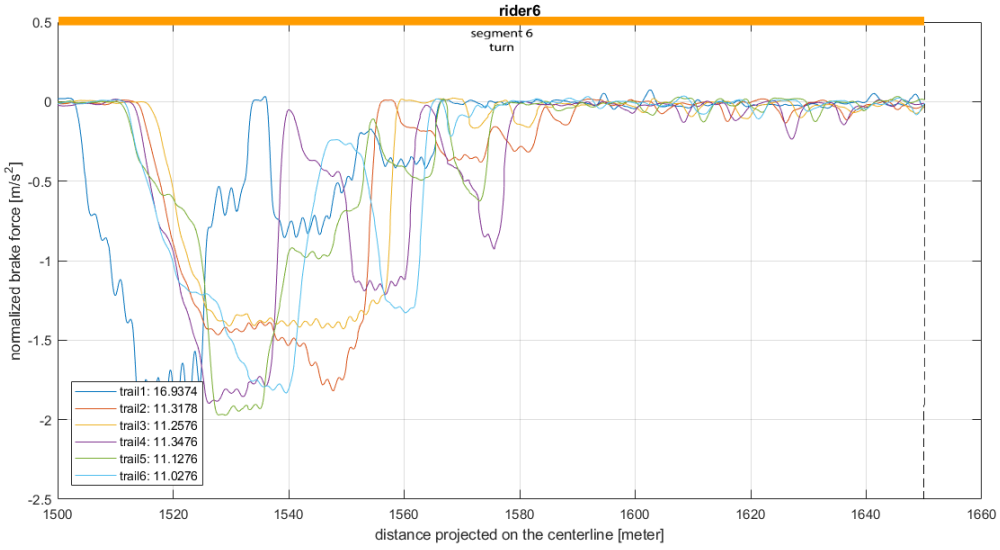

Figure G.17: Brake sensor data from rider 6 with sensor drift removed

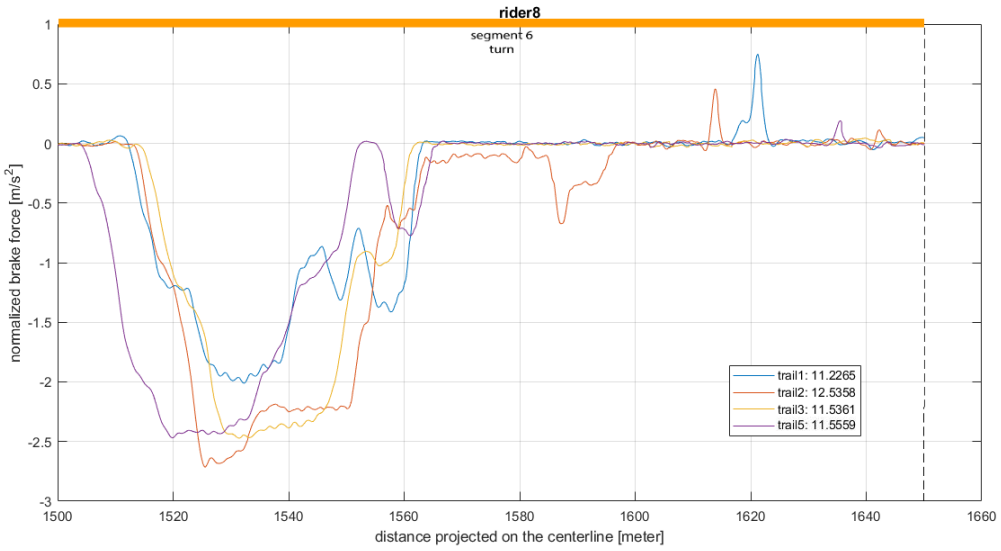

Figure G.18: Brake sensor data from rider 8 with sensor drift removed

H

Re-Calibrated Acceleration Data

This Appendix contains the re-calibrated acceleration data (for re-calibration, see Appendix K.3).

Figure H.1, H.2, H.3, H.4, H.5, H.6 and H.7 show the acceleration in x (forward) direction of all trails per rider.

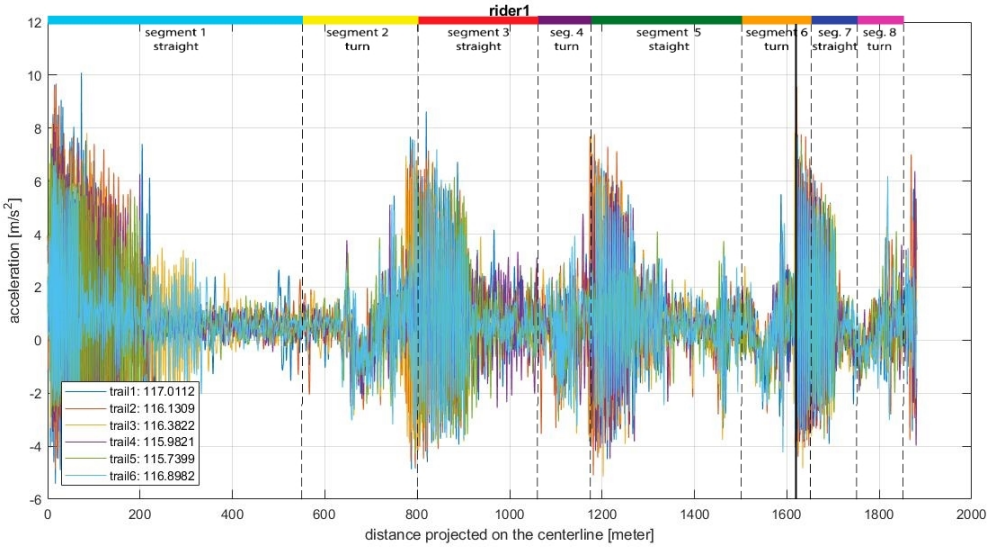

Figure H.1: Forward acceleration of rider 1. Pedalling starts around 1620 m.

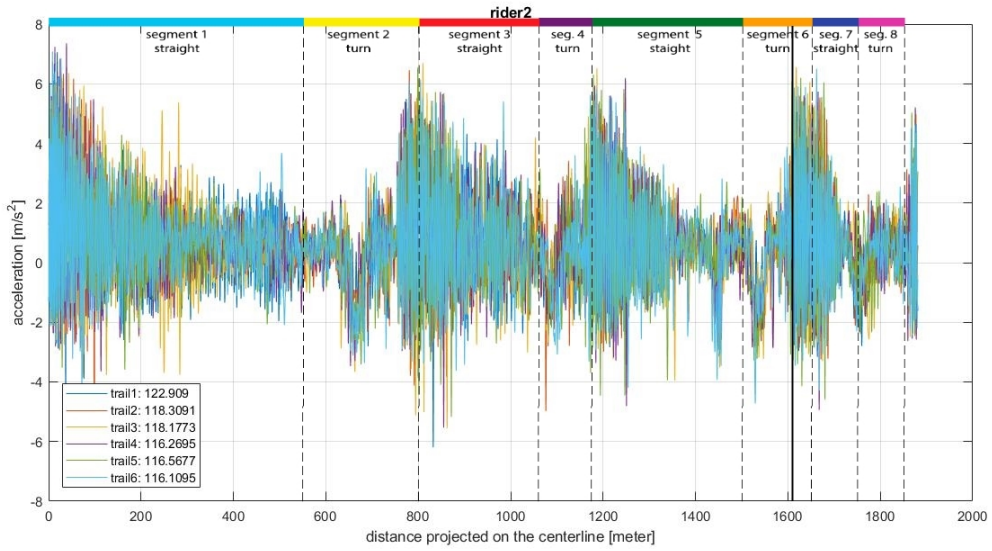

Figure H.2: Forward acceleration of rider 2. Pedalling starts around 1610 m.

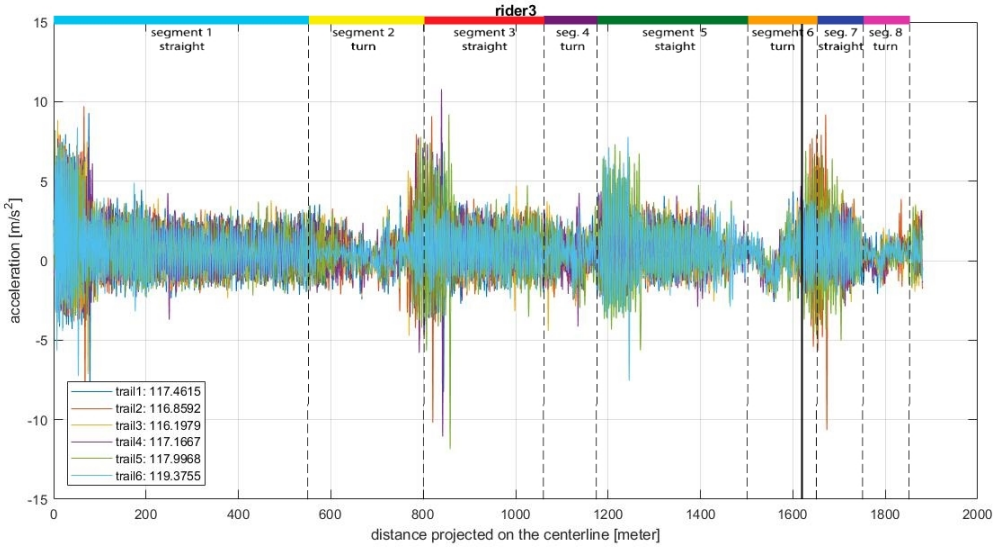

Figure H.3: Forward acceleration of rider 3. Pedalling starts around 1620 m.

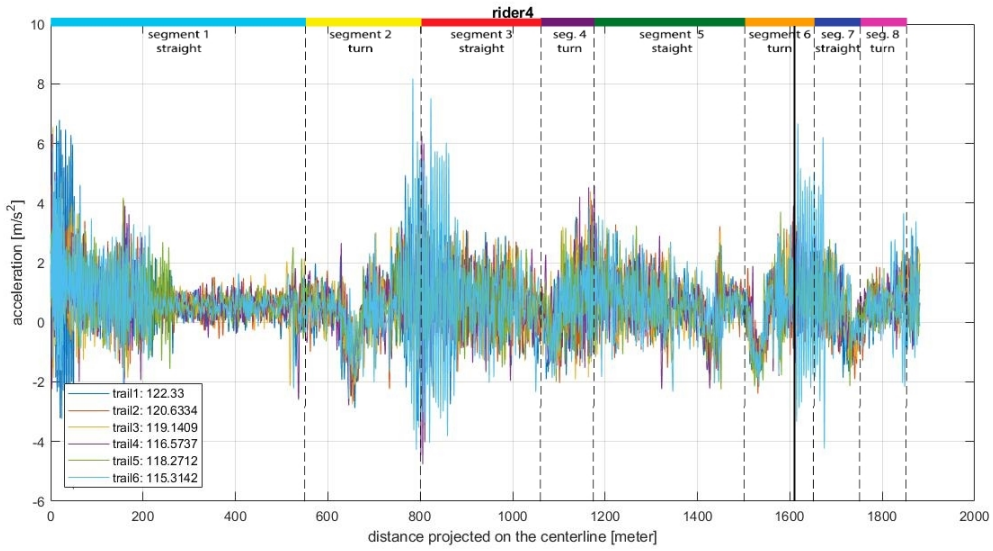

Figure H.4: Forward acceleration of rider 4. Pedalling starts around 1610 m.

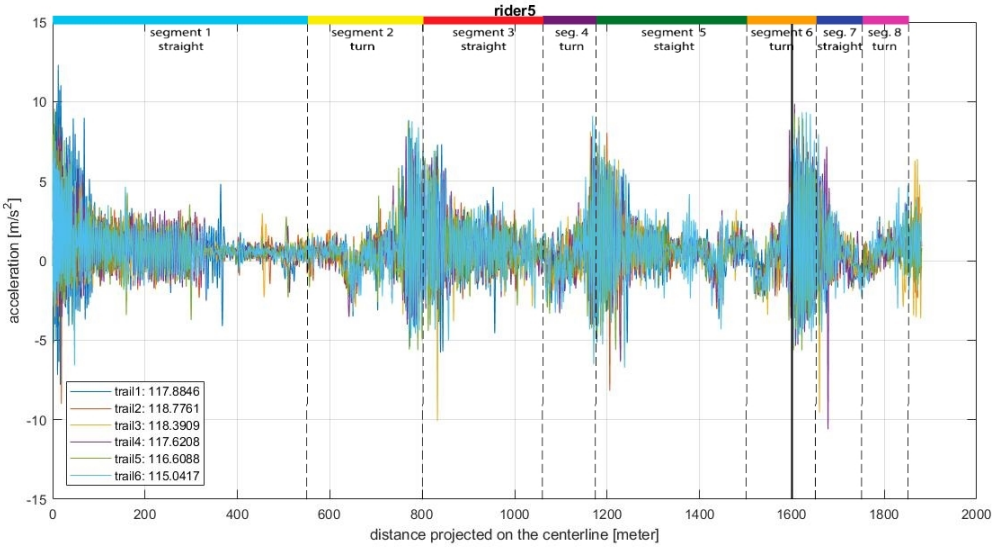

Figure H.5: Forward acceleration of rider 5. Pedalling starts around 1600 m.

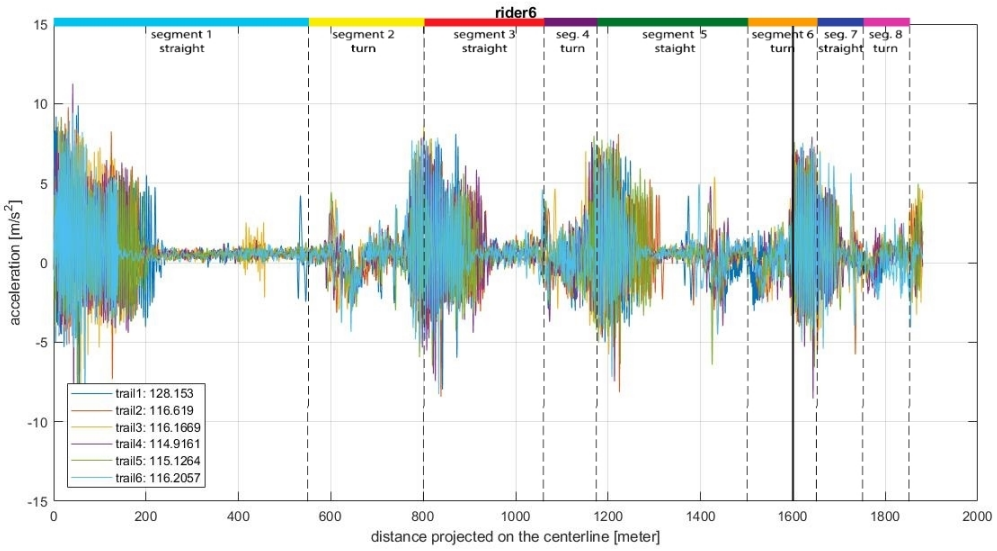

Figure H.6: Forward acceleration of rider 6. Pedalling starts around 1600 m.

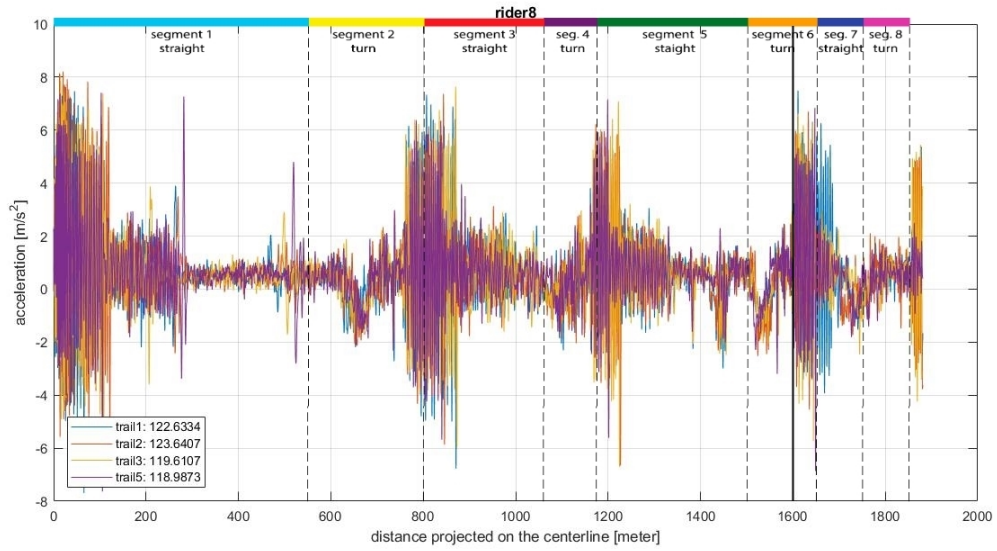

Figure H.7: Forward acceleration of rider 8. Pedalling starts around 1600 m.

Figure H.8, H.9, H.10, H.11, H.12, H.13 and H.14 show the acceleration in y (sideways) direction of all trails per rider.

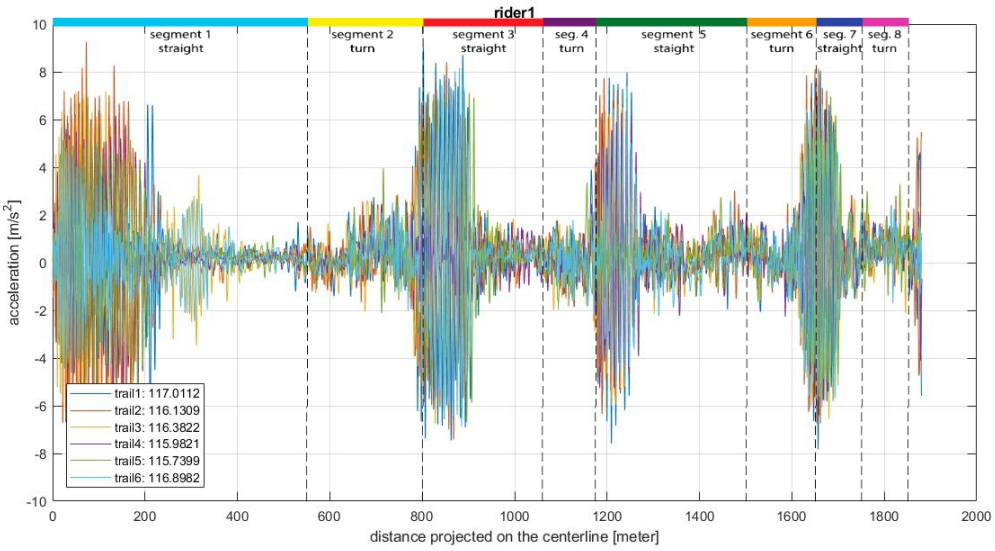

Figure H.8: Sideways acceleration of rider 1.

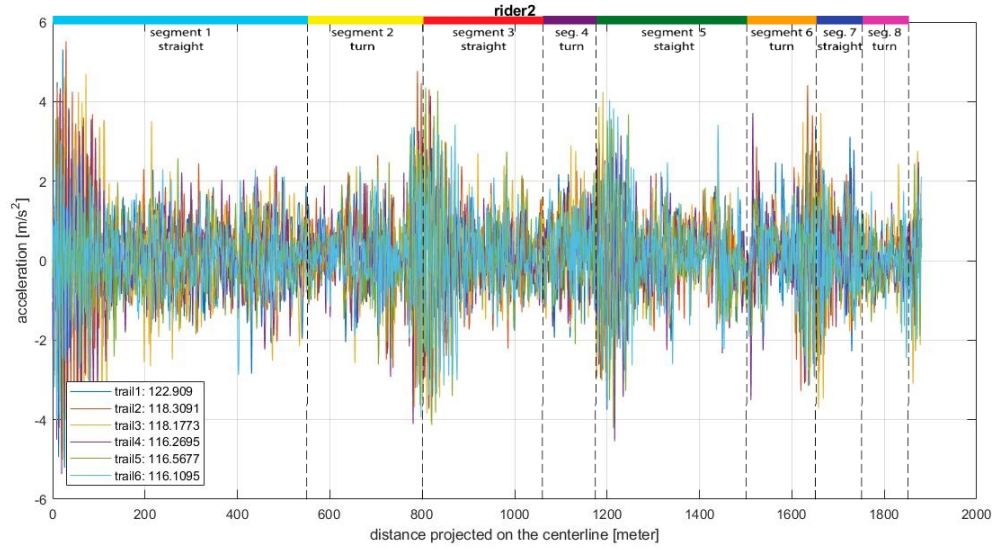

Figure H.9: Sideways acceleration of rider 2.

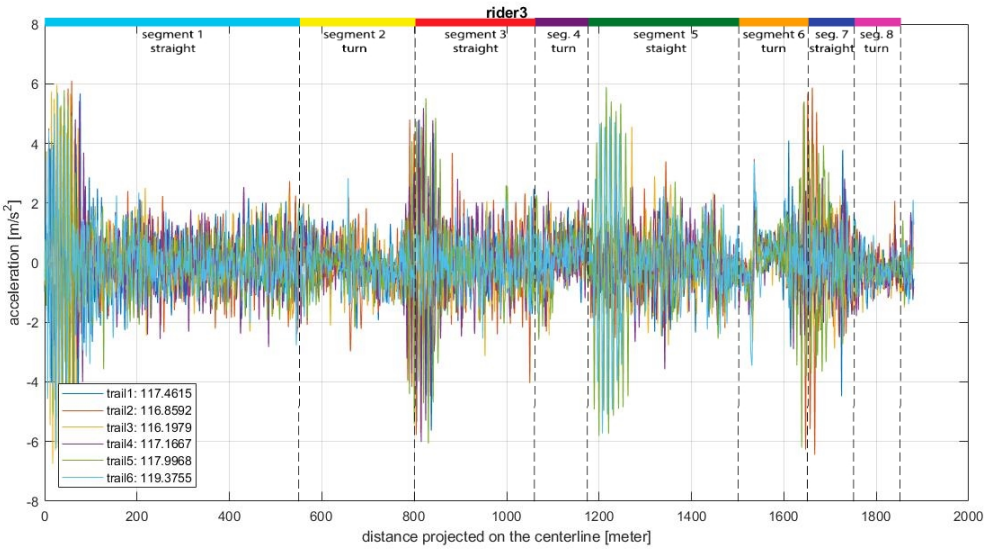

Figure H.10: Sideways acceleration of rider 3.

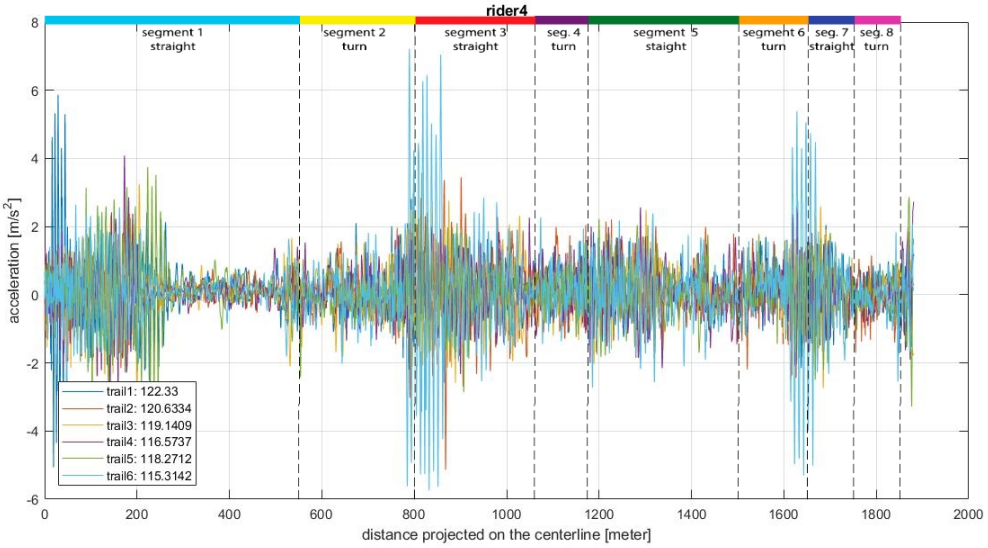

Figure H.11: Sideways acceleration of rider 4.

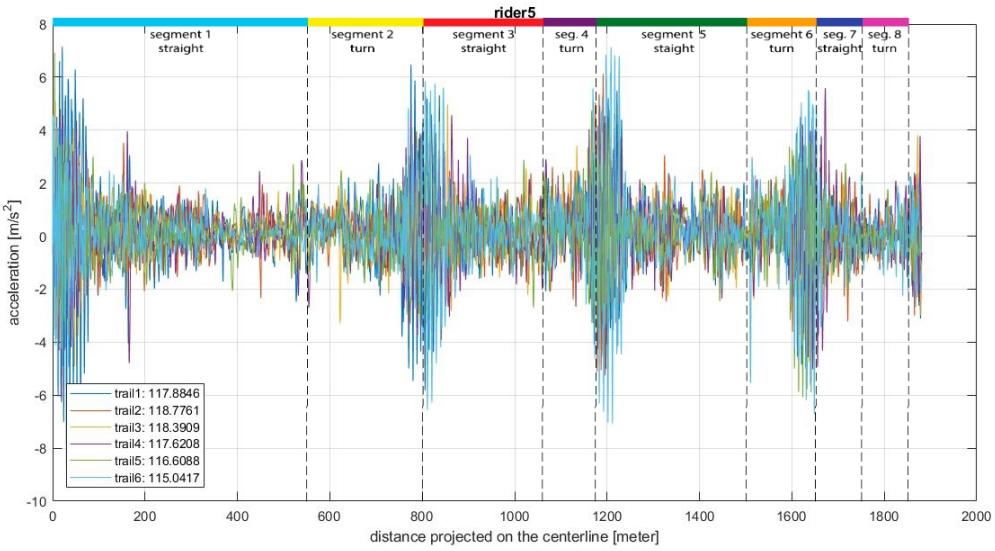

Figure H.12: Sideways acceleration of rider 5.

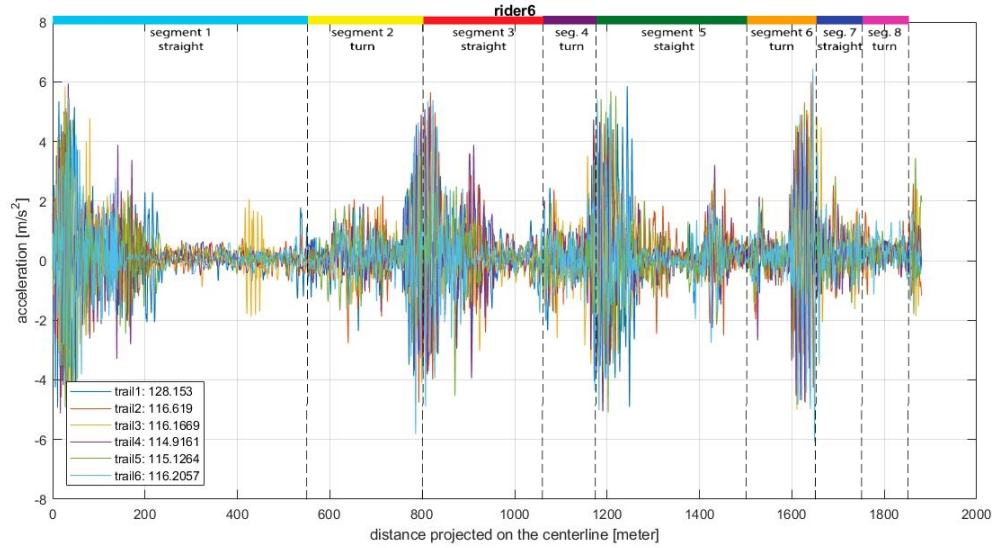

Figure H.13: Sideways acceleration of rider 6.

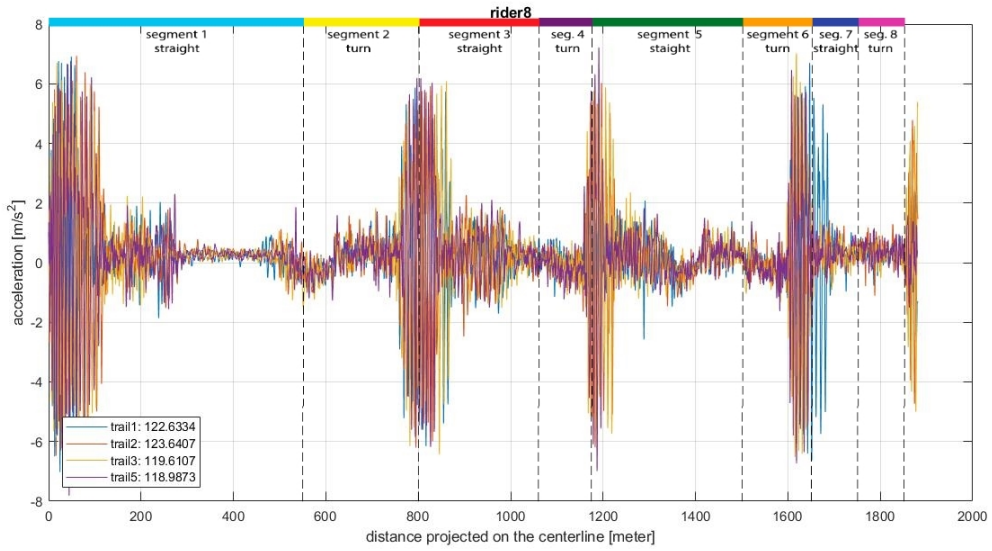

Figure H.14: Sideways acceleration of rider 8.

Figure H.15, H.16, H.17, H.18, H.19, H.20 and H.21 show the acceleration in z (upwards direction) direction of all trials per rider.

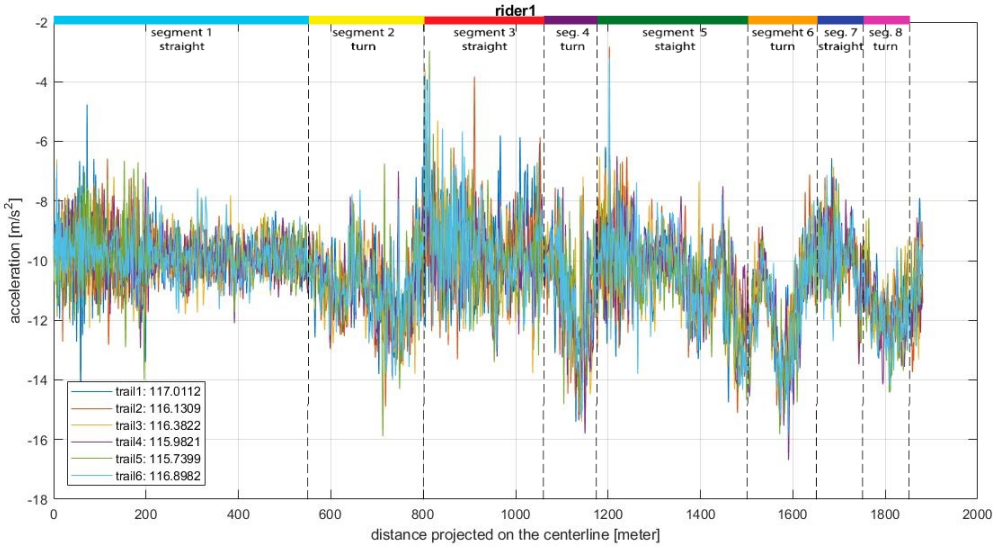

Figure H.15: Upwards acceleration of rider 1.

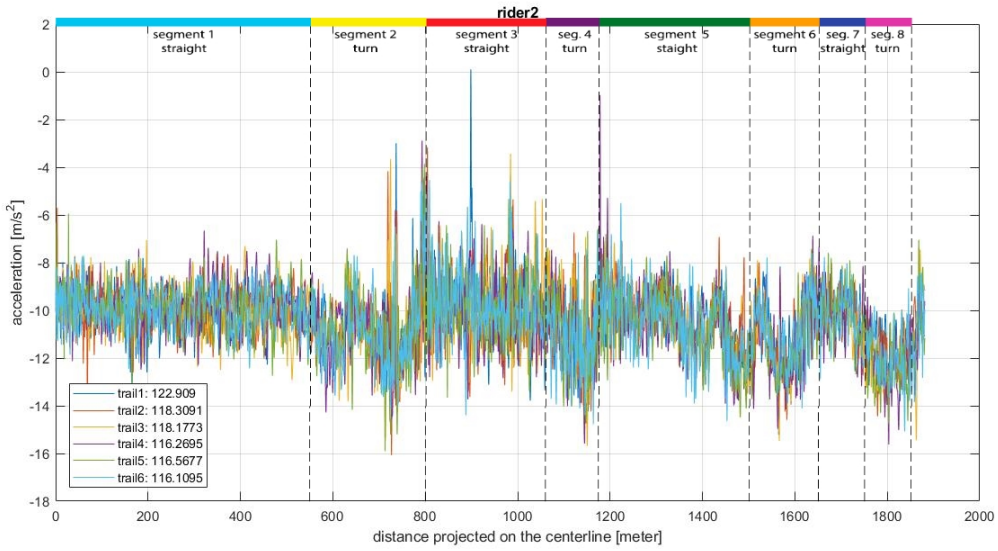

Figure H.16: Upwards acceleration of rider 2.

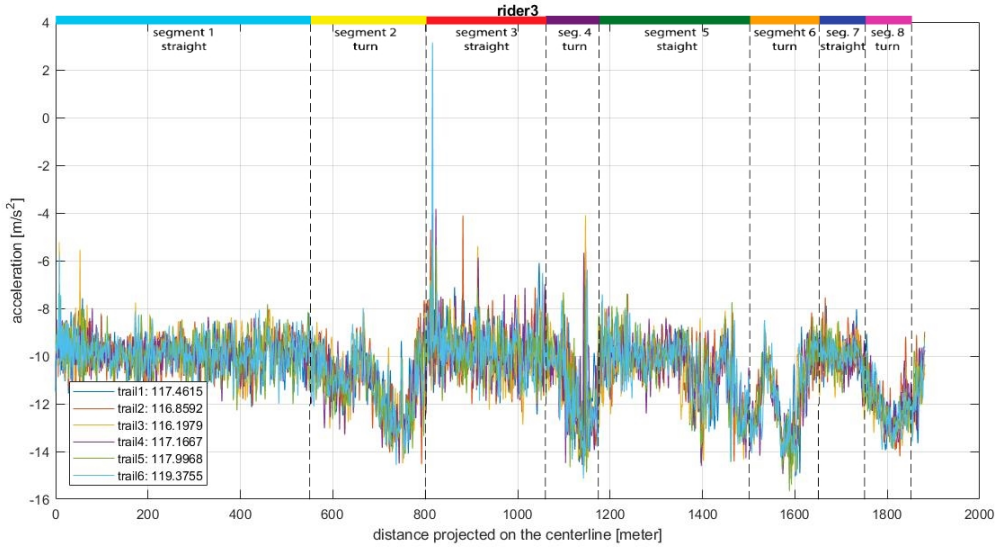

Figure H.17: Upwards acceleration of rider 3.

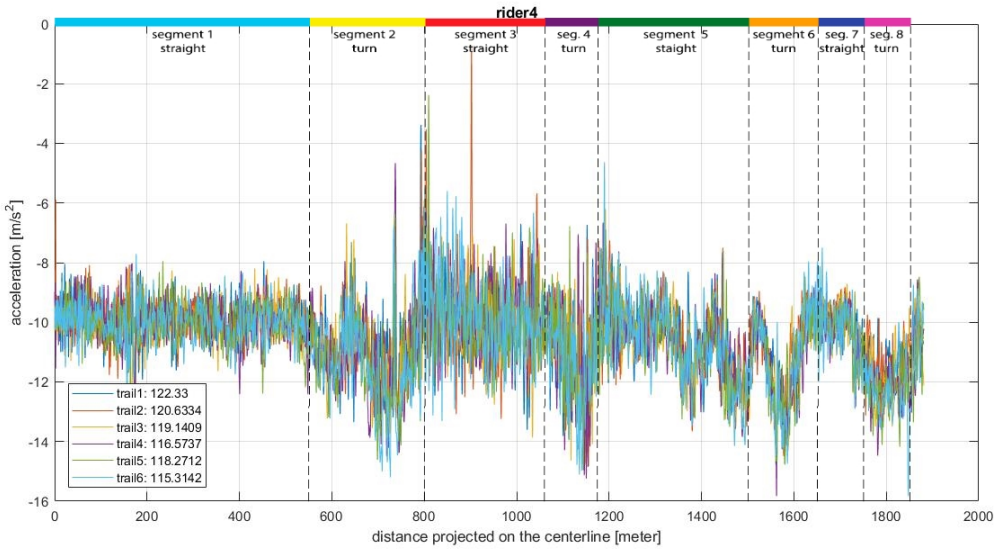

Figure H.18: Upwards acceleration of rider 4.

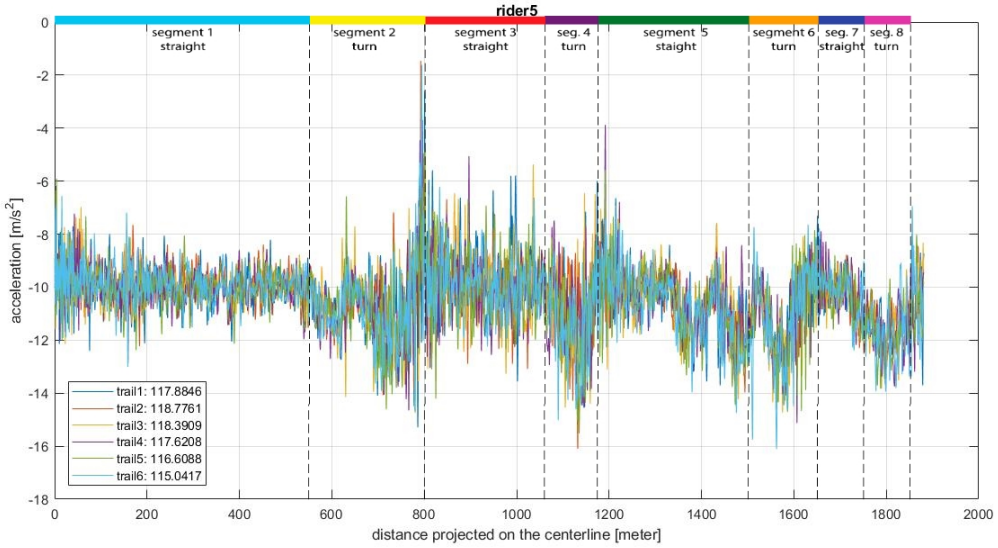

Figure H.19: Upwards acceleration of rider 5.

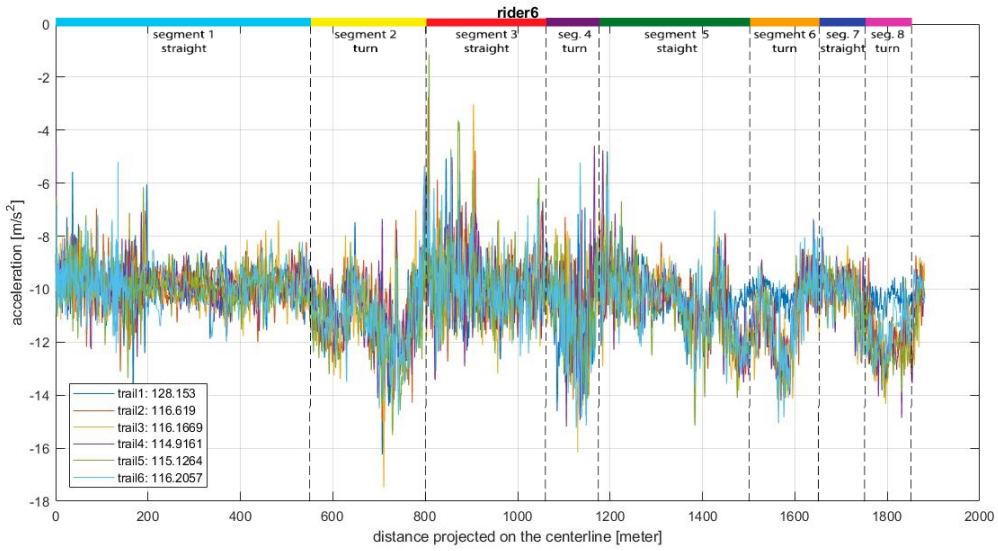

Figure H.20: Upwards acceleration of rider 6.

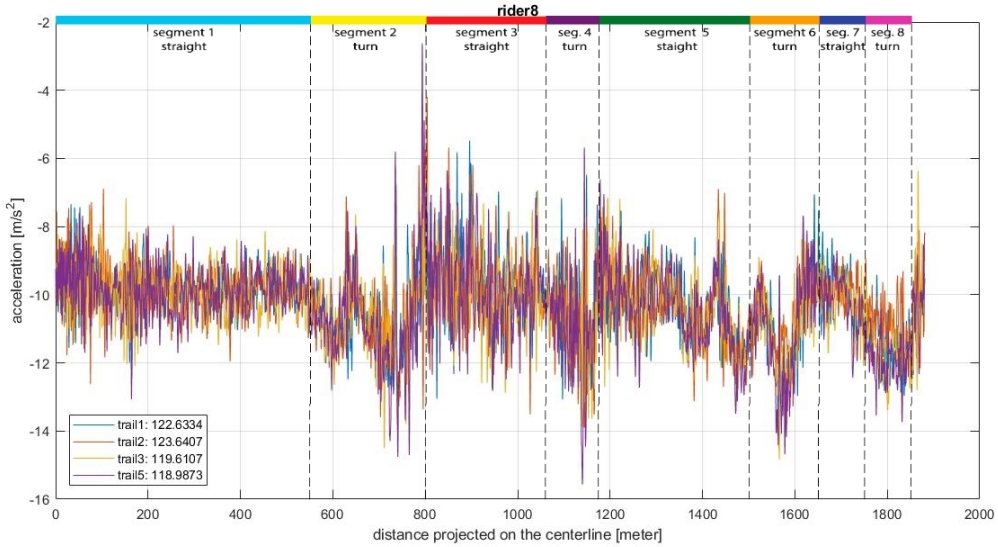

Figure H.21: Upwards acceleration of rider 8.

Speed Data

I.1. Results of Full Descent Trials

This Appendix contains plots with GPS speed data for whole descend. Any GPS recording gaps are filled in using the accelerometer data in combination with forward integration[1].

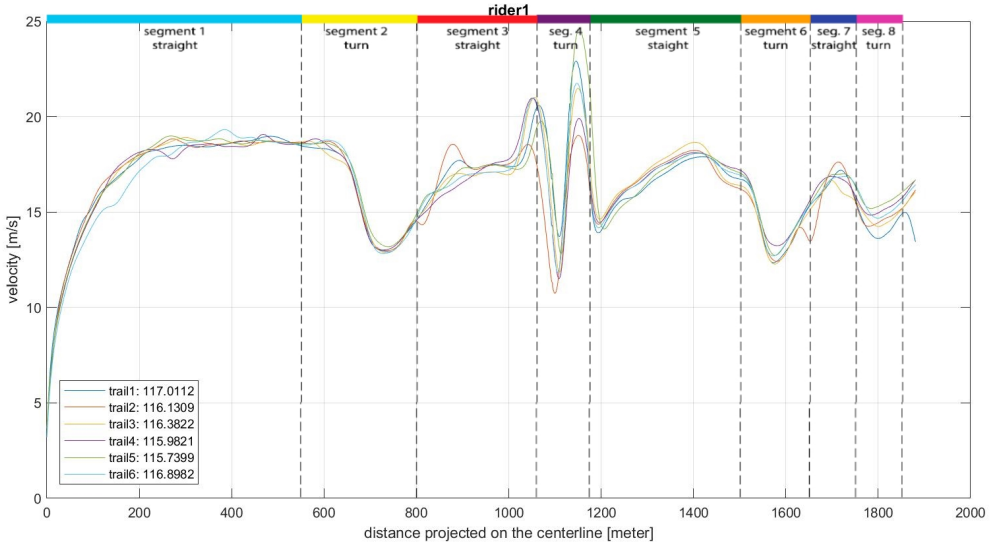

Figure I.1: Speed data rider 1

[1] credit is due to Marco Reijne for making the Matlab script.

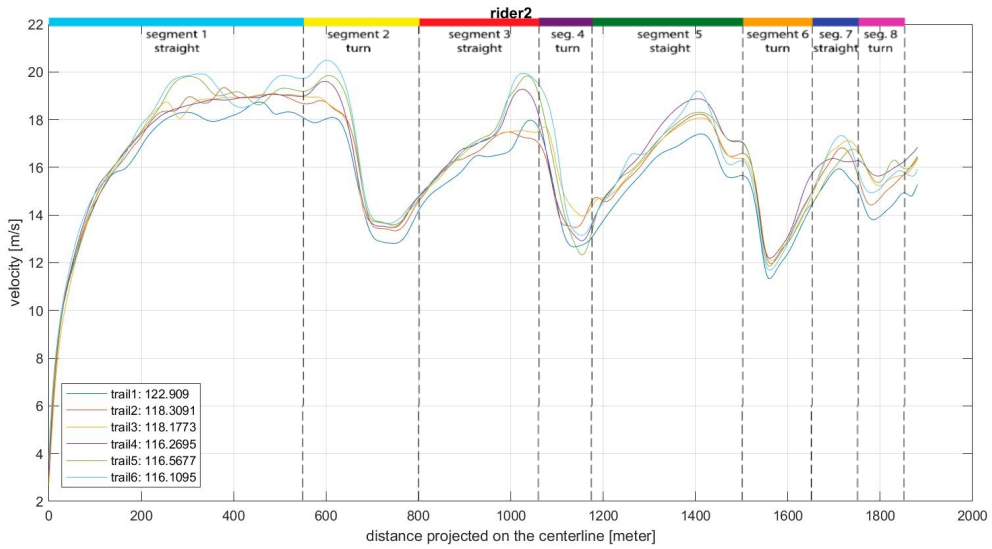

Figure I.2: Speed data rider 2

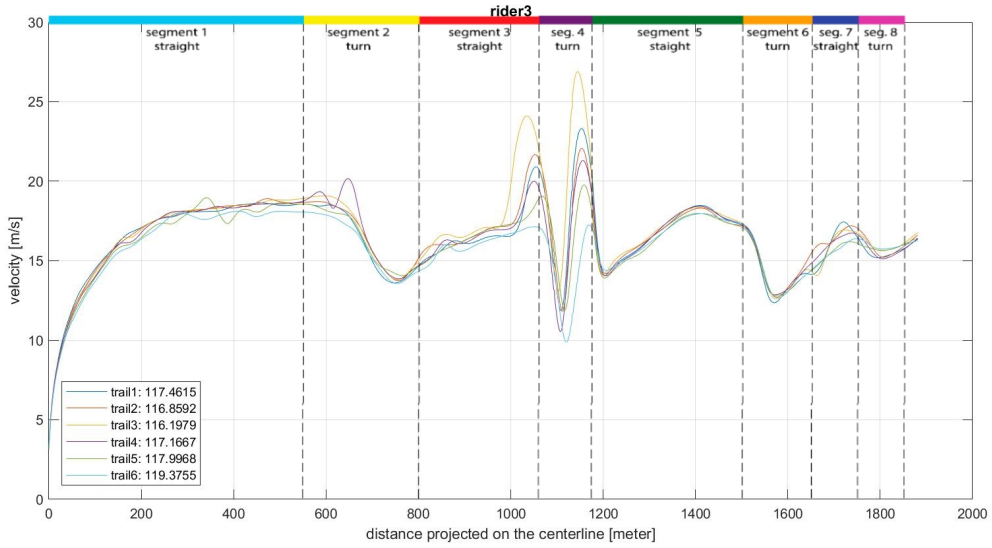

Figure I.3: Speed data rider 3

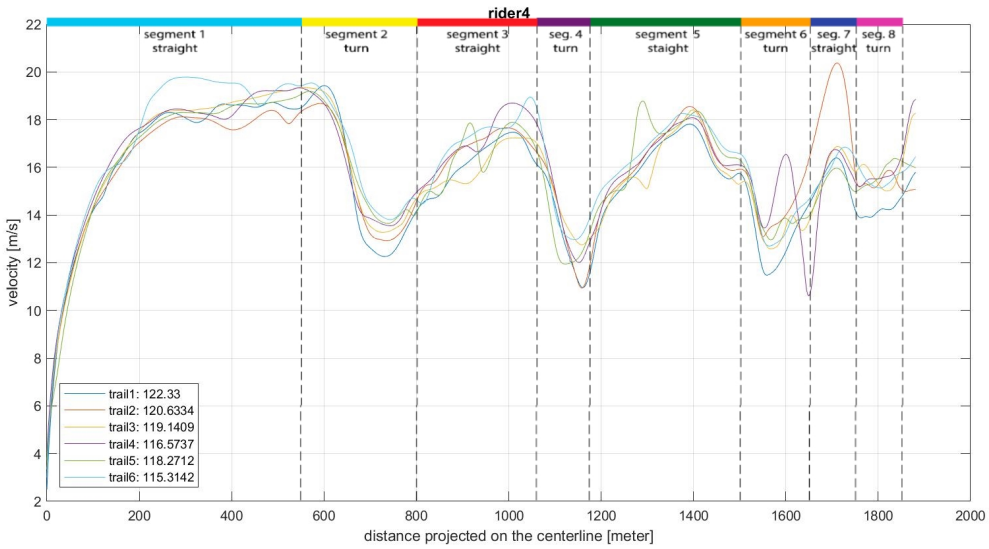

Figure I.4: Speed data rider 4

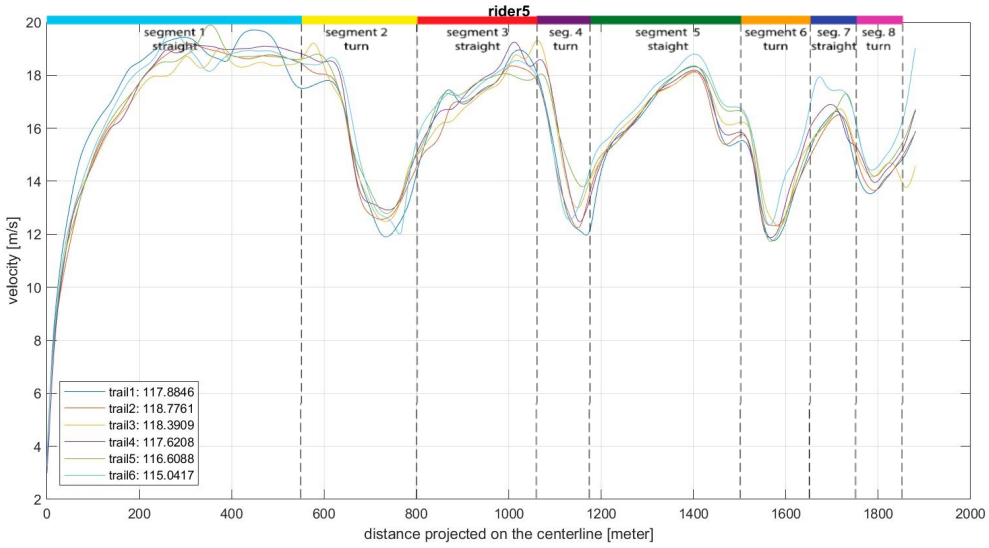

Figure I.5: Speed data rider 5

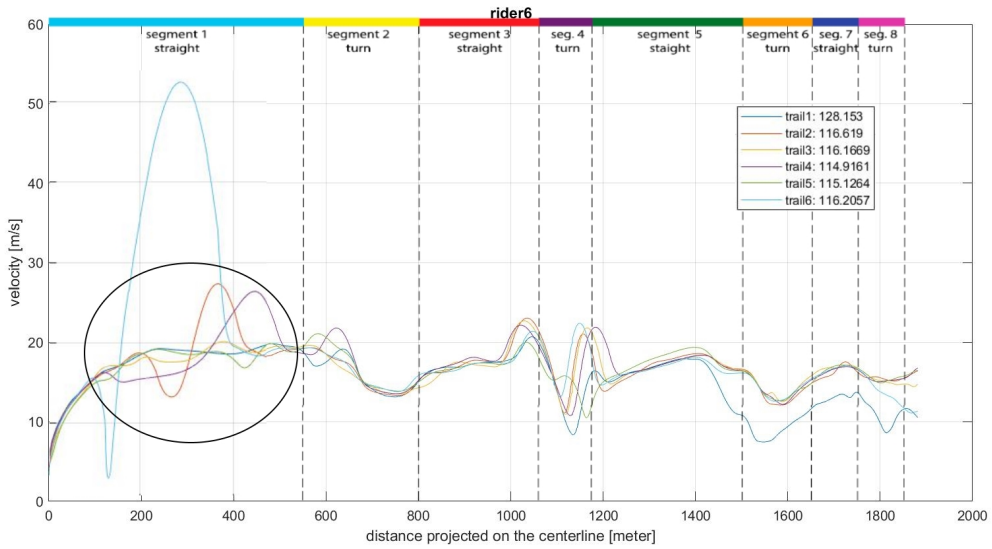

Figure I.6: Speed data rider 6. In the area marked with a circle, GPS signal is lost.

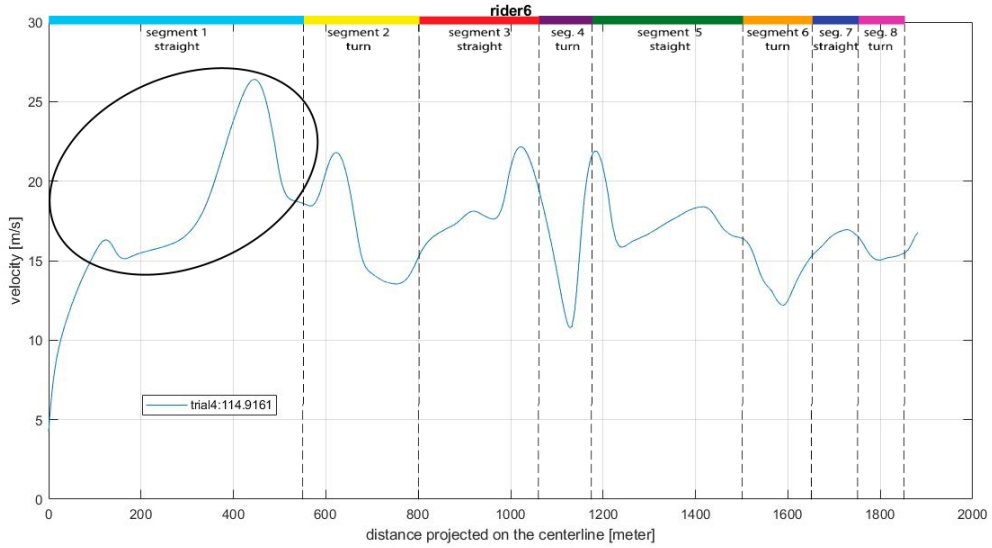

Figure I.7: Speed data rider 6. In the area marked with a circle, GPS signal is lost.

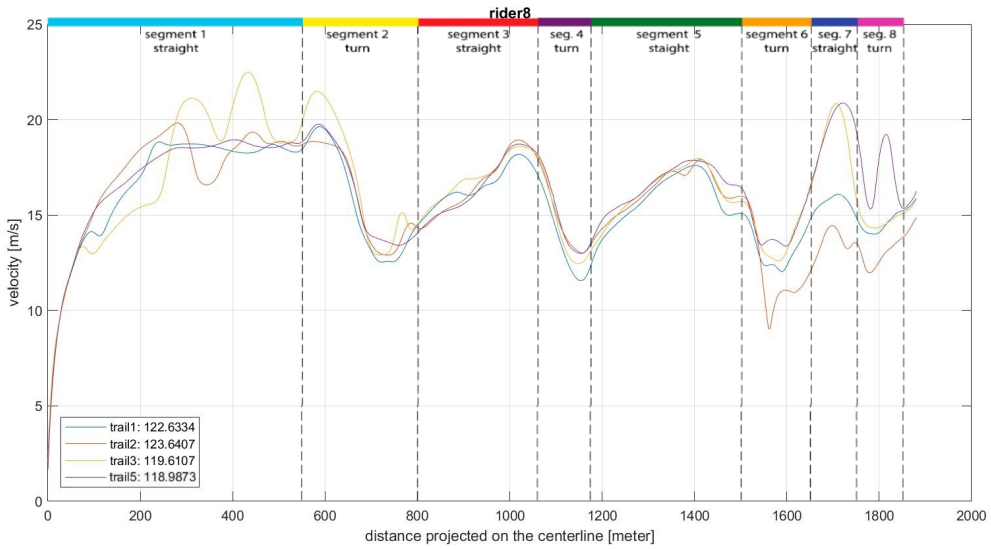

Figure I.8: Speed data rider 8

I.2. Cornering - Segment 6

This section contains the speed data for segment 6 only.

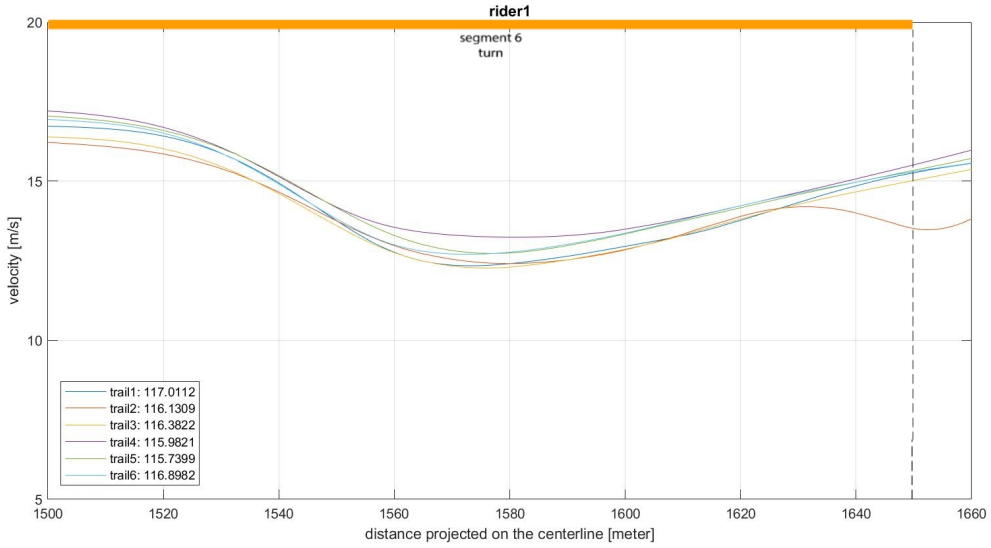

Figure I.9: Speed data rider 1

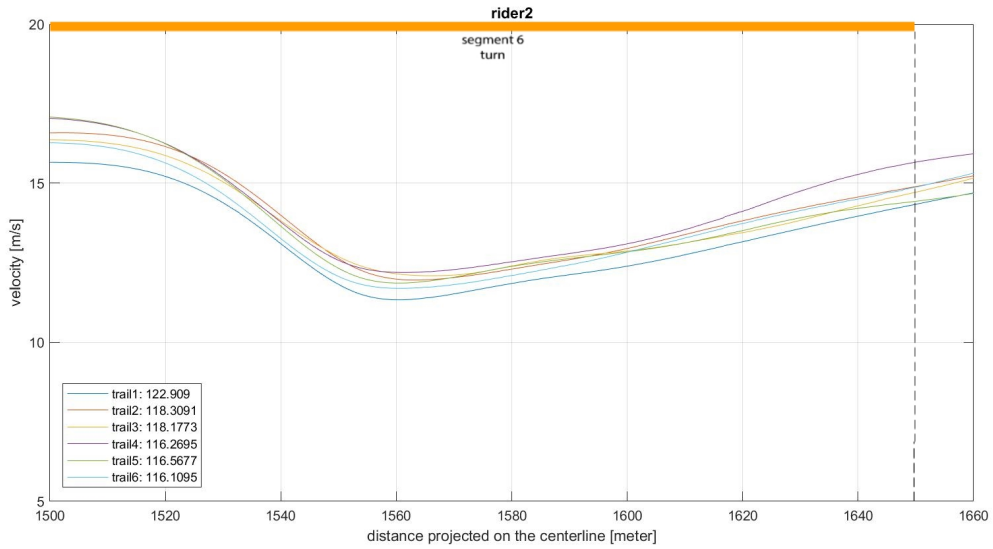

Figure I.10: Speed data rider 2

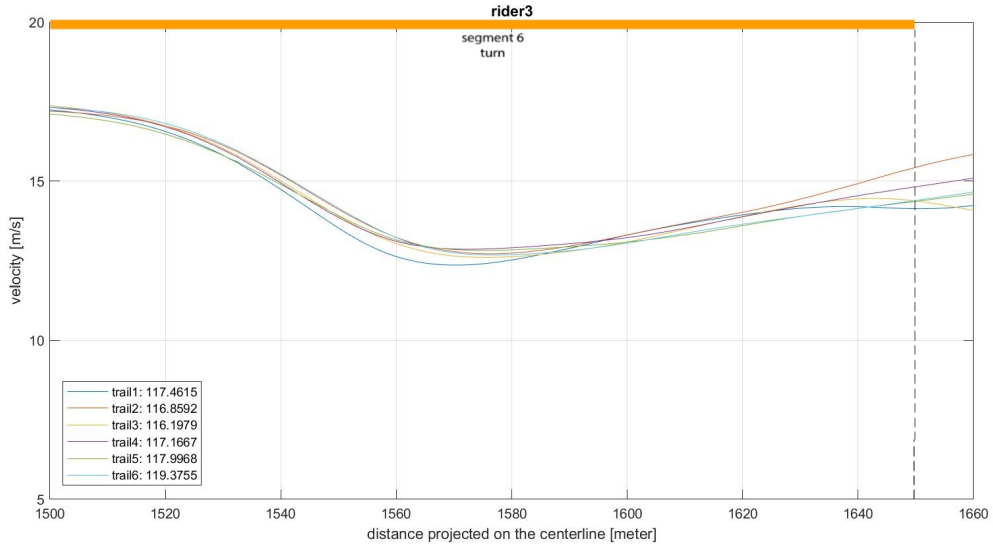

Figure I.11: Speed data rider 3

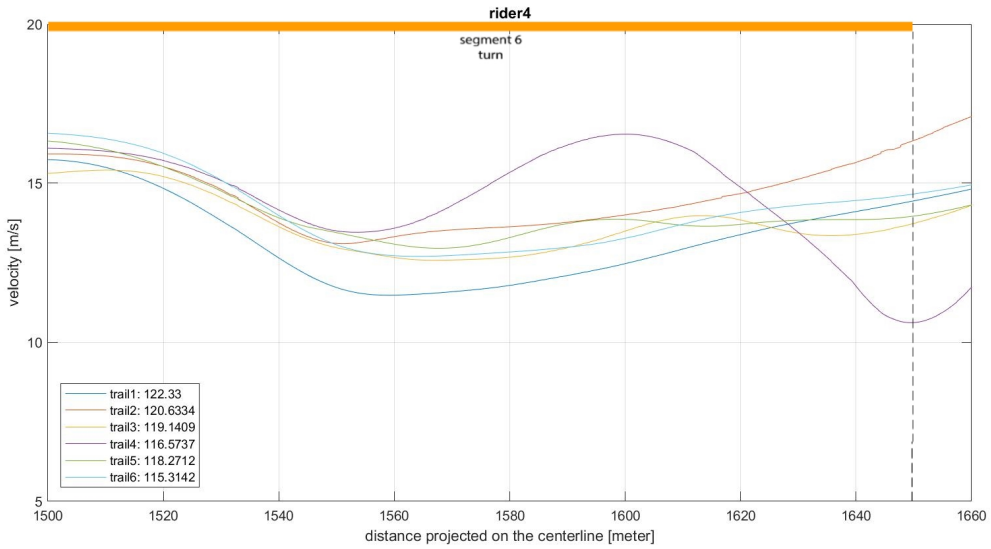

Figure I.12: Speed data rider 4

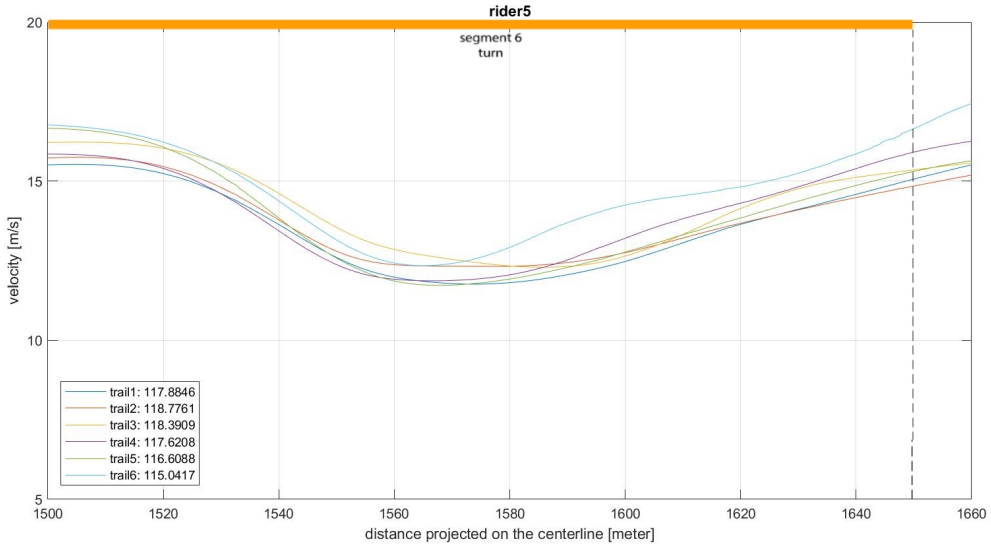

Figure I.13: Speed data rider 5

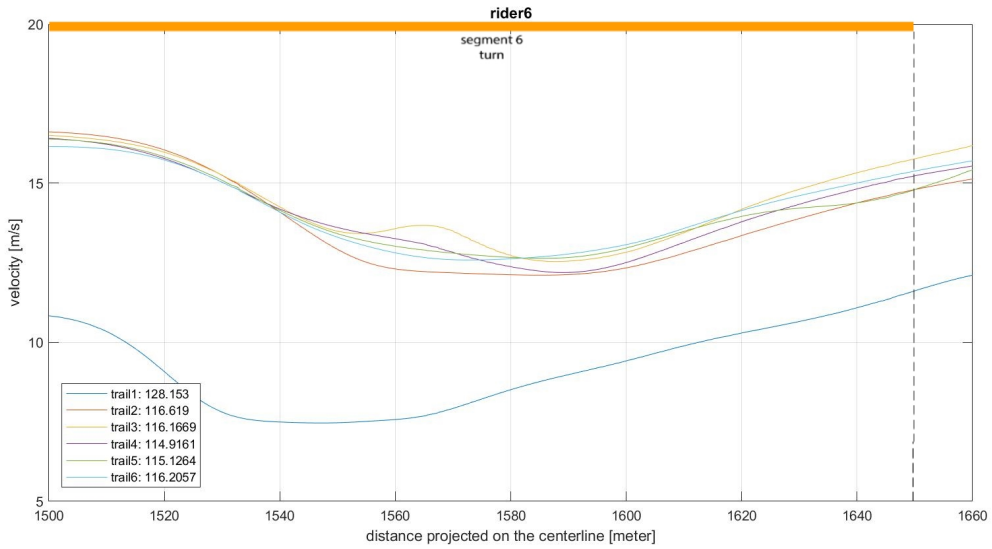

Figure I.14: Speed data rider 6

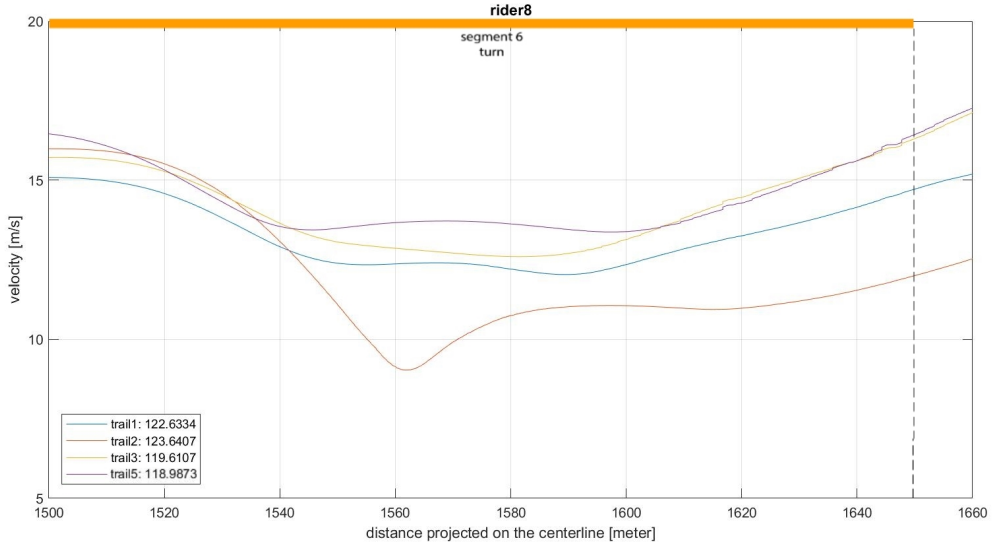

Figure I.15: speed data rider 8

J

Rider Remarks

Listed below are the remarks given by each rider after finishing a trial.

Rider 1:
Trail 1: No
Trail 2: Knee against steering angle sensor, changed position during the descent from saddle to top tube.
Trail 3: Tired legs
Trail 4: No
Trail 5: Pedal hit the ground, leg against steering handle
Trail 6: Forgot to put on glasses, did this during the descent, happy during the descent as this is the last one.

Rider 2:
Trail 1: Knee hit the measurement system
Trail 2: No
Trail 3: No
Trail 4: No
Trail 5: Brake in the last corners for car
Trail 6: No

Rider 3:
Trail 1: No, pedal hit the ground
Trail 2: Last corner there was a motorbike on the other side
Trail 3: No
Trail 4: Motorbike on the other side in turn
Trail 5: Feels not safe with motorbikes
Trail 6: Less power and less concentration

Rider 4:
Trail 1: Saw a rock on the road
Trail 2: No
Trail 3: No
Trail 4: No
Trail 5: Did not click immediately into the pedal at the start
Trail 6: Stones in the corner

Rider 5:
Trail 1: No
Trail 2: More on technique than speed
Trail 3: Car form the right
Trail 4: No
Trail 5: Caught up with a car

Trail 6: No

Rider 6:
Trail 1: Motor in the way
Trail 2: No
Trail 3: No
Trail 4: No
Trail 5: No
Trail 6: Car in the way

Rider 8:
Trail 1: 3rd of 4th corner is very wet, touched the steering angle sensor, different handling due to camera
Trail 2: Caught up with a car
Trail 3: Getting into it
Trail 4: Best one yet
Trail 5: The best
Trail 6: Road is slowly drying

K

Re-Calibrating the Accelerometer

As shown in Appendix L. The original method used to calculate acceleration data in the bike frame coordinates, resulted in low data quality.

The best method to get acceleration data in the bike frame coordinates would be to calibrate the accelerometer in the bike frame coordinates when mounted on the bicycle.
With the frame size differences between the bicycles, calibration is dependent on the used bicycle. As a result, a new calibration would be needed after switching the Sensor-Set. This would increase the time needed to switch the Sensor-Sets between bikes.

Another solution is to calibrate the accelerometer in the Sensor-Set frame. The calibrated data can then be rotated around the y-axis (side ways direction of bicycle and Sensor-Set). The question is the amount of rotation needed the go from Sensor-Set to bike coordinates.

The Gaint TCR bicycles used during the experiment, are not present in the bicycle lab. Making it impossible to measure the angles of the down-tube. Assuming the different frame sizes have a comparable angle. A picture of the Giant TCR form the Giant website figure K.1 can be used to determine this angle. A photo editing programme (paint.net [18]) is used to determine the angle between the line through the wheel axis and the down-tube. An angle of 48 deg is found.

Figure K.1: Picture form the Giant website[6] with the lines used to get the down-tube angle.

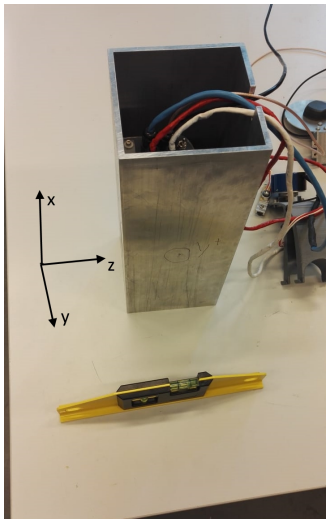

Figure K.2: Aluminium profile used to statically calibrate the accelerometer in the senor-set axis

To calibrate the accelerometer in the Sensor-Set axis, the chosen X, Y and Z axis need to be aligned with

the gravitational field in both positive and negative direction. In order to do this in a repeatable and accurate way, the Sensor-Set is mounted inside a square aluminium profile see picture K.2.
A level horizontal calibration surface is created, allowing alignment of the X, Y and Z axis with the gravitational field.
The positive X axis is set in the direction of the cable exits, the z axis is set upwards and the y axis to the left of the sensor unit.
A perfect sensor is to give the output of table K.1.

Table K.1: The theoretical output when aligning with gravity

axis towards gravity	ideal sensor set output		
	sensor set x	sensor set y	sensor set z
x+	g	0	0
x-	-g	0	0
y+	0	g	0
y-	0	-g	0
z+	0	0	g
z-	0	0	-g

As expected, the output of the accelerometer from the Sensor-Set differs from table K.1. The sensor is not perfect, the output in bit has to be converted to acceleration, there is some cross-axis sensitivity and misalignment between accelerometer and Sensor-Set frame. A plot of the sensor output data converted according to the sensor data sheet is shown in figure K.3.

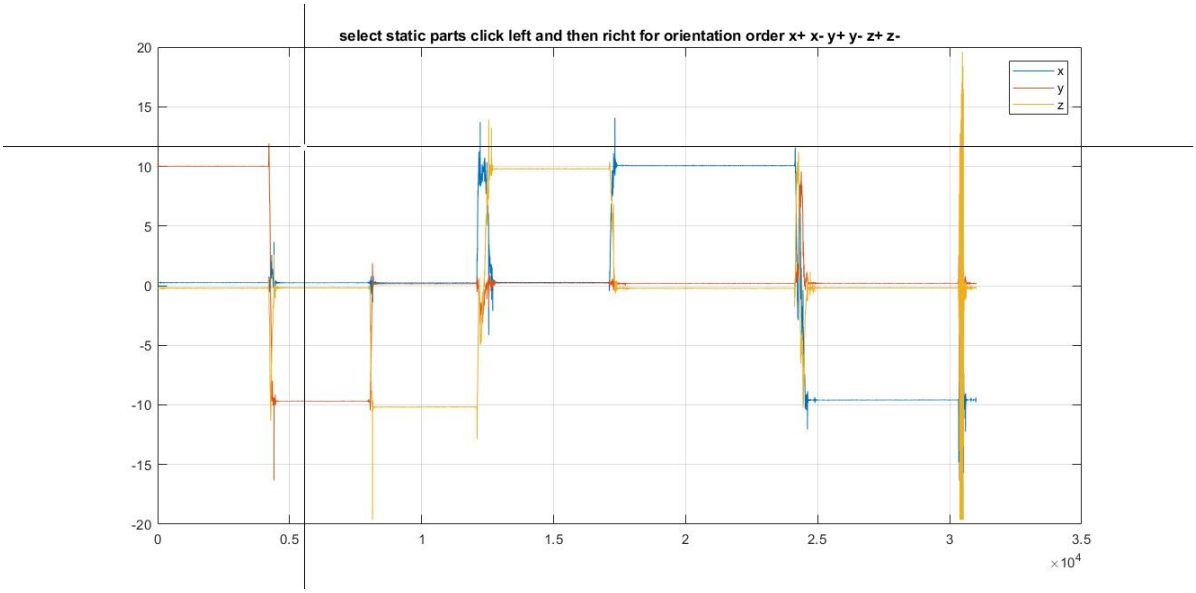

Figure K.3: Raw acceleration data form Sensor-Set1 with the selection lines used to select the six different orientations.

A Matlab program is made that allows for selecting the left and right side of the static parts in the plot of the data. Over the static parts the mean is calculated. The raw x, y and z data from all six orientations are stored in a matrix. An equal matrix with the theoretical output is generated. The output matrices from this script are show in table K.2 K.3

Table K.2: Calibration output of senor-set 1

axis towards gravity	sensor set data output		
	sensor set x	sensor set y	sensor setz
x+	0.2493	10.012	-0.2082
x-	0.2425	-9.6786	-0.1847
y+	0.2309	0.1575	-10.177
y-	0.2714	0.2203	9.7941
z+	10.079	0.1802	-0.2194
z-	-9.5880	0.1975	-0.1892

Table K.3: Calibration output of senor-set 2

axis towards gravity	sensor set data output		
	sensor set x	sensor set y	sensor setz
x+	0.2231	10.081	0.0293
x-	0.2839	-9.5837	0.0795
y+	0.2761	0.2625	-9.8555
y-	0.2596	0.2248	9.9656
z+	10.095	0.2697	0.0318
z-	-9.5853	0.2181	0.0710

The tables K.2 and K.3 show the data produced by the accelerometer, is not similar to the ideal output.
The axis in the Sensor-Set do not align with the accelerometer-chip axis.
The two Sensor-Sets also give different output. This raw sensor output needs to be converted to correspond to the ideal output.
Conversion of the data is done using equation K.1. The output from the sensor is noted as x_{raw}, y_{raw} and z_{raw}. The calibrated accelerations are noted as x, y, z.

$$\begin{bmatrix} x \\ y \\ z \end{bmatrix} = \begin{bmatrix} xx & xy & xz \\ yx & yy & yz \\ zx & zy & zz \end{bmatrix} \begin{bmatrix} x_{raw} \\ y_{raw} \\ z_{raw} \end{bmatrix} + \begin{bmatrix} x_{bias} \\ y_{bias} \\ z_{bias} \end{bmatrix} + \begin{bmatrix} x_{noise} \\ y_{noise} \\ z_{noise} \end{bmatrix} \tag{K.1}$$

The noise is an unknown input in the calibration trial. Any potential noise is filtered by taking the mean over approximately 4 seconds of the 100Hz accelerometer data. Removing the noise from equation K.1 and rewriting it for easier computation we get equation K.2.

$$\begin{bmatrix} x & y & z \end{bmatrix} = \begin{bmatrix} x_{raw} & y_{raw} & z_{raw} & 1 \end{bmatrix} \begin{bmatrix} xx & yx & zx \\ xy & yy & zy \\ xz & yz & zz \\ x_{bias} & y_{bias} & z_{bias} \end{bmatrix} \tag{K.2}$$

$$Out = In * Cal \tag{K.3}$$

Out is the calibrated output, In is the input from the sensor and Cal is the 12 parameter calibration matrix. To determine the parameters inside the Cal matrix the six orientations with known output and input are used. The output should be equal to what is inside table K.1 and the input is from table K.2 this leads to 18 equations and only 12 parameters thus an over defined problem.
Matlab is used to solve this system of matrices. Typing $Cal = In \backslash Out$ inside the Matlab programming environment this automatically performs a least-squares fit when a system is over determined [16].

Bike 1 calibration matrix results

$$Cal = In \backslash Out = \begin{bmatrix} 0.000873 & -0.0015 & 0.9976 \\ 0.9964 & -0.0012 & -0.000349 \\ 0.0031 & 0.9824 & 0.0020 \\ -0.1817 & -0.1933 & -0.2473 \end{bmatrix} \tag{K.4}$$

Bike 2 calibration matrix results

$$Cal = In\backslash Out = \begin{bmatrix} -0.0026 & -0.0020 & 0.9969 \\ 0.9977 & -0.0025 & 0.0030 \\ -0.0019 & 0.9899 & -0.00083 \\ -0.2444 & 0.0543 & -0.2586 \end{bmatrix} \tag{K.5}$$

Multiplying the raw data with this matrix and plotting this in figure K.4 and K.5. It can be seen that in all orientations the calibrated data is around 9.81 for the axis aligned with gravity and the other two axis around zero.

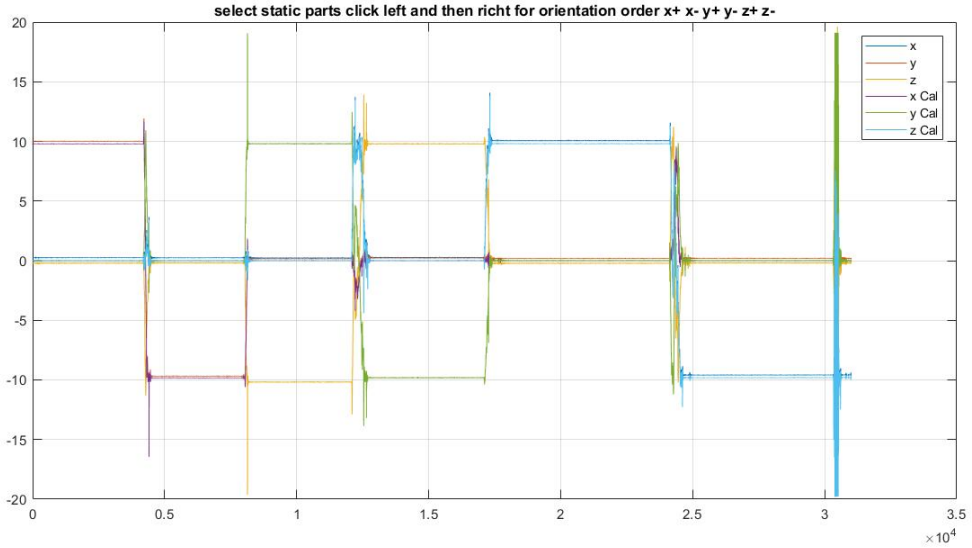

Figure K.4: Raw and calibrated accelrometer data of sensor-set 1

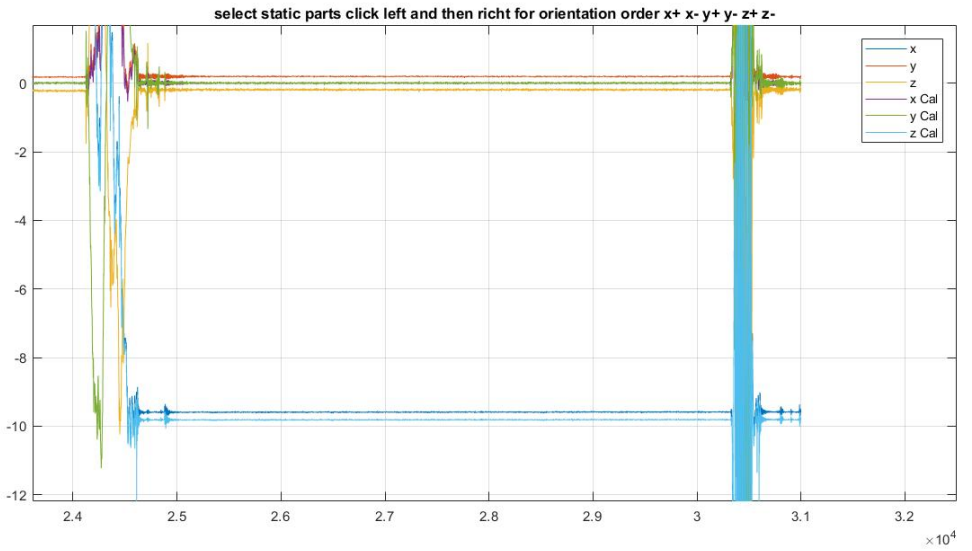

Figure K.5: Zoom of raw and calibrated accelrometer data of sensor-set 1

With the data calibrated in the Sensor-Set axis, the data can be rotated to align with the chosen axis of the bicycle. This is done using $roty(48)$ in Matlab to get a rotation matrix around the y axis.

The test data filtered and is multiplied with the calibration matrix and the rotation matrix in order to get the acceleration data into the bike frame co-ordinates. x, y and z acceleration data of the first trial of every rider is shown in figure K.6, K.7, K.8, K.9, K.10, K.11, K.12 and K.13.

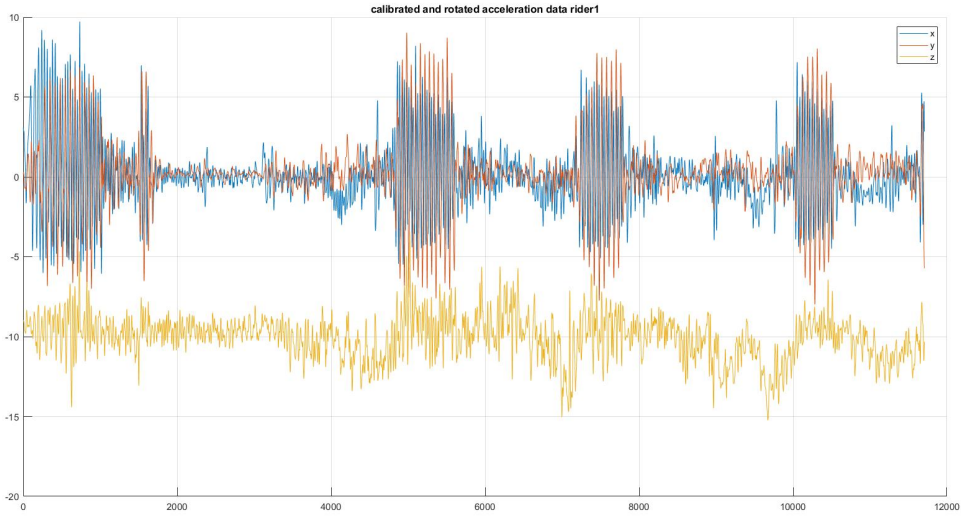

Figure K.6: Acceleration data rider 1

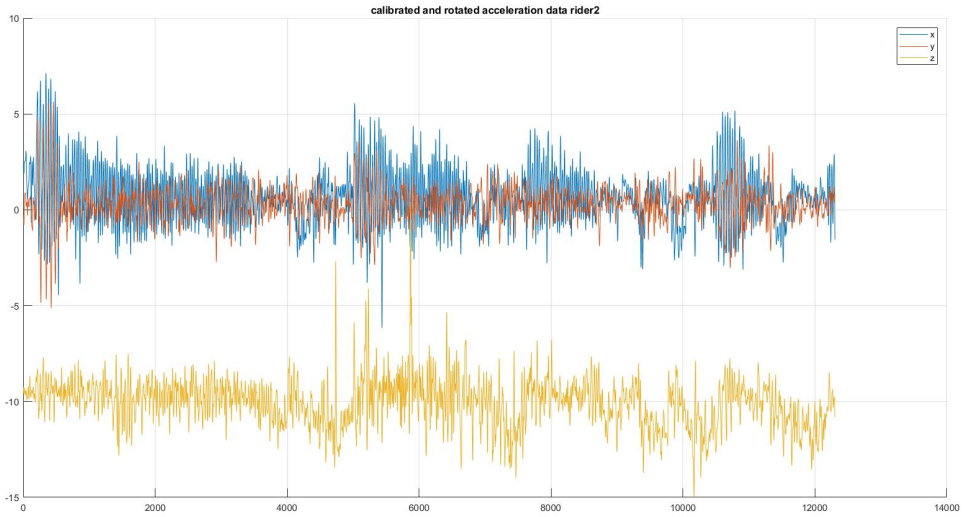

Figure K.7: Acceleration data rider 2

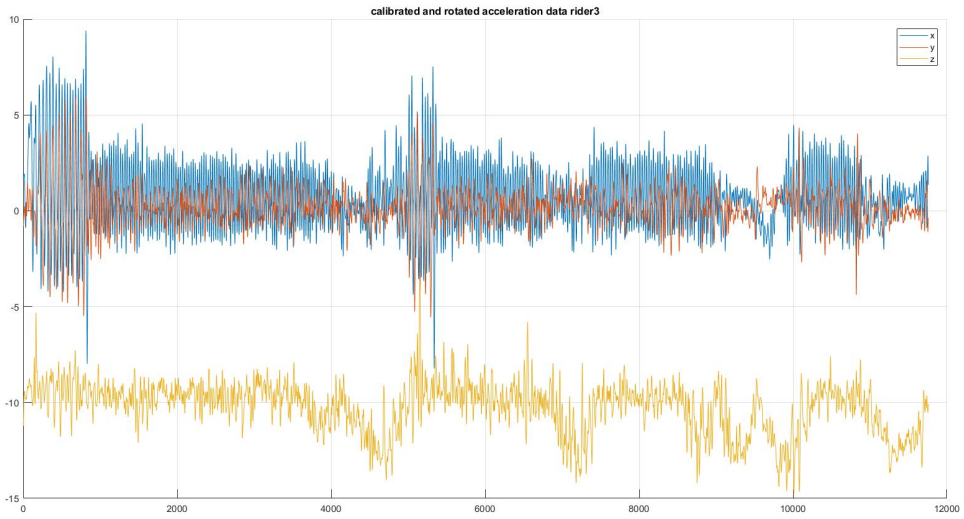

Figure K.8: Acceleration data rider 3

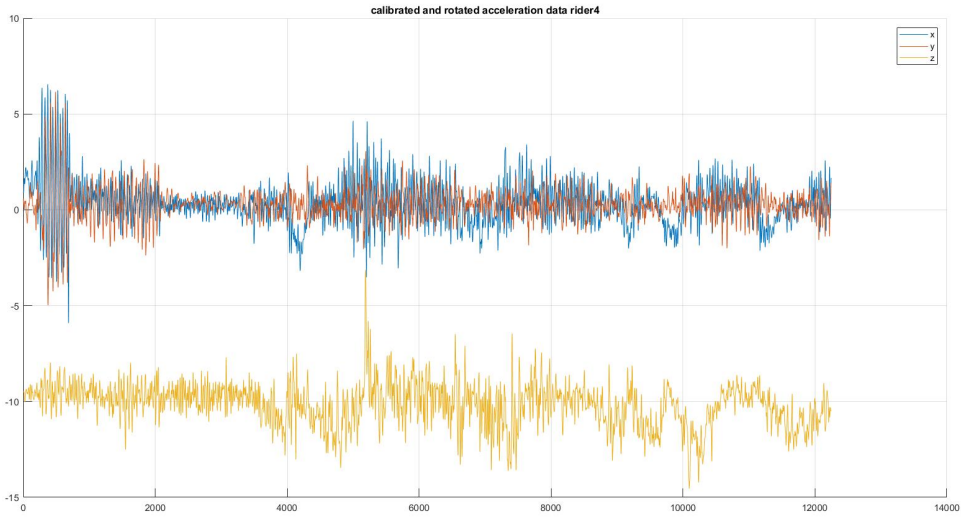

Figure K.9: Acceleration data rider 4

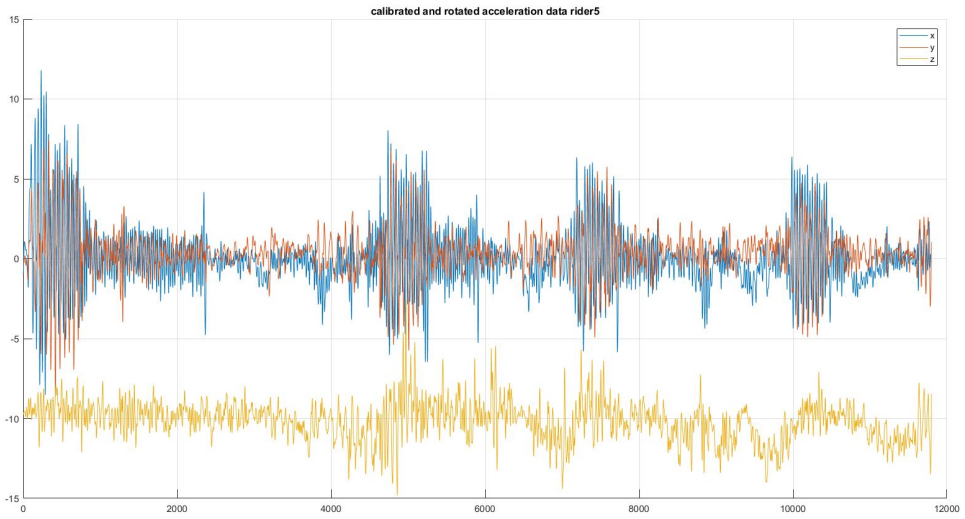

Figure K.10: Acceleration data rider 5

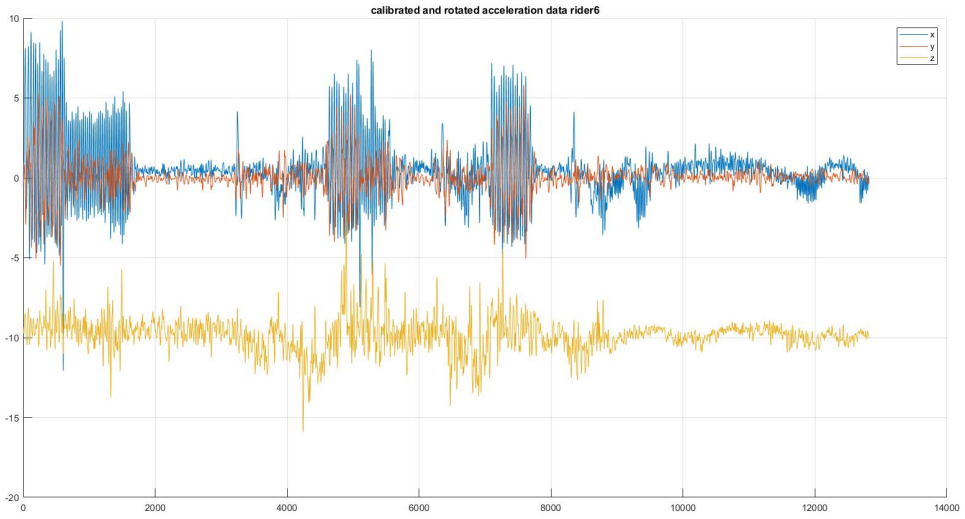

Figure K.11: Acceleration data rider 6

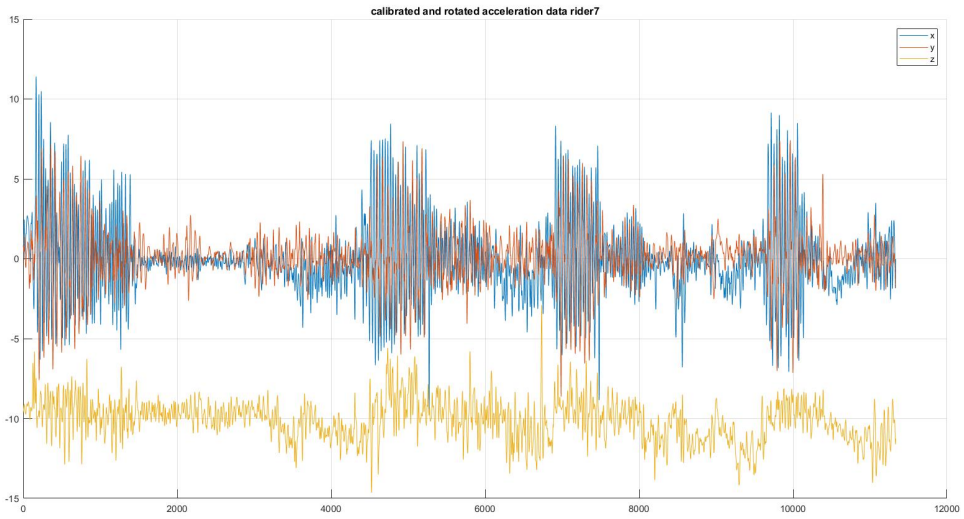

Figure K.12: Acceleration data rider 7

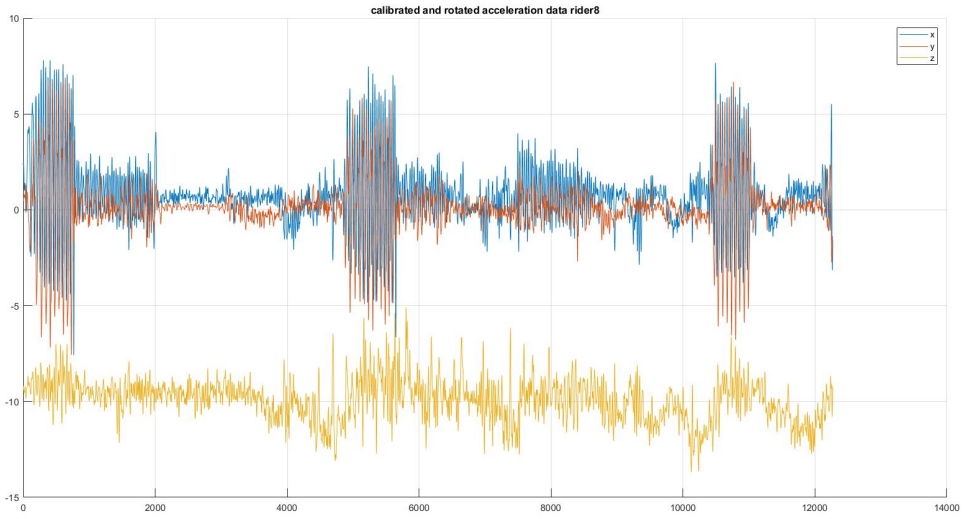

Figure K.13: Acceleration data rider 8

We see that the y zero average is closer to zero which is good. But not good is the variation between the average of the x data that differs between the trials, this should be equal on every trial because its determined by the road incline. The z data is very close to 9.81 m/s^2. At first the accelerations in z direction does not look correct. During and after braking the acceleration in downwards direction z axis gets larger than the gravitational force. At first this looks like an calibration error but it could be explained by the centripetal forces in the coroners.
This calibration is an improvement over the method used by Marco Reijne. This is for example proven by the fact that the bike motion form sprinting out of the corners is less visible in the z data.
But the method of rotating the accelerations in the sensors set frame by 48 degree to transfer Sensor-Set frame to the bike frame is not perfect. The different frame sizes have different down tube angles. Leading to varying zero offset for the accelerations in x direction. The fact that these down-tube angles are unknown makes it hard to solve this problem. The angle of rotation needs to be determined with the currently available data.
To improve the data quality its only possible to make an optimisation for the rotation angle using the data

form the Duren tests. The problem is to determine the goal of these optimisation.
For the calibration of the brake sensor the accelerations in longitudinal direction of the bicycle are most important. The optimisation of the rotation angle is thus done to get the x direction data as good as possible. Using a short part on the course where the cyclist don't peddle, I assume constant velocity for this part. The acceleration force measured by the sensor should then be equal to the force of gravity (due to incline of the road this will not be zero see figure K.14).
The riders do not peddle between 350meter and 500meter this part of the track it is also clear of any corners. The average gradient of this part is taken from the data made during the measurement of the centerline of the road. This data is made at slower speeds resulting in more samples per meter and thus better data quality. The average gradient is -5.688 %. The acceleration in forward bike detection measured by the accelrometer from the gradient should then average 0.5570 m/s^2

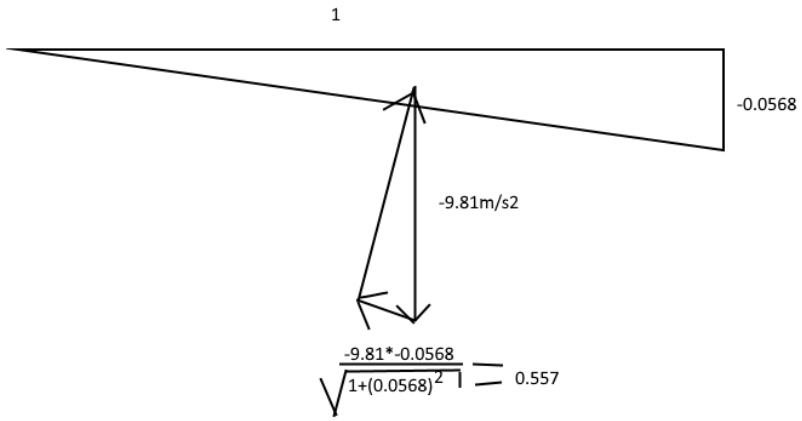

Figure K.14: Measured acceleration due to road incline.

A Matlab function is made where rider, trial and rotation angel around the y axis are the input. The output is the mean of the x acceleration between 350 and 500 meter minus 0.5570 form the gravity. Using this function the rotation can be optimised with Matlab using fmincon. A Matlab script is made that automatically run's fmincon for each rider and trial. After finding an optimal angle this angel is stored in a matrix where the rows represent the trials and the columns the riders. When the angles for one rider are determined the mean and standard deviation is calculated per rider. The results form this are shown in K.4.

	rider1	rider2	rider3	rider4	rider5	rider6	rider7	rider8
trial1	51,24	47,72	47,58	50,01	52,17	48,56	-	47,53
trial2	51,35	47,93	47,91	49,79	51,97	48,61	-	47,27
trial3	51,12	48,19	47,49	49,58	51,58	48,31	-	47,21
trial4	51,01	47,98	47,70	49,76	51,72	48,82	-	-
trial5	51,11	48,14	47,74	49,80	51,89	48,76	-	47,25
trial6	51,54	47,22	47,82	49,70	51,91	48,62	-	-
mean	51.23	47.86	47.70	49.77	51.87	48.61	-	47.31
SD	0.1937	0.3540	0.1527	0.1417	0.2050	0.1788	-	0.1446

Table K.4: Table with the optimised rotation angles form senor to bike frame. Part of track from 350m to 500m

The results are better than expected as the standard deviation shows the differences between trials are small. Using the mean angles of the optimisation to transform the measurement data from Sensor-Set axis to the bike axis these results are saved in the data structure as riderx_trialx.acc.b_static.
The resulting data is plotted in Appendix H

L

Original Accelerometer Data

This Appendix contains the accelerometer data as processed by the first Matlab script [1] that synchronised all measurement data.
In this script a first accelrometer calibration and rotation is done. The conversion from bit to acceleration is done as specified by the accelerometer data-sheet.
The acceleration data is then rotated from the accelerometer chip coordinates to the bike frame coordinates by selecting a short straight part of the route and assuming that the bike is level and steady for that part or the route.
The steps done in the Matlab script to transform accelerometer, gyroscope, magnetometer from sensor to body coordinate frame. As described by Marco Reijne are listed below:

- Select straight road;
- Calculate linear slope gradient;
- Assume no roll –> y-offset;
- Calculate forward acceleration form velocity;
- Calculate pitch angle orientation frame;
- Pitch angle: x offset z offset;
- Transform acc, gyro, magneto.

Plot L.1, L.2, L.3, L.4, L.5, L.6 and L.7 show the acceleration in x (forward) direction of all trails per rider.

[1] credit is due to Marco Reijne for making the Matlab script

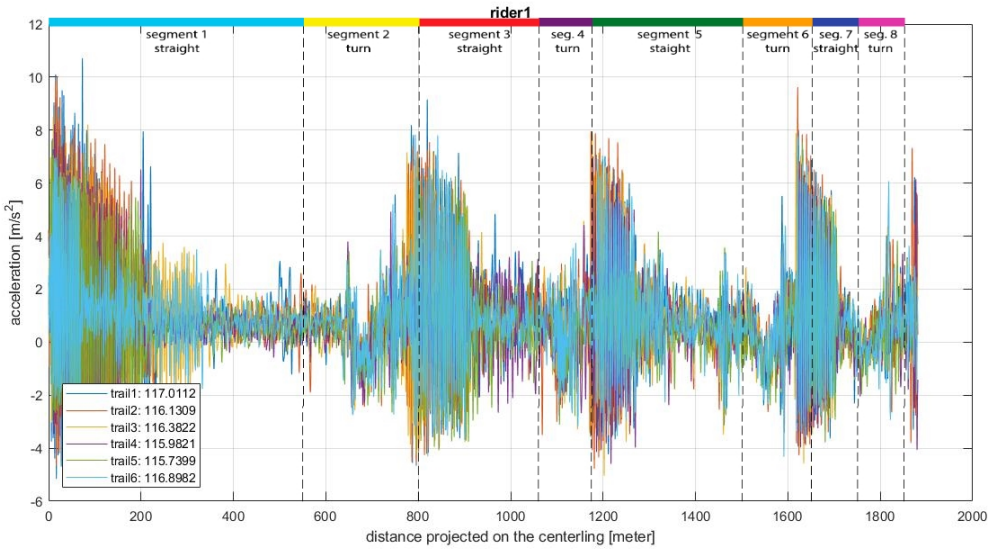

Figure L.1: Acceleration data rider 1

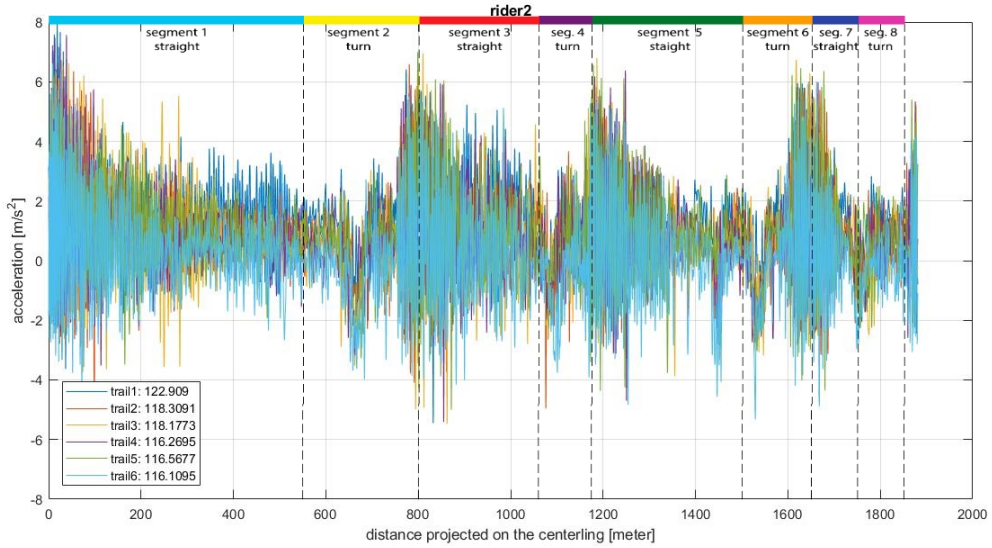

Figure L.2: Acceleration data rider 2

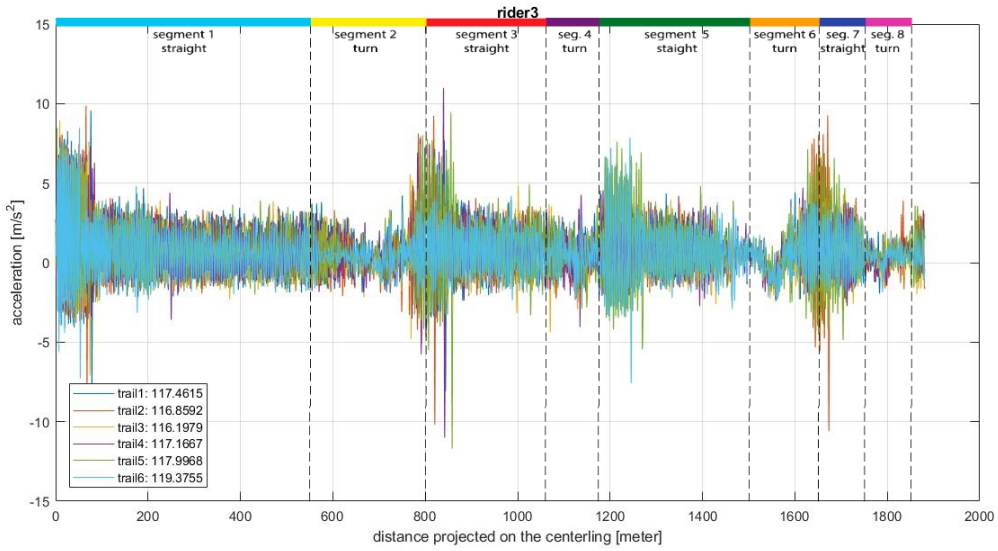

Figure L.3: Acceleration data rider 3

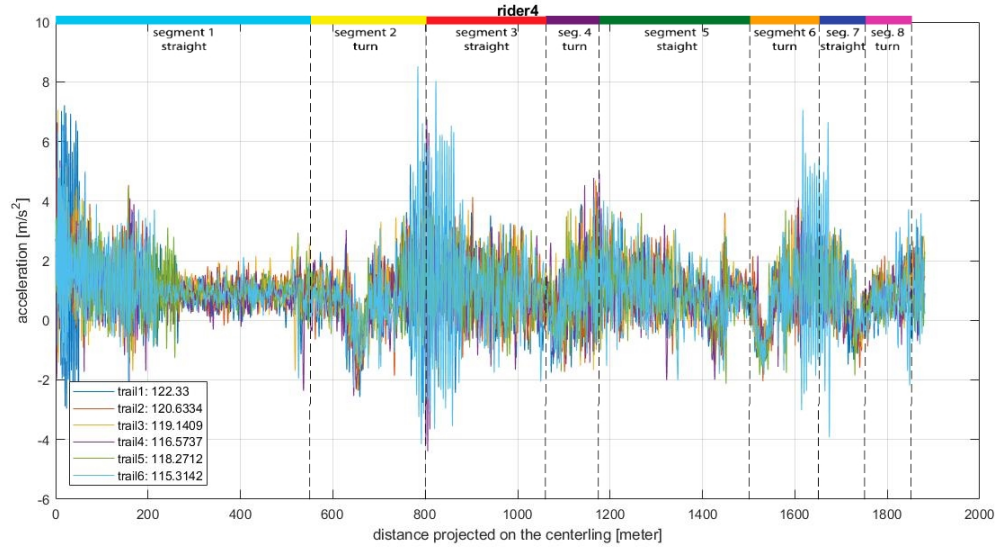

Figure L.4: Acceleration data rider 4

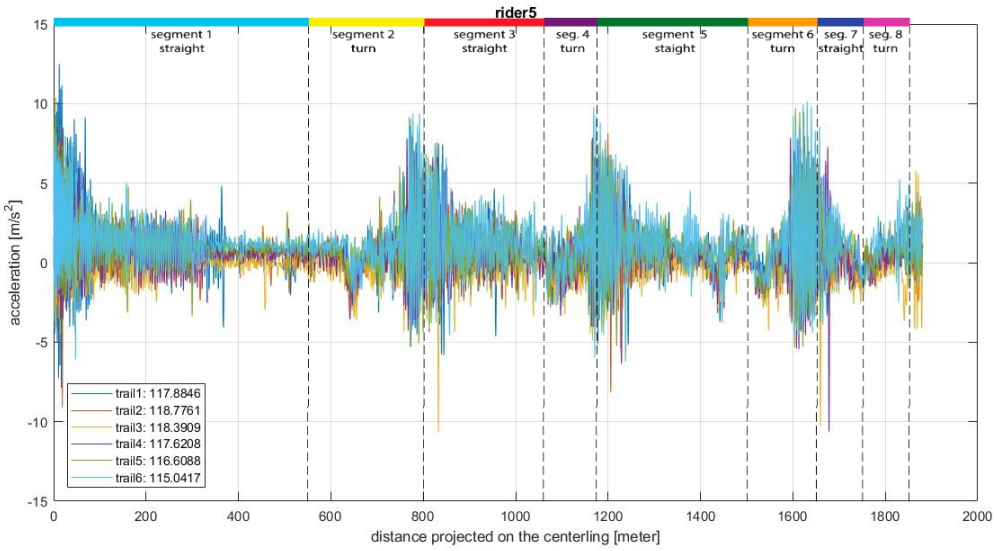

Figure L.5: Acceleration data rider 5

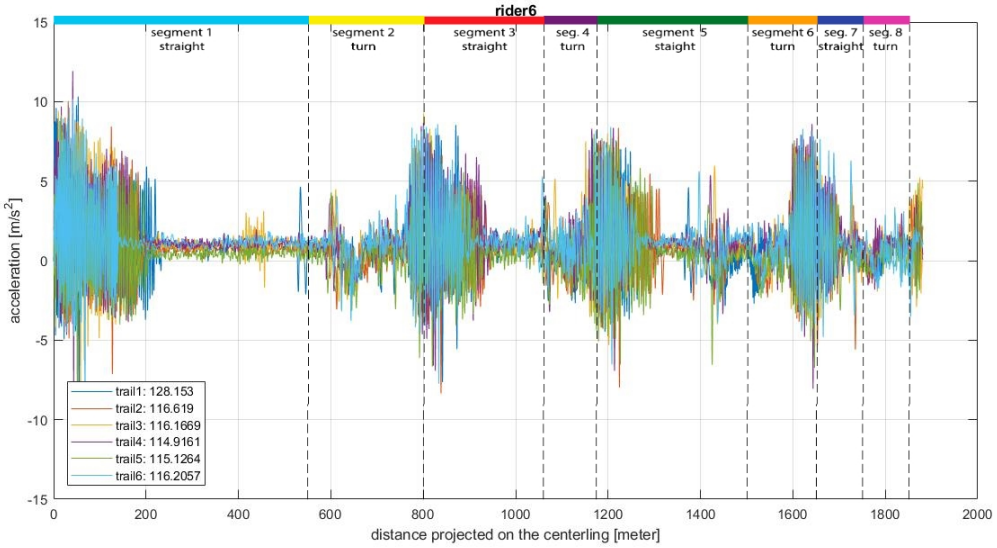

Figure L.6: Acceleration data rider 6

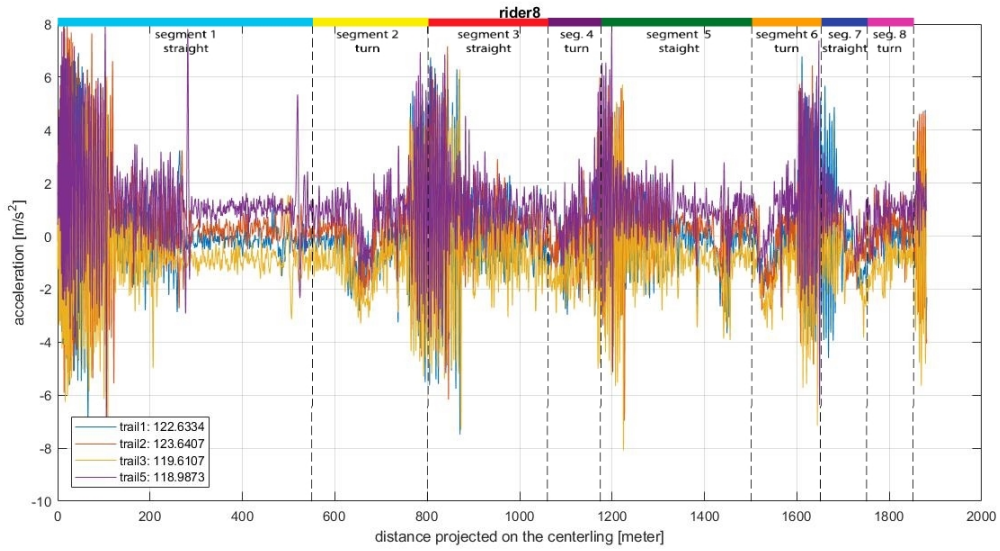

Figure L.7: Acceleration data rider 8

Looking at the accelerometer data in forward direction the following things can be observed:

1. The average of the x acceleration data is not equal for all the riders and also differ between trails of a single rider. This indicates that the transformation from sensor chip to bike frame is not good;
2. That the x acceleration mean is not zero on average as expected. The incline of the road gives a small forward gravitational force measured by the accelerometer;
3. The amount of 'noise' in the acceleration data shows how and when the riders are peddling. When riders are sprinting out of corners and over the start line the data has noise with a large amplitude from swinging the bike form left to right. Peddling in the saddle gives a smaller noise amplitude. When the riders are coasting on the fast straight parts or true the corners, road vibrations still give noise on the acceleration data;
4. Before the corners when the riders brake, this braking can be seen as a dip in the x acceleration data.

Plot L.8, L.9, L.10, L.11, L.12, L.13 and L.14 show the acceleration in y (sideways direction right side positive) direction of all trails per rider.

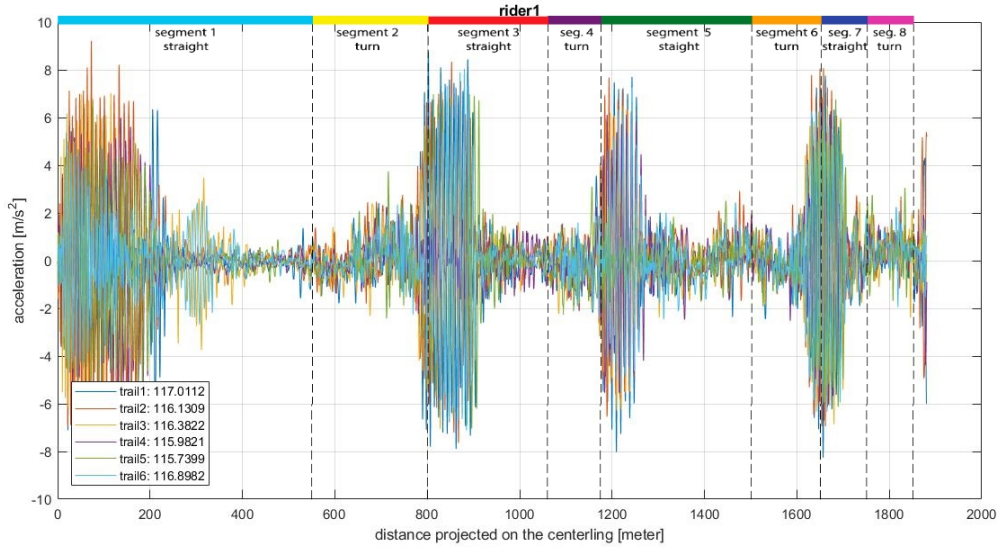

Figure L.8: Acceleration data rider 1

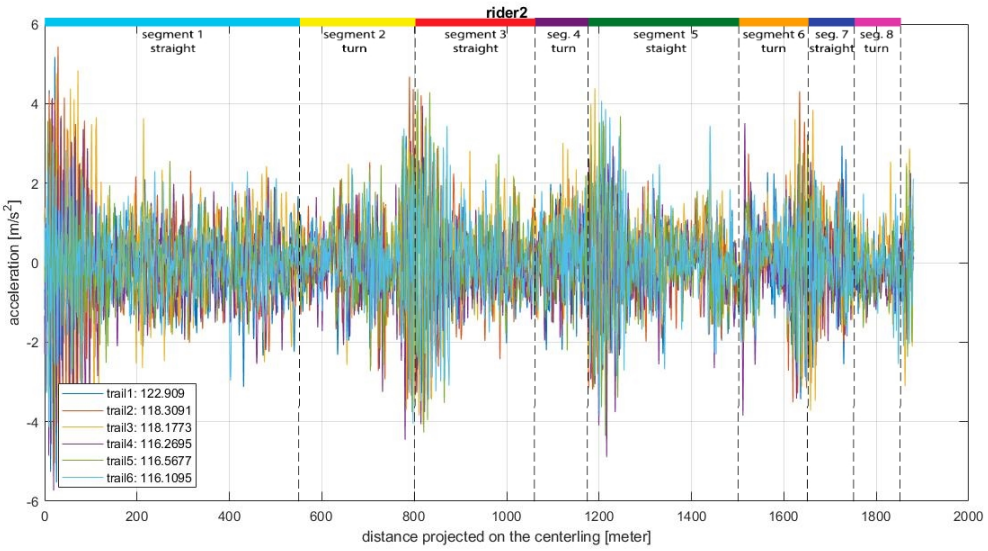

Figure L.9: Acceleration data rider 2

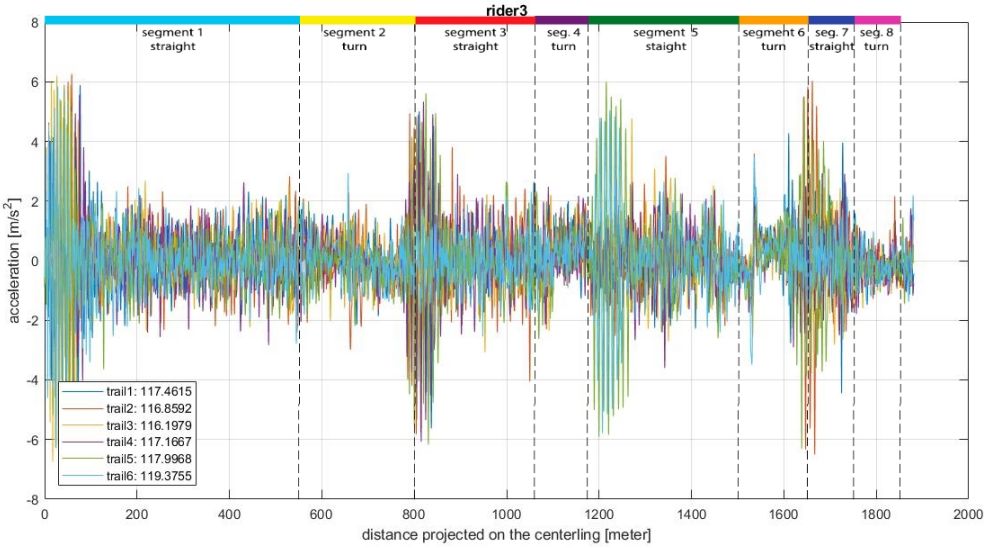

Figure L.10: Acceleration data rider 3

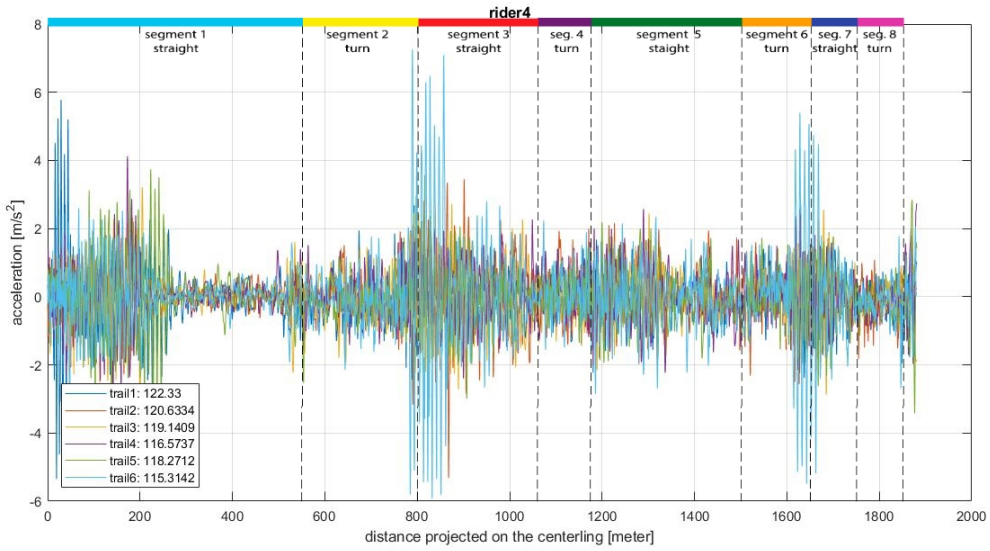

Figure L.11: Acceleration data rider 4

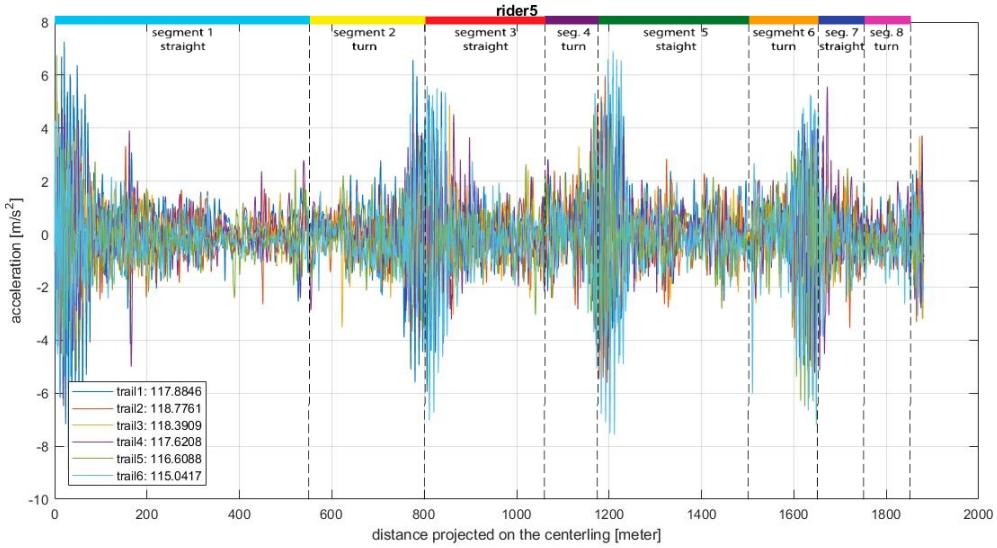

Figure L.12: Acceleration data rider 5

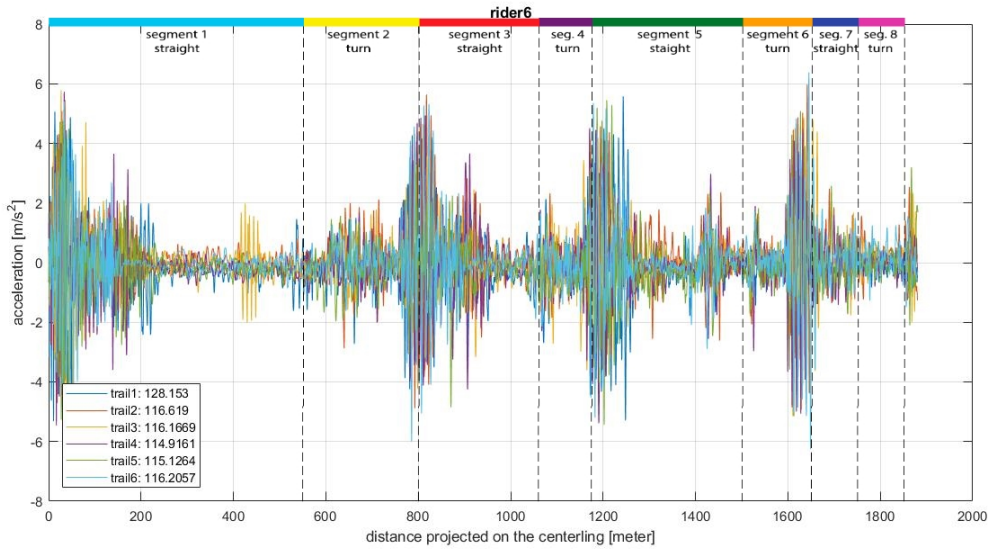

Figure L.13: Acceleration data rider 6

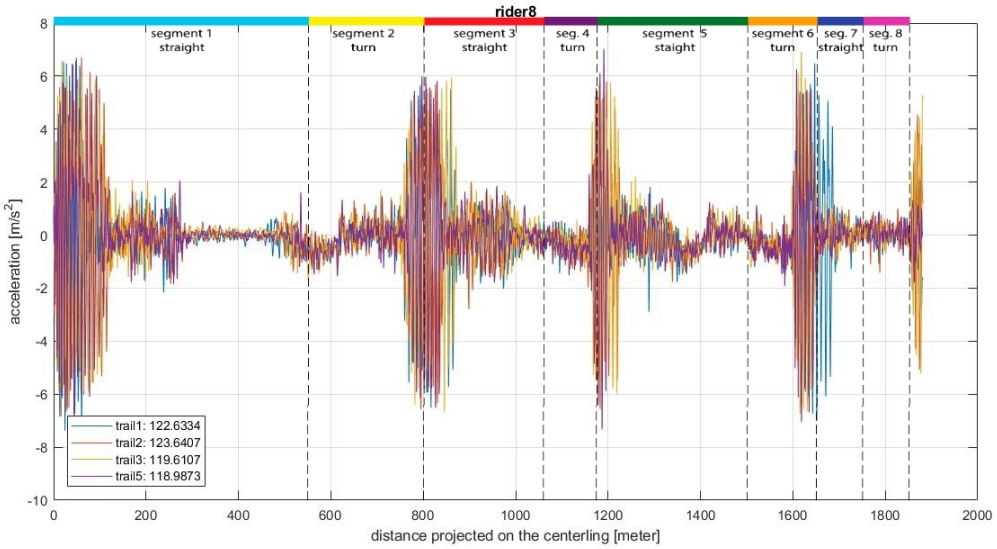

Figure L.14: Acceleration data rider 8

Looking at the accelerometer data in sideways direction the following things can be observed:

1. The y acceleration data shows the same 'noise' differences with the different peddling techniques as the x acceleration.

Plot L.15, L.16, L.17, L.18, L.19, L.20 and L.21 show the acceleration in z (upwards direction) direction of all trails per rider.

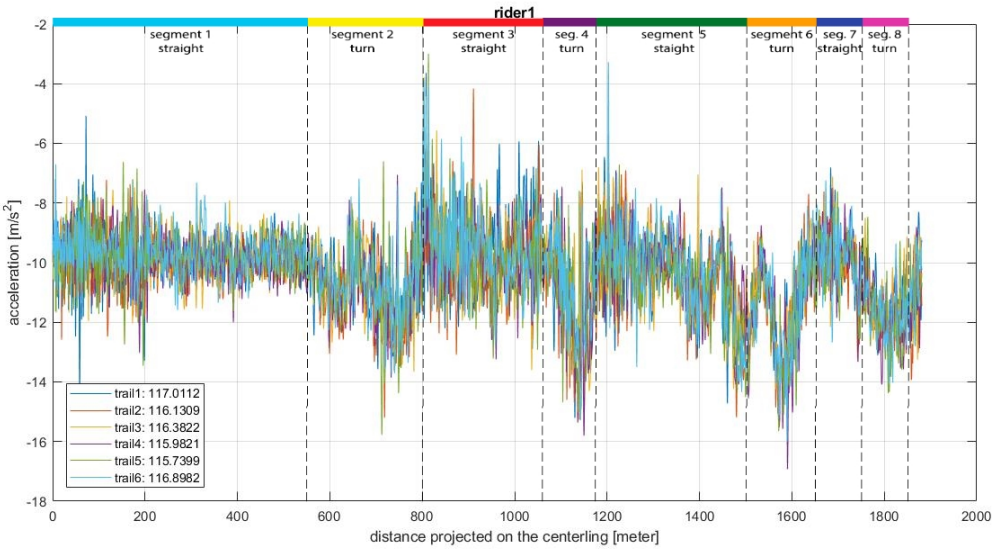

Figure L.15: Acceleration data rider 1

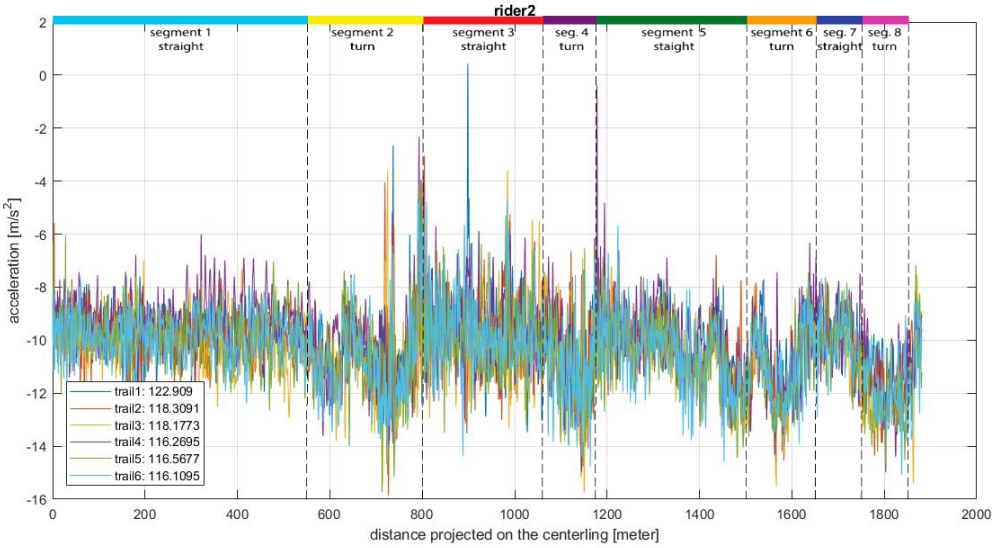

Figure L.16: Acceleration data rider 2

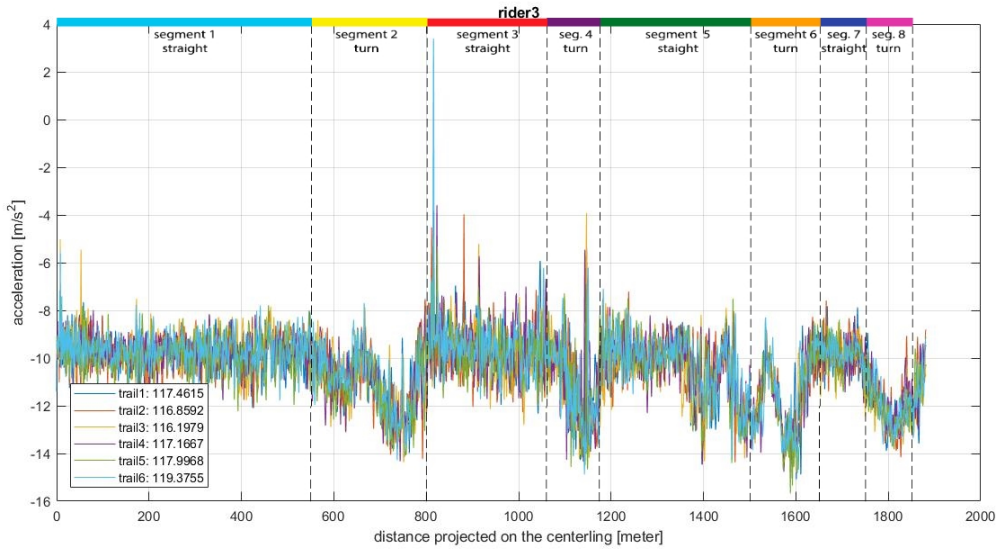

Figure L.17: Acceleration data rider 3

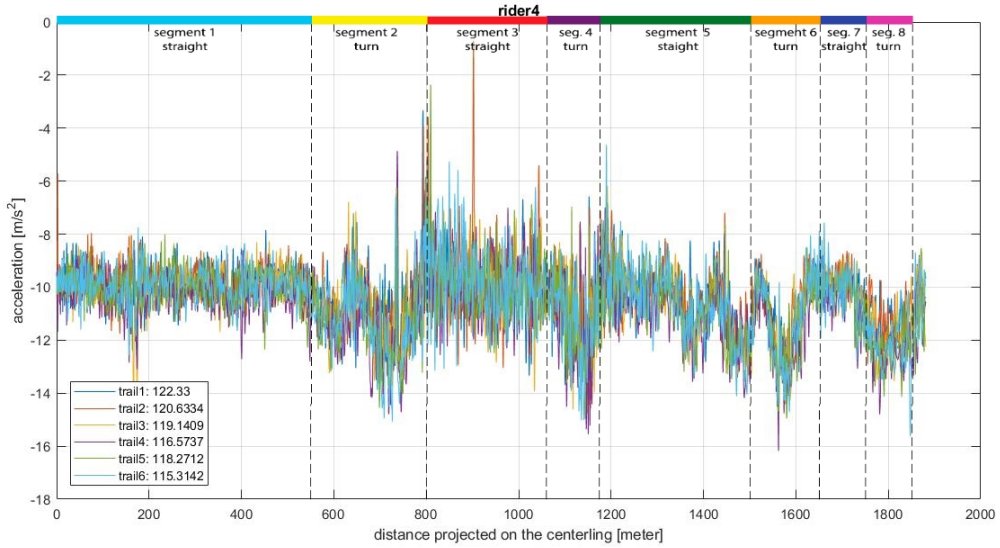

Figure L.18: Acceleration data rider 4

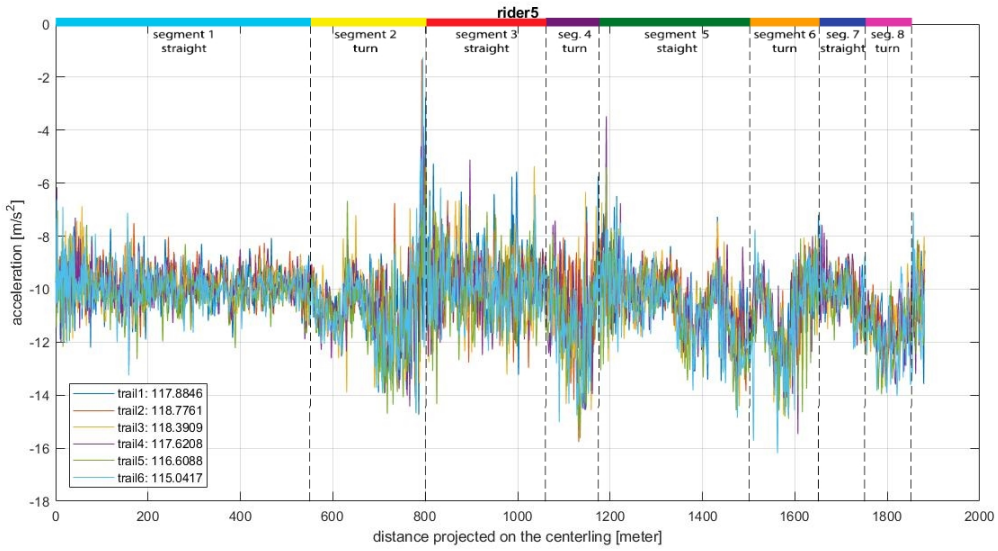

Figure L.19: Acceleration data rider 5

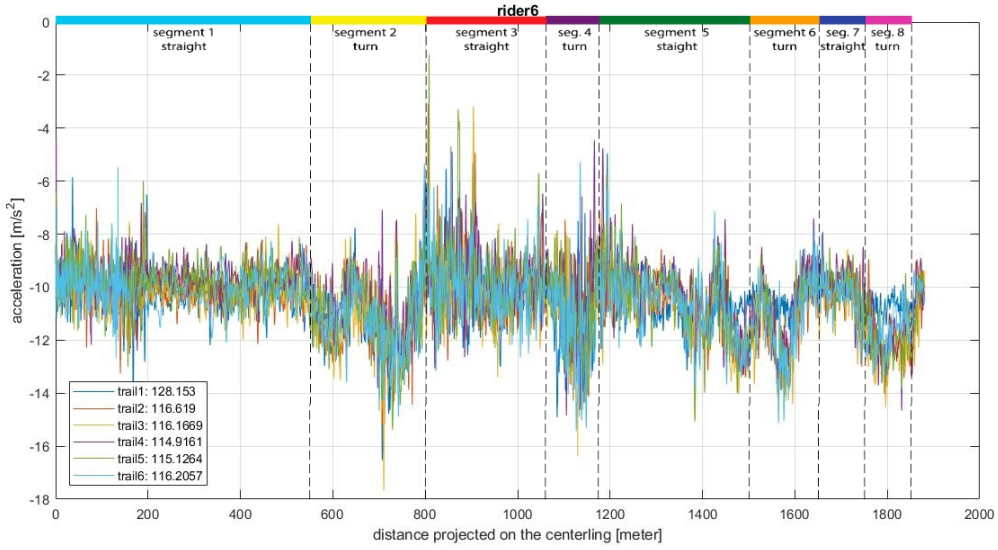

Figure L.20: Acceleration data rider 6

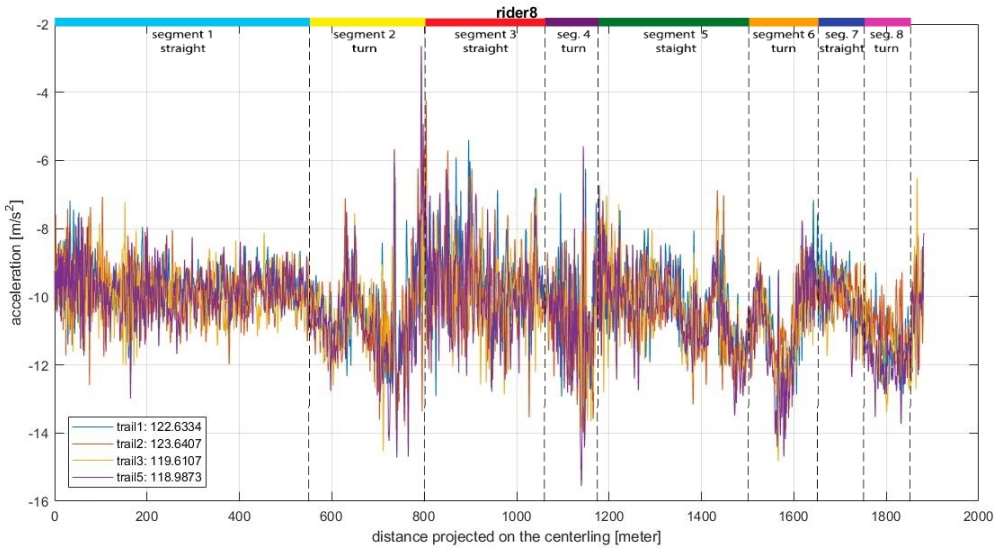

Figure L.21: Acceleration data rider 8

Looking at the accelerometer data in upward direction the following things can be observed:

1. When giving a quick glance at the z accelerations its looks strange that the acceleration is larger than 9.81g. As the cyclist cannot go through the ground. But this can be explained by the centripetal force in the corners;
2. For rider 1, 6 and 8 the sprinting motion creates extra 'noise' in the z data while the bike is not going up and down.

Combining the observations made about the acceleration data in x, y and z direction, it can be concluded the data is not properly calibrated and/or rotated. This is especially clear when looking at the offsets differing between riders and trails on the same road segments.

M

Power Meter Data

The broadcasted power meter data is not stored in the Sensor-Set data. The power meters entered sleeping mode before or in between trials resulting in a lost connection. If the power-meters get out of sleeping mode when pedalling is started, the Sensor-Set did not automatically reconnect resulting in the power data being absent.
An attempt is made to regain parts of the missing power-meter data. This data is collected from the head-units where, some riders collected their power-meter data. The results form synchronising the power-meter ans Sensor-Set data are included in this Appendix. The quality of the resulting data is not sufficient for further analysis. As there are still a lot of trials missing and timing is far from perfect.

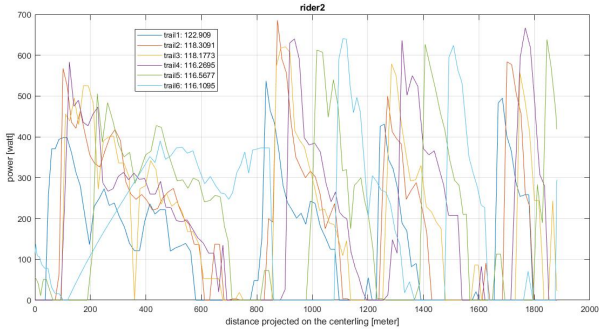

Figure M.1: Power data form rider 2

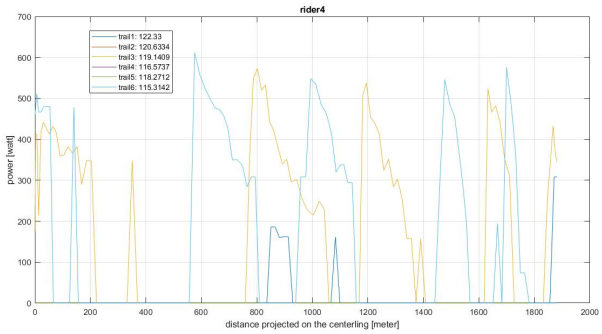

Figure M.2: Power data form rider 4

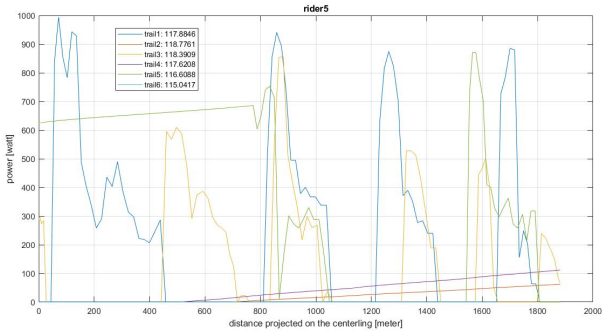

Figure M.3: Power data form rider 5

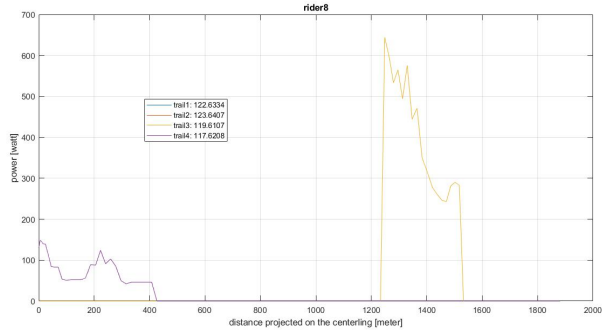

Figure M.4: Power data form 8rider

N

Brake Sensor Data Offset Removal

The below figures contain brake sensor data as processed by the script used to organise, filter and synchronise the raw Sensor-Set data.
In this script the brake sensor drift is removed by seating the first sample of each rider to zero. As can be observed, the data is still drifting after this first sample.

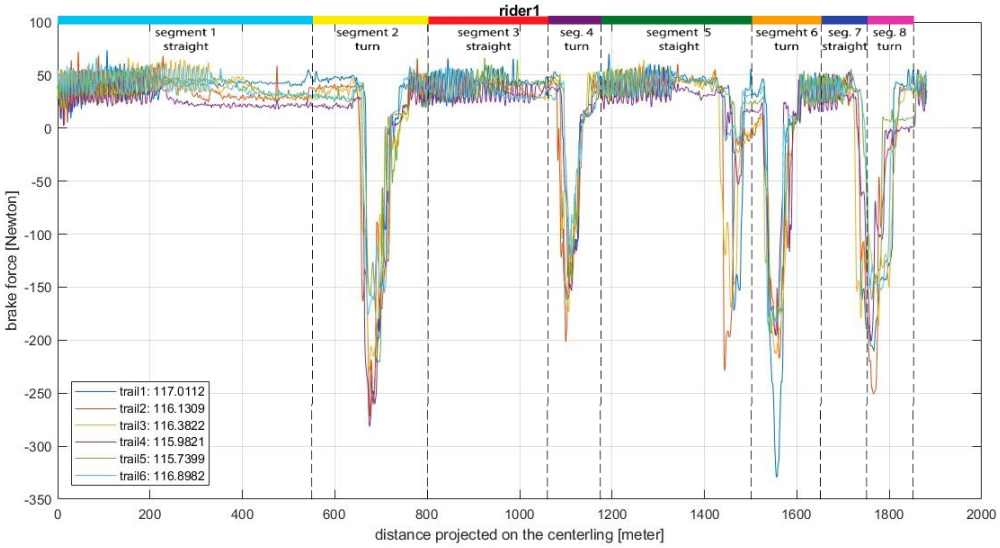

Figure N.1: Zero offset is not zero, the wheel rubs the brake pad when peddling forces flex the bike frame.

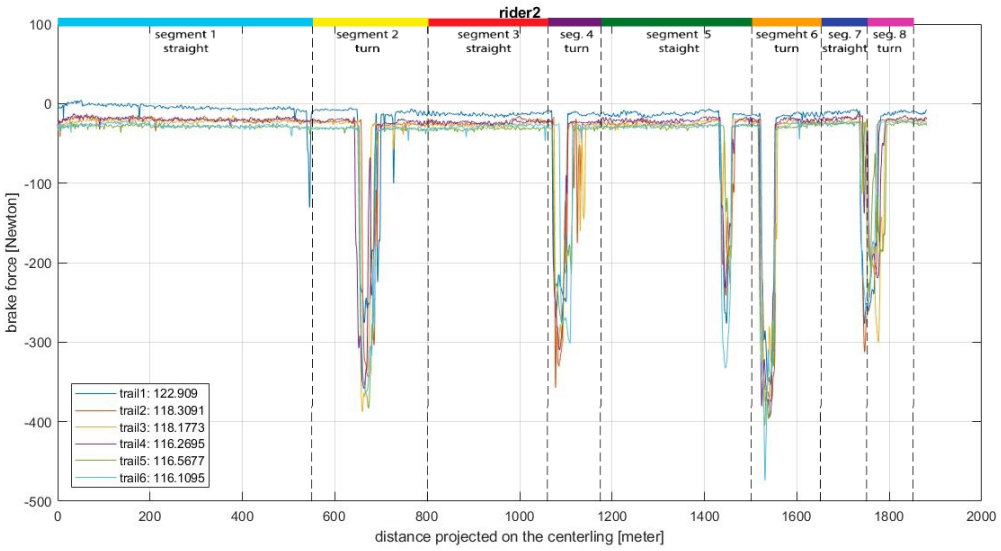

Figure N.2: Zero offset drifts in time at start of trial 1, it was good.

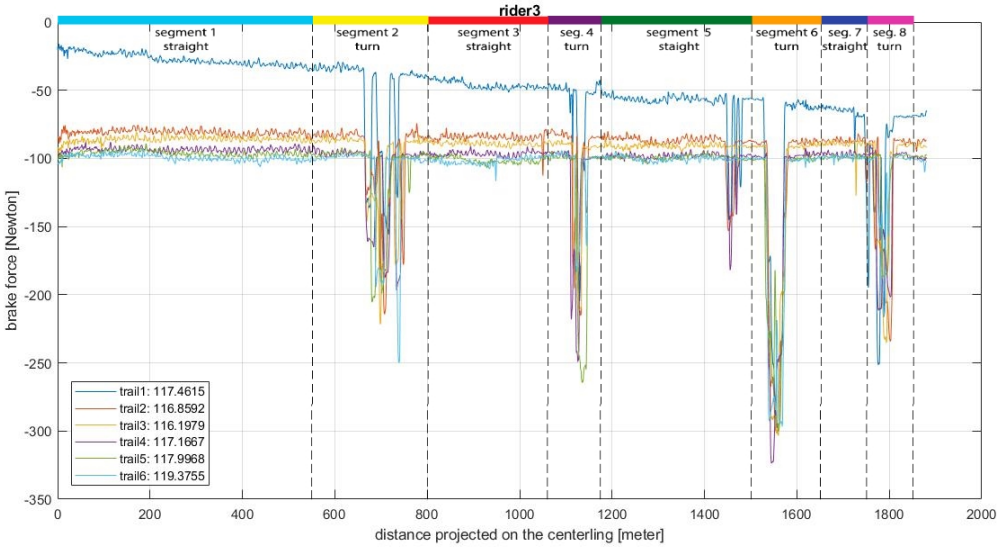

Figure N.3: Zero offset drifts in time at start of trial 1, it was good.

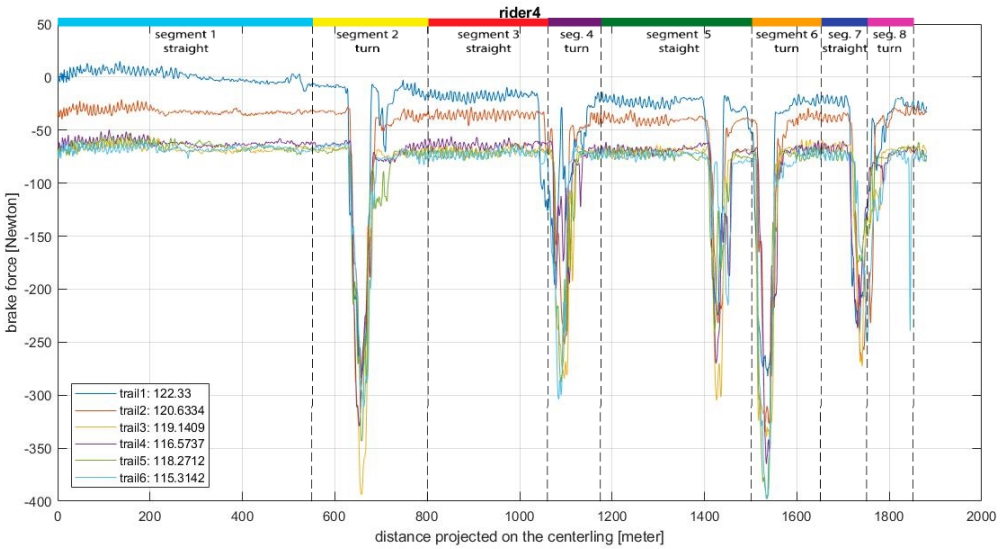

Figure N.4: Zero offset drifts in time at start of trial 1, it was good, there is also brake rub form frame flex when peddling.

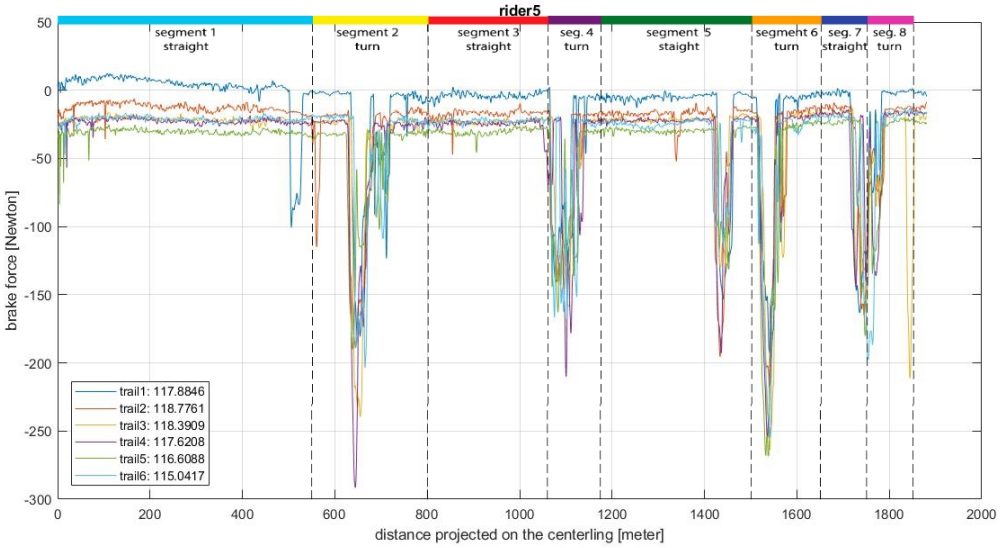

Figure N.5: Drift in zero offset, On the first trial there is a small braking peak in the fast blind corner.

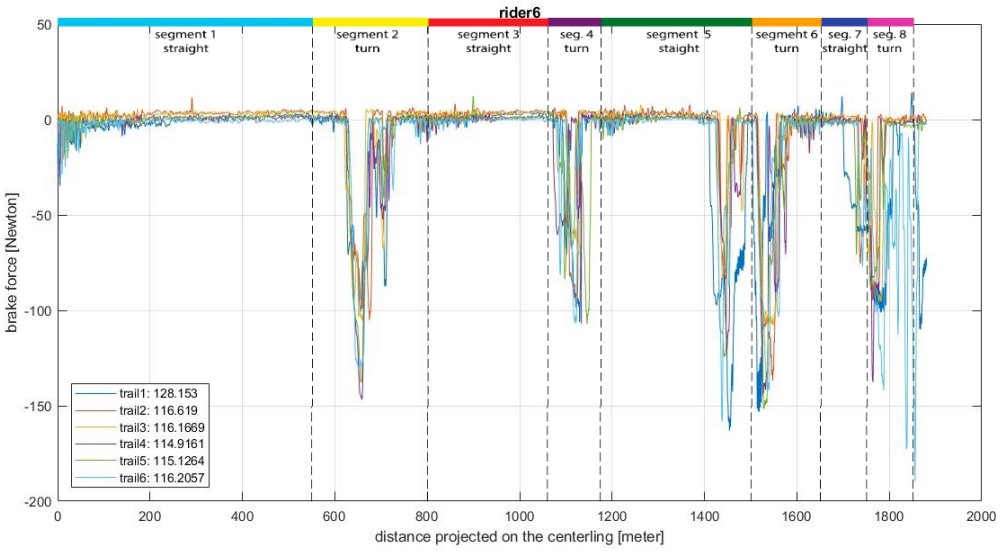

Figure N.6: Zero offset almost good, brake rub when peddling

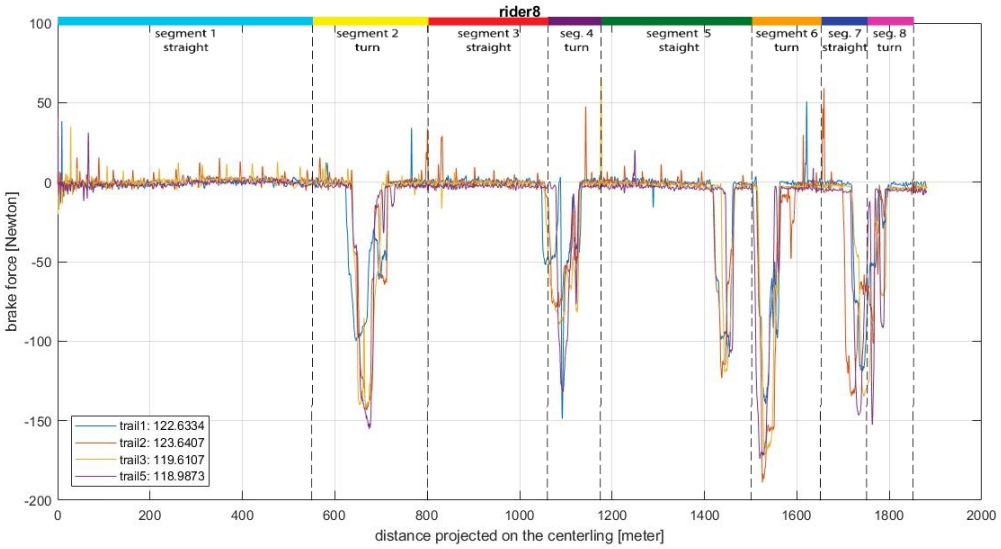

Figure N.7: Zero offset almost good, strange spikes in upwards direction.

As the above plot show, brake sensor data is drifting in time. This drift can be removed without affecting data quality as tested and explained in chapter F.
The brake data is shifted linear to remove the brake sensor drift. The offset at the front and rear of the brake data is noted down. A straight line through these two points is subtracted from the brake data.

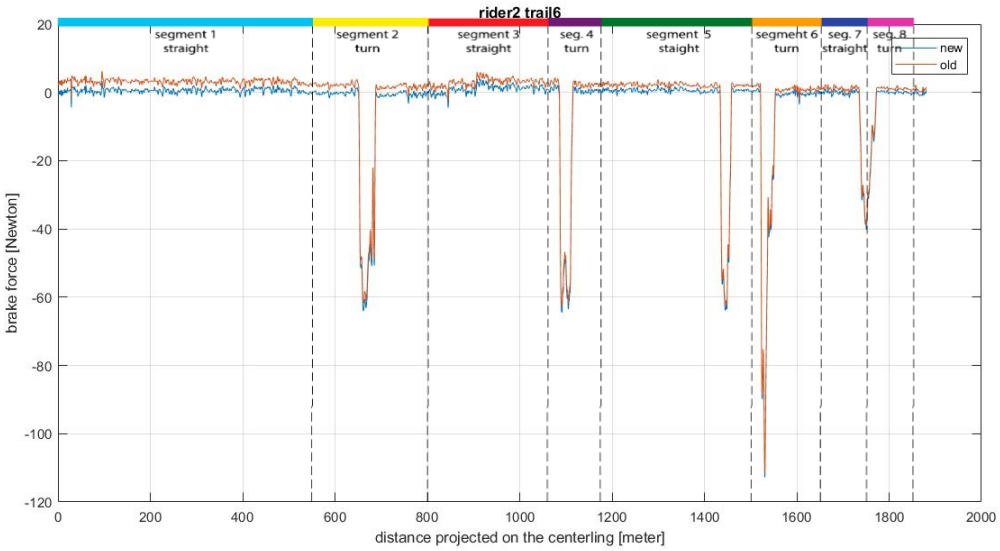

Figure N.8: Example of shifted brake data

trial 4 and 6 of rider 8 do not have the distance projected on the interline. This means that the script does not work. I did not make an extra script because this trials will not be useful without distance projected on the centreline.

	rider 1		rider 2		rider 3		rider 4		rider 5		rider 6		rider 8	
	s1	s2	s1	s2	s1	s2	s1	s2	s1	s2	s1	s2	s1	s2
trial 1	11 11	-53 -53	13 13	-8 -1	25 27	3 37	3 30	0 0	-	1 4	2 -1	-2 -1	0 -1	0 2
trial 2	9 12	-49 -50	25 22	-3 0	32 35	47 52	35 36	-7 3	12 8	9 6	-4 -4	-1 2	-2 -1	2 3
trial 3	8 12	-45 -49	26 23	-4 0	39 40	50 50	69 65	0 0	11 9	11 9	-6 -4	1 3	-3 0	2 3
trial 4	14 20	-45 -45	26 22	-7 -3	44 46	49 51	60 65	-4 3	12 9	11 8	-4 -3	1 3	—-	—-
trial 5	13 16	-60 -60	37 23	-3 1	50 50	45 48	69 71	-5 2	-3 -6	14 10	-3 -3	1 4	-5 0	3 5
trial 6	8 17	-55 -55	37 23	-3 -1	55 53	44 46	69 72	-5 -1	12 9	10 9	-3 -2	3 4	—-	—-

Appendix G shows plots containing brake data with the zero offset removed. This data is also normalised to compensate for rider weight differences.

O

Brake Distribution

Plots containing the distribution of brake force between the front and rear brake. With 1 being only front braking and 0 being only rear braking. The result contains a lot of noise when the riders do not apply brake force. This noise is a result of the brake sensor output oscillating around 0 when not loaded. Dividing these small non relevant numbers will result in output.
When riders brake the data is smooth. Looking at the smooth parts, it can be observed that riders use different brake force distributions.

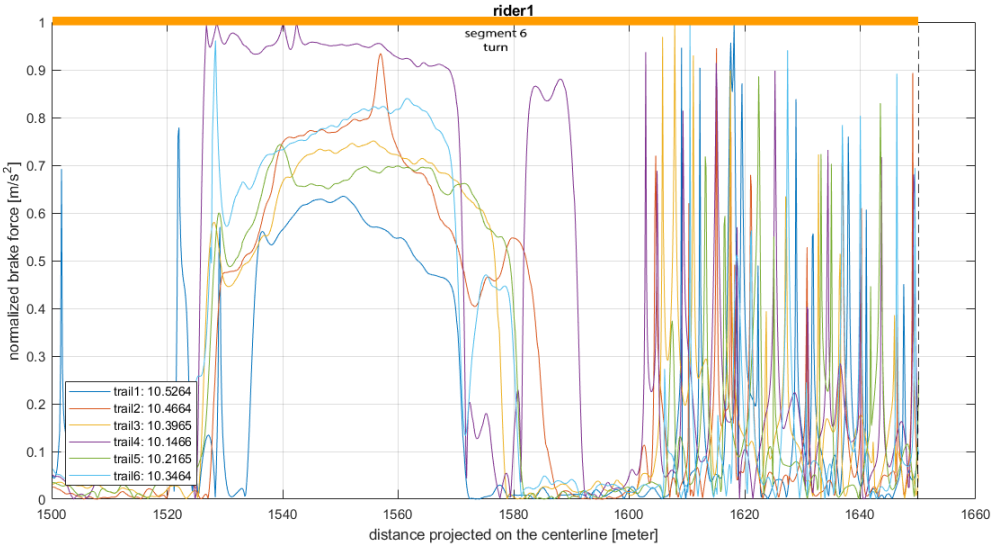

Figure O.1: Brake distribution between front and rear for rider 1.

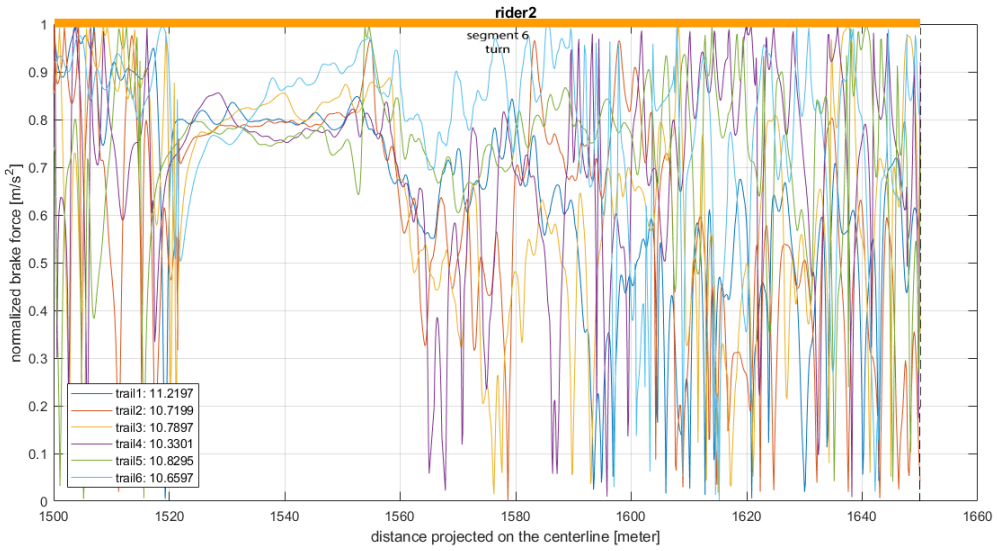

Figure O.2: Brake distribution between front and rear for rider 2.

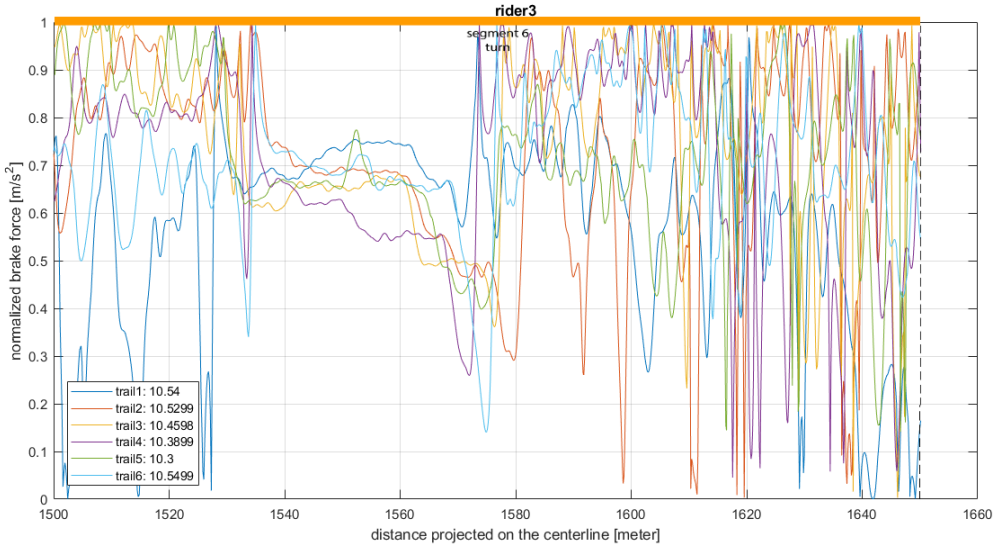

Figure O.3: Brake distribution between front and rear for rider 3.

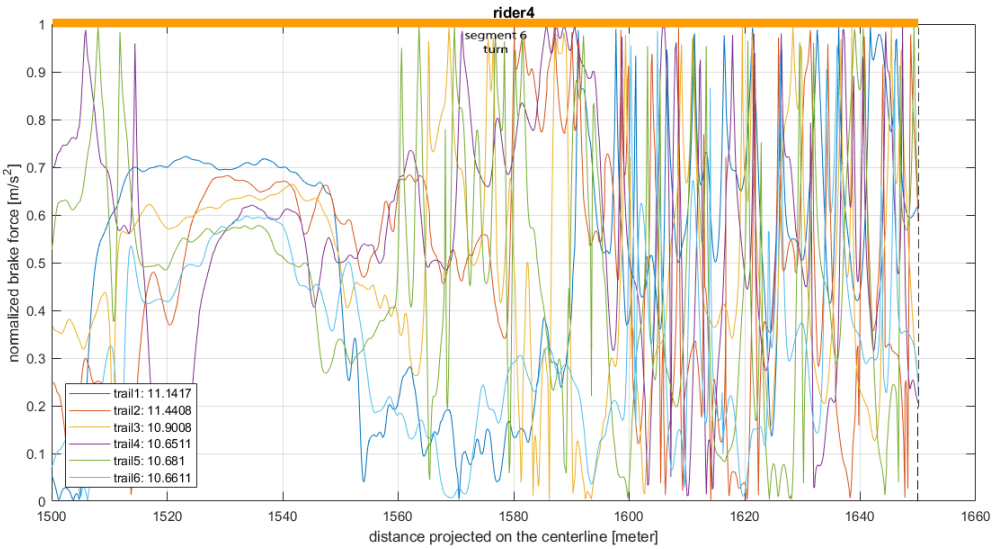

Figure O.4: Brake distribution between front and rear for rider 4.

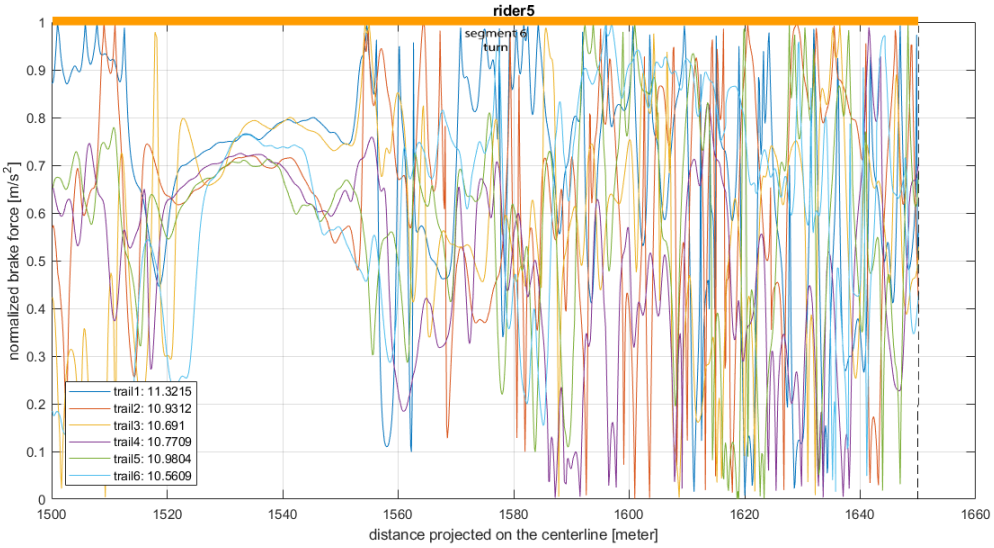

Figure O.5: Brake distribution between front and rear for rider 5.

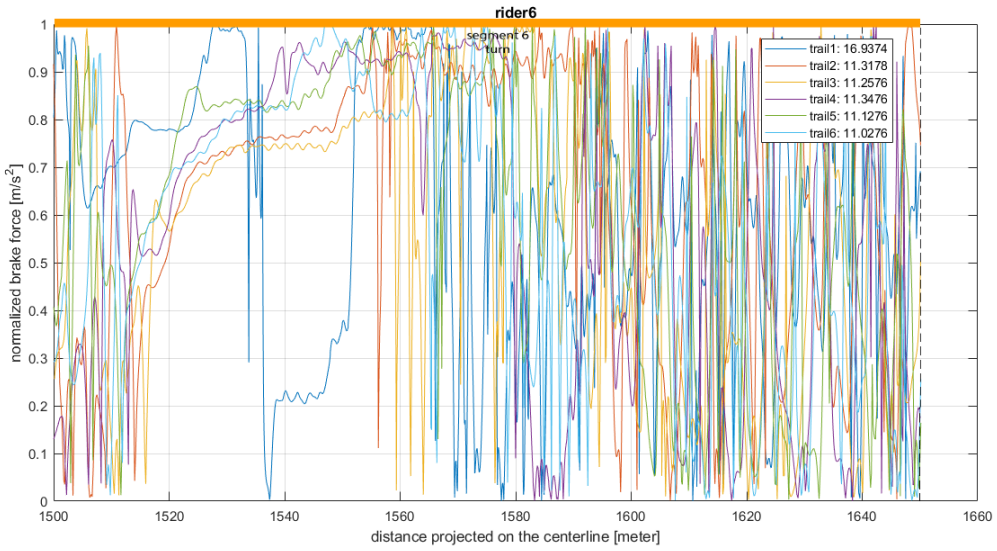

Figure O.6: Brake distribution between front and rear for rider 6.

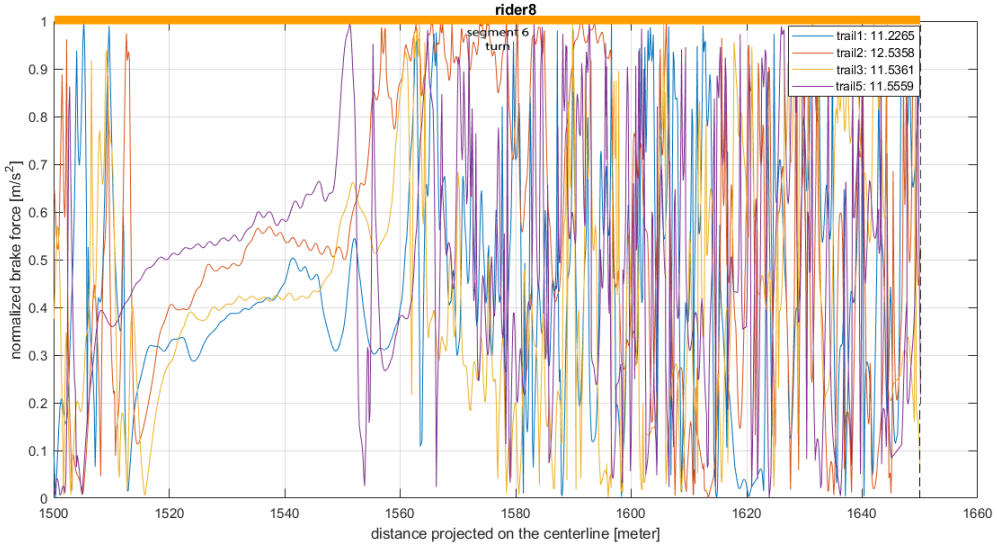

Figure O.7: Brake distribution between front and rear for rider 8.

P

Overarching Research

This research is conducted as an integral part of an overall research plan for optimising cycling using a 'sensor' bike
The description of the project from the official paperwork is: 'The project consists of developing four identical measurement kits. With such a measurement kit, any bicycle can be transformed into a measurement-cycle, a 'sensor bike'. The measurements provide insights into the inclination angle, the speed and the cyclist's behaviour with regard to steering and braking. Via an app, the athletes and coaches receive feedback on decisions made during trial runs. This way, they can determine optimal steering and braking patterns.'[8]

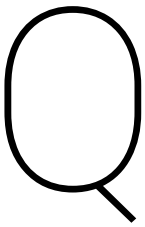

Informed Consent

TECHNICAL UNIVERSITY DELFT

Consent Form

Investigation: **Optimal cornering and descent technique in elite race cycling**

Investigators:
Ir. Marco Reijne – researcher
Email : m.m.reijne@tudelft.nl
Tel : 0646554526

Dr. A.L. Schwab – supervisor
Dr. D.J.J. Bregman - researcher

Introduction: Before agreeing to participate in this study, it is important that the following explanation of the proposed procedures be read and understood. This document describes the purpose, procedures, benefits, risks, and possible discomforts of the study. It also describes the right to withdraw from the study at any time.

Purpose of the study: Goal of the experiment is to obtain data on elite race cyclist behaviour during a descent. The data will be used to explore differences in riding behaviour in-between elite race cyclists and to identify relevant cyclist behaviour variables for performance that will be further tested. The participant will perform 10 descents of approximately 2 km on his own bicycle equipped with a measurement system developed by the TU Delft. The results of this experiment will be analysed and possibly published in a scientific article. Participants will remain anonymous throughout this process.

Duration of the experiment: The experiment will take approximately 1.5 hours to complete of which 10 trials of approximately 2 min.

Procedure: During the experiment a measurement system (containing steering angle encoder, accelerometers, gyroscopes, magnetometers, load cells, GNSS and GoPro) will be installed on your bicycle. Your bicycle is already prepared at the bottom of the descent when you arrive. When the measurement system is installed, you will first be weighted together with the bicycle on a scale. Next you will be driven to the start location of the descent together with your bicycle. Here the measurement system will be switched on and calibrated. Next the real test will start. When given the signal by the starter you will ride the descent track as you would normally do (approximately 2 km). At the end of the descent you will wait at the side of the road where the measurement system will be calibrated again and switched off. During the experiment, you adhere to all road regulations and remain on the right side of the road. You will be followed by a team car that will bring you back up to the start location. Here you will rest before we repeat the test (total of 10 repetitions).

Confidentiality: All the data collected in this study will be kept confidential and will be used for research purposes only. Throughout the study, you will only be identified by a subject number only.

Right to refuse or withdraw: Your participation is strictly voluntary and you may refuse to participate, or discontinue your participation at any time, without negative consequences.

Questions: If you have any questions concerning this study, you may contact M.M. Reijne (contact details included at the top).

I have read and understood the information provided above.
I give permission to process the data for the purposes described above.
I give permission to store the data for a period of 3 years.
I voluntarily agree to participate in this study.

Name:

Signature Participant date:

Signature Investigator

R

Procedure Rider

Goal of the study

Experiment

For the experiment, you have to ride a descent of approximately 2 km as fast as possible (but safety first). The experiment is repeated 10 times. You must remain on the right lane at all times and be aware of other traffic. You are allowed to pedal **and take on any position you like (be aware of the measurement system).** The experiment will be performed with two riders at the same time (1 minute interval on the descent).

Procedure

- You will be picked up by car at the hotel (**already in cycling clothes, shoes and helmet?**), from which you will be driven to the location of the descent.
- In the car, you are asked to fill in a questionnaire and sign a consent form.
- **You will ride down the descent by car before the experiment start**
- For the experiment your bicycle will be equipped with a measurement system. Your bike is already prepared for you and waiting at the bottom of the descent.
- At the bottom of the descent you will meet Chris, Marco and Daan. They will explain the sensor system to you if you like and give further instruction on the experiment.
- First you will be weighted together with the bicycle.
- Next, you and the bicycle will be driven back up the climb to the start location.
- Before your first trial, at the start location, the measurement system will be switched on and calibrated (this takes approximately 5 minutes).
- After this you will be placed at the start location, where you will be asked to remain for several seconds to calibrate the GPS and mark the start of the trial.
- Next you will start the descent when given the sign by the starter.
- Go down as fast as possible. Always remain in the right lane and be aware of other traffic.
- At the bottom of the descent you will return to the parking place where you started.
- You will be asked several questions on how you experienced the descent.
- Your bicycle will then be placed back on the car and you will be driven back up to the start location where you will repeat the experiment (a total of 10 trials).
- After the final trial, the measurement system will be switched off.
- You will be asked a final two questions.
- You can wait until the measurement system is removed from your bicycle and ride back to the hotel or you can be brought back by car.

The data we will collect during the experiment will be given back to you within 1-2 days. You will be able to see your descent trajectory and braking points and force of your fastest trial. You will be able to see the descent time and velocities in the turns of all your trials.

Thank you for your participation.

Bibliography

[1] Roman F Beck. Mountain bicycle acceleration and braking factors. *Accident Reconstruction Journal*, 19 (4):49–56, 2009.

[2] CeremicSpeed. Driven, CeramicSpeed.com. https://www.ceramicspeed.com/en/driven/. [online; accessed 21-nov-2018].

[3] Jim Papadopoulos David Gordon Wilson. *Bicycling Science*. MIT Press, 2004.

[4] Jos J de Koning, Maarten F Bobbert, and Carl Foster. Determination of optimal pacing strategy in track cycling with an energy flow model. *Journal of Science and Medicine in Sport*, 2(3):266–277, 1999.

[5] Ben Delaney. Lab test: what causes brake rub - the wheels or the frame? - BikeRadar. https://www.bikeradar.com/road/gear/article/bicycle-brake-rub-wheels-vs-frame-49344/. [online; accessed 13-feb-2019].

[6] Giant. TCR-Advanced-SL-0–DA-Carbon.jpg (1519×1000). https://images.giant-bicycles.com/b_white,c_pad,h_1000,q_80/uoawr1grdm1zftrnjoj6/TCR-Advanced-SL-0--DA_Carbon.jpg. [online; accessed 23-mei-2018].

[7] TE Graham and LL Spriet. Performance and metabolic responses to a high caffeine dose during prolonged exercise. *Journal of applied physiology*, 71(6):2292–2298, 1991.

[8] TU Delft Sports Engineering Institute. Award for 'sensor-bike' project TU Delft. http://sportsengineering.tudelft.nl/national-sportinnovator-award-for-measurement-cycle-project-tu-delft/ [online; accessed 19-April-2018].

[9] GREG KOPECKY. Debunking Wheel Stiffness - Slowtwitch.com. https://www.slowtwitch.com/Tech/Debunking_Wheel_Stiffness_3449.html. [online; accessed 13-feb-2019].

[10] Chester R Kyle. Reduction of wind resistance and power output of racing cyclists and runners travelling in groups. *Ergonomics*, 22(4):387–397, 1979.

[11] Alejandro Lucía, Jesús Hoyos, and José L Chicharro. Physiology of professional road cycling. *Sports medicine*, 31(5):325–337, 2001.

[12] RA Lukes, SB Chin, and SJ Haake. The understanding and development of cycling aerodynamics. *Sports engineering*, 8(2):59–74, 2005.

[13] Mantel.com. Giant Propel Advanced 1 kopen? https://www.mantel.com/giant-propel-advanced-1?spec%5B%5D=10739&spec%5B%5D=17268&utm_source=google&utm_medium=shopping&gclid=CjwKCAiAwojkBRBbEiwAeRcJZC4EJvr60OKiT9fGo69LxcJP4amE0jrxP0cyS2_gG-cxBMUweXLNnhoC-0kQAvD_BwE. [online; accessed 8-march-2019].

[14] James C Martin, Douglas L Milliken, John E Cobb, Kevin L McFadden, and Andrew R Coggan. Validation of a mathematical model for road cycling power. *Journal of applied biomechanics*, 14(3):276–291, 1998.

[15] JC Martin and WW Spirduso. Determinants of maximal cycling power: crank length, pedaling rate and pedal speed. *European journal of applied physiology*, 84(5):413–418, 2001.

[16] Mathworks. Systems of Linear Equations. https://nl.mathworks.com/help/matlab/math/systems-of-linear-equations.html. [online; accessed 10-okt-2018].

[17] Matthew C Miller, Philip W Fink, Paul William Macdermid, Blake G Perry, and Stephen R Stannard. Validity of a device designed to measure braking power in bicycle disc brakes. *Sports biomechanics*, 17(3): 303–313, 2018.

[18] Paint.NET. Free Software for Digital Photo Editing. https://www.getpaint.net/. [online; accessed 23-mei-2018].

[19] Wayne Pein. *High Speed Bicycling*. North Carolina Coalition for Bicycle Driving, 2007.

[20] MM Reijne, DJJ Bregman, and AL Schwab. Measuring and comparing descend in elite race cycling with a perspective on real-time feedback for improving individual performance. In *Multidisciplinary Digital Publishing Institute Proceedings*, volume 2, page 262, 2018.

[21] Philip Friere Skiba, Weerapong Chidnok, Anni Vanhatalo, and Andrew M Jones. Modeling the expenditure and reconstitution of work capacity above critical power. *Medicine and science in sports and exercise*, 44(8):1526–1532, 2012.

[22] sportinnovator.nl. Met de sensorbike sneller en veiliger door de bocht. http://sportinnovator.nl/projecten/met-de-sensorbike-sneller-en-veiliger-door-de-bocht. [online; accessed 8-march-2019].

[23] David P Swain. A model for optimizing cycling performance by varying power on hills and in wind. *Medicine and Science in Sports and Exercise*, 29(8):1104–1108, 1997.

[24] C. van Trigt. Measuring bicycle brake forces during a descent. 2018.

[25] Vittoria. Corsa Speed is the fastest bike tire. https://www.vittoria.com/eu/fastest-bike-tire. [online; accessed 21-nov-2018].